Return to Dan Lussman

REPORT NO. DOT-TSC-OST-77-54

ELEVATED GUIDEWAY COST-RIDE QUALITY STUDIES FOR GROUP RAPID TRANSIT SYSTEMS

D.N. Wormley
J.K. Hedrick
L. Eglitis
D. Costanza

Department of Mechanical Engineering
Massachusetts Institute of Technology
Cambridge MA 02139

OCTOBER 1977

FINAL REPORT

DOCUMENT IS AVAILABLE TO THE U.S. PUBLIC THROUGH THE NATIONAL TECHNICAL INFORMATION SERVICE, SPRINGFIELD, VIRGINIA 22161

Prepared for

U.S. DEPARTMENT OF TRANSPORTATION
OFFICE OF THE SECRETARY
Office of the Assistant Secretary for Systems Development and Technology
Office of Systems Engineering
Washington DC 20590

NOTICE

This document is disseminated under the sponsorship of the Department of Transportation in the interest of information exchange. The United States Government assumes no liability for its contents or use thereof.

NOTICE

The United States Government does not endorse products or manufacturers. Trade or manufacturers' names appear herein solely because they are considered essential to the object of this report.

Technical Report Documentation Page

1. Report No. DOT-TSC-OST-77-54	2. Government Accession No.	3. Recipient's Catalog No.
4. Title and Subtitle ELEVATED GUIDEWAY COST-RIDE QUALITY STUDIES FOR GROUP RAPID TRANSIT SYSTEMS		5. Report Date October 1977
		6. Performing Organization Code
7. Author(s) D.N. Wormley, J.K. Hedrick, L. Eglitis, D. Costanza		8. Performing Organization Report No. DOT-TSC-OST-77-54
9. Performing Organization Name and Address Department of Mechanical Engineering* Massachusetts Institute of Technology Cambridge MA 02139		10. Work Unit No. (TRAIS) OS749/R8505
		11. Contract or Grant No. DOT-TSC-1206
12. Sponsoring Agency Name and Address U.S. Department of Transportation Office of the Secretary Office of the Assistant Secretary for Systems Development and Technology Office of Systems Engineering Washington DC 20590		13. Type of Report and Period Covered FINAL REPORT September 1976-May 1977
		14. Sponsoring Agency Code
15. Supplementary Notes *Under contract to:	U.S. Department of Transportation Transportation Systems Center Kendall Square Cambridge MA 02142	

16. Abstract

A methodology is developed for relating cost to ride quality in elevated guideway system design, based upon directly relating guideway structural properties and construction tolerances to both cost and ride quality. It is illustrated in detail for group-rapid-transit precast concrete elevated guideway systems. These detailed cost-ride quality studies include an assessment of span properties, construction-related tolerances such as joint discontinuities, pier height variations, camber, and local surface roughness, and the effect of vehicle properties on cost and vehicle ride quality.

17. Key Words Group Rapid Transit, Elevated Guideways, Ride Quality		18. Distribution Statement DOCUMENT IS AVAILABLE TO THE U.S. PUBLIC THROUGH THE NATIONAL TECHNICAL INFORMATION SERVICE, SPRINGFIELD, VIRGINIA 22161	
19. Security Classif. (of this report) Unclassified	20. Security Classif. (of this page) Unclassified	21. No. of Pages 202	22. Price

Form DOT F 1700.7 (8-72) Reproduction of completed page authorized

PREFACE

The authors wish to acknowledge the assistance of C.E. Maguire, Inc., which performed the structural and costing studies contained in this report. The detailed cost calculations were performed under the direction of Sam Wasfy.

The authors also wish to acknowledge the assistance provided by representatives of the precast concrete industry, particularly Donald Reeves of San-Vel Concrete Corporation, in providing information on the technical aspects of casting and cost reduction for pre-cast beam elements.

This study was supported by the Transportation Advanced Research Projects (TARP) Program of the U.S. Department of Transportation, Office of the Secretary, and the Transportation Systems Center. We wish to acknowledge the fruitful suggestions and assistance of the project technical monitors, Donald Sussman and Robert Ravera. The authors also acknowledge Mrs. Leslie Regan, who prepared the report manuscript.

METRIC CONVERSION FACTORS

Approximate Conversions to Metric Measures

Symbol	When You Know	Multiply by	To Find	Symbol
		LENGTH		
in	inches	2.5	centimeters	cm
ft	feet	30	centimeters	cm
yd	yards	0.9	meters	m
mi	miles	1.6	kilometers	km
		AREA		
in^2	square inches	6.5	square centimeters	cm^2
ft^2	square feet	0.09	square meters	m^2
yd^2	square yards	0.8	square meters	m^2
mi^2	square miles	2.6	square kilometers	km^2
	acres	0.4	hectares	ha
		MASS (weight)		
oz	ounces	28	grams	g
lb	pounds	0.45	kilograms	kg
	short tons (2000 lb)	0.9	tonnes	t
		VOLUME		
tsp	teaspoons	5	milliliters	ml
Tbsp	tablespoons	15	milliliters	ml
fl oz	fluid ounces	30	milliliters	ml
c	cups	0.24	liters	l
pt	pints	0.47	liters	l
qt	quarts	0.95	liters	l
gal	gallons	3.8	liters	l
ft^3	cubic feet	0.03	cubic meters	m^3
yd^3	cubic yards	0.76	cubic meters	m^3
		TEMPERATURE (exact)		
°F	Fahrenheit temperature	5/9 (after subtracting 32)	Celsius temperature	°C

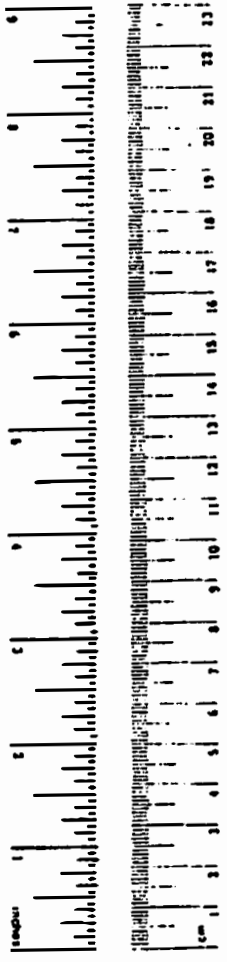

Approximate Conversions from Metric Measures

Symbol	When You Know	Multiply by	To Find	Symbol
		LENGTH		
mm	millimeters	0.04	inches	in
cm	centimeters	0.4	inches	in
m	meters	3.3	feet	ft
m	meters	1.1	yards	yd
km	kilometers	0.6	miles	mi
		AREA		
cm^2	square centimeters	0.16	square inches	in^2
m^2	square meters	1.2	square yards	yd^2
km^2	square kilometers	0.4	square miles	mi^2
ha	hectares (10,000 m^2)	2.5	acres	
		MASS (weight)		
g	grams	0.035	ounces	oz
kg	kilograms	2.2	pounds	lb
t	tonnes (1000 kg)	1.1	short tons	
		VOLUME		
ml	milliliters	0.03	fluid ounces	fl oz
l	liters	2.1	pints	pt
l	liters	1.06	quarts	qt
l	liters	0.26	gallons	gal
m^3	cubic meters	35	cubic feet	ft^3
m^3	cubic meters	1.3	cubic yards	yd^3
		TEMPERATURE (exact)		
°C	Celsius temperature	9/5 (then add 32)	Fahrenheit temperature	°F

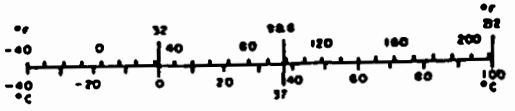

CONTENTS

Section		Page
1.	INTRODUCTION	1-1
1.1	Background	1-1
1.2	Scope and Objectives of Study	1-4
1.3	Guideway Cost-Construction Tolerance-Ride Quality Relationships	1-5
1.4	Study Methodology	1-9
2.	GUIDEWAY STRUCTURAL DESIGN AND COST ANALYSIS	2-1
2.1	Configuration Definition	2-1
2.2	Structural Design Basis	2-1
2.3	Cost Basis	2-5
2.4	Configuration Parametric Studies	2-9
2.4.1	Superstructure Studies	2-9
2.4.2	Support Structure Tradeoff Studies	2-18
2.5	Baseline Designs and Cost Summary	2-22
3.	RIDE QUALITY ANALYSIS	3-1
3.1	Ride Quality Measurement	3-1
3.2	Vehicle-Guideway Model	3-3
3.2.1	Guideway Representation	3-4
3.2.2	Vehicle Representation	3-7
3.2.3	Summary of Ride Quality Computation Techniques	3-10
3.3	Summary of Baseline Vehicle-Guideway Parameters	3-13
3.4	Influence of Guideway Static Irregularities on Ride Quality	3-13
3.5	Influence of Simple Span Deflection, Mean Camber and Irregularities on Vehicle Response	3-31
3.6	Influence of Multiple Span Deflection, Mean Camber and Irregularities on Vehicle Response	3-40

CONTENTS (cont.)

Section		Page
3.7	Influence of Vehicle Suspension Properties on Ride Quality	3-45
4.	RIDE QUALITY COST TRADEOFF STUDIES	4-1
4.1	Scope of Tradeoff Studies	4-1
4.2	Baseline Guideway Configuration	4-1
4.3	Lateral Ride Quality Cost Relationships	4-2
4.4	Vertical Ride Quality Cost Relationships	4-7
5.	SUMMARY AND CONCLUSIONS	5-1
6.	REFERENCES	6-1
APPENDIX A	SUMMARY OF STRUCTURAL DESIGN CALCULATIONS FOR SMALL GUIDEWAY	A-1
APPENDIX B	SUMMARY DESIGN COST CALCULATIONS	B-1
APPENDIX C	VEHICLE-GUIDEWAY MODEL DESCRIPTION	C-1
	C.1 Guideway Representation	C-1
	C.2 Vehicle Representation	C-18
	C.3 Computation of Vehicle Acceleration	C-34
APPENDIX D	REPORT OF INVENTIONS	D-1

LIST OF ILLUSTRATIONS

Figure		Page
1.1	Relationships of Ride Quality, Construction Tolerance and Guideway Cost	1-7
1.2	Construction Generation Surface Profile Irregularities	1-8
1.3	Cost-Construction Tolerance-Ride Quality Design Methodology	1-10
2.1	Guideway Configuration	2-2
2.2	Superstructure Guideway Configurations	2-10
2.3	Distribution of Prestressing Strands	2-13
2.4	Small and Large Superstructure Designs	2-16
2.5	Construction of Continuous Spans	2-17
2.6	Pier Designs and Costs	2-21
2.7	Cost Breakdown by Structural Components	2-23
2.8	Design Cost Summary	2-25
2.9	Distribution of Guideway Costs	2-27
3.1	Lateral I.S.O. Specification	3-2
3.2	Vertical I.S.O. Specification	3-2
3.3	Construction Generation Surface Profile Irregularities	3-5
3.4	Vertical Plane Vehicle Model	3-8
3.5	Lateral Plane Vehicle Model	3-9
3.6	Time and Frequency Analysis Techniques	3-12
3.7	Vertical Single Span Dimensional Irregularity Input PSD	3-17
3.8	Small Vehicle Vertical I.S.O. Single Span Response to Separate Irregularities, 60 Foot Span Length, 60 MPH	3-19
3.9	Large Vehicle Vertical I.S.O. Single Span Response to Separate Irregularities 60 Foot Span Length, 60 MPH	3-20

LIST OF ILLUSTRATIONS (cont.)

Figure		Page
3.10	Maximum Vertical Construction Tolerance to Meet 25 Minute I.S.O. Specifications	3-22
3.11	Large and Small Vehicle Irregularity I.S.O. Response 60 Foot Span Length, 60 MPH	3-23
3.12	Lateral Single Span Dimensional Irregularity Input PSD	3-25
3.13	Small Vehicle Lateral I.S.O. Separate Irregularity Response 60 Foot Span Length, 60 MPH	3-26
3.14	Large Vehicle Lateral I.S.O. Separate Irregularity Response 60 Foot Span Length, 60 MPH	3-27
3.15	Maximum Lateral Construction Tolerance to Meet 25 Minute I.S.O. Specifications	3-29
3.16	Large and Small Lateral I.S.O. Single Span Response, 60 Foot Span Length at 60 MPH	3-30
3.17	Small Vehicle Lateral Total RMS Response as a Function of Span Length and Velocity	3-32
3.18	Large Vehicle Lateral Total RMS Response as a Function of Span Length and Velocity	3-33
3.19	Large and Small Vertical Single Span I.S.O. Response 60 Foot Span Length, 60 MPH	3-34
3.20	Small Vehicle Vertical I.S.O. Single Span Response as a Function of Velocity and Span Length	3-36
3.21	Large Vehicle Vertical I.S.O. Single Span Response as a Function of Velocity and Span Length	3-37
3.22	Small Vehicle Six Span I.S.O. and Deflection Response of 80 Foot Span Length at 60 MPH	3-41
3.23	Large Vehicle Six Span I.S.O. and Deflection Response of 80 Foot Span Length at 60 MPH	3-42
3.24	Large Vehicle Single Span RMS Response as a Function of Sprung and Unsprung Natural Frequency	3-46
4.1	Cost Lateral Ride Quality Tradeoff for Lateral Surface Profile Modifications	4-6
4.2	Beam Cost, Camber, Unit Deflection, and Stiffness for a 60 Foot Simple Span Large Guideway	4-8

LIST OF ILLUSTRATIONS (cont.)

Figure		Page
4.3	Beam Cost, Camber and Unit Deflection as a Function of Continuity for a 100 Foot Span Large Guideway	4-12
4.4	Cost-Vertical Ride Quality Tradeoff as a Function of Continuity for 100 Foot Span Large Guideway	4-13
4.5	Cost-Vertical Ride Quality for Modification of Vertical Surface Profile on the 60 Foot Simple Span Large Guideway	4-16
C.1	General Elevated Guideway Configuration	C-2
C.2	Multispan Reinforcing Strands	C-2
C.3	Mode Shapes for Multispan Guideways	C-8
C.4	Surface Roughness Measurement Device	C-11
C.5	Guideway Surface Roughness Profiles	C-14
C.6	Mean Camber Profile	C-15
C.7	Non-Dimensional Vehicle Acceleration Transfer Function Magnitude as a Function of Non-Dimensional Frequency	C-23
C.8	Lateral Vehicle Schematic	C-28
C.9	Small Vehicle Root Locus	C-32
C.10	Large Vehicle Root Locus	C-33
C.11	Vertical Vehicle Analysis Program	C-39

LIST OF TABLES

Table		Page
1.1	Group Rapid Transit Vehicle Characteristics	1-5
2.1	Factors Which Influence Structural Design	2-6
2.2	Structural and Cost Characteristics of Constant and Variable Depth Section Simple Spans	2-14
2.3	Deflection, Camber and Cost for Simple and Continuous Spans	2-19
2.4	Summary of Span Design Structural Properties	2-28
3.1	Baseline Vehicle Parameters	3-14
3.2	Baseline Construction Tolerances	3-15
3.3	Small Vehicle RMS Acceleration on Single Span Guideway Design 6	3-38
3.4	Large Vehicle RMS Acceleration on Single Span Guideway Design 3a	3-39
3.5	RMS Vehicle Accelerations for Three Span Continuous Guideways	3-43
3.6	RMS Vehicle Accelerations for Six Span Continuous Guideways	3-44
4.1	Large Vehicle Lateral Ride Quality for Selected Construction Tolerance Levels	4-5
4.2	Large Vehicle Vertical Ride Quality for Baseline Levels of Construction Tolerance as a Function of Beam Depth for 60 Foot Simple Spans	4-10
C.1	First NS Eigenvalues $\bar{\lambda}_m = \lambda_m \ell_s$ for Semicontinuous Beams	C-6
C.2	Nondimensional Modal Coefficients of ϕ_m for Three Span Semi-Continuous Beams	C-6
C.3	Vertical Vehicle Transfer Function Coefficients	C-21
C.4	Lateral Vehicle Model Nomenclature	C-26

LIST OF SYMBOLS

a	vehicle c.g. to front axle distance
a_m	modal beam shape coefficient
a_{ms}	modal span shape coefficient
A	surface roughness coefficient, also guideway cross-section area
A_b	guideway beam cross section area
A_m	time varying mode amplitude coefficient
A_1	camber deviation coefficient
A_2	camber deviation coefficient
b	vehicle c.g. to rear axle distance
b_b	vertical secondary suspension damping
b_m	modal beam shape coefficient
b_{ms}	modal span shape coefficient
b_1	first coefficient of Fourier sine camber shape
b_2	third coefficient of Fourier sine camber shape
b_3	fifth coefficient of Fourier sine camber shape
c_m	modal beam shape coefficient
c_{ms}	modal span shape coefficient
d_m	modal beam shape coefficient
d_{ms}	modal span shape coefficient
E	Young's modulus for beam material
$f(x,t)$	vehicle force distribution acting on beam
f_e	span encounter frequency V/ℓ_s
$H(\omega)$	frequency response function of linear system
I_b	beam cross section moment of inertia
I_v	vehicle pitch moment of inertia
$\bar{I}_v$	vehicle nondimensional pitch moment of inertia $\frac{12\ I_v}{m_v\ \ell_a^2}$
I_y	vehicle yaw moment of inertia
j	$\sqrt{-1}$
k	number of spans per beam in a semicontinuous guideway

LIST OF SYMBOLS (cont.)

k_b	vehicle secondary suspension stiffness
k_{sr}	vehicle primary suspension (tire) stiffness
K	vehicle primary to secondary suspension stiffness ratio, k_{sr}/k_b
K_c	vehicle lateral steering controller overall gain
ℓ_a	vehicle distance between front and rear axles
ℓ_b	beam length ($n\,\ell_s$)
ℓ_h	interval spacing distance in multivehicle trains
ℓ_i	irregularity characteristic wavelength
L_c	length of midchord deviation surface roughness measurement device
L^*	vehicle lateral controller gain on yaw angle
m	mode number
m_R	vehicle total mass
m_u	vehicle unsprung mass
m_v	vehicle sprung mass
M_u	vehicle unsprung to sprung mass ratio, m_u/m_v
n	span number in multispan guideway
S_a	angular-fixed datum irregularity single sided power spectral density (PSD)
S_o	joint offset irregularity single sided PSD
S_{rw}	angular relative datum irregularity single sided PSD
S_{sr}	surface roughness irregularity single sided PSD
S_{y_f}	front wheel input PSD
S_{y_r}	rear wheel input PSD
S_{δ_m}	midchord deviation PSD of surface roughness measurement device
$\hat{S}$	nondimensional single sided irregularity PSD, $S/\sigma^2\ell_i$
T_c	nondimensional front (rear) acceleration transfer function due to input at front (rear)
T_s	nondimensional front (rear) acceleration transfer function due to input at rear (front)
V	vehicle forward velocity
V_c	vehicle crossing velocity frequency ratio, $V/2\pi\omega_1\ell_s$

LIST OF SYMBOLS (cont.)

x	coordinate denoting displacement along length of guideway
X	frequency domain description of input to linear system
y	coordinate denoting vertical displacement
$\bar{y}_c$	mean camber mid span magnitude
y_d	vertical vehicle input due to guideway deflection
y_s	vertical vehicle input due to guideway static shape
y_t	total vertical vehicle guideway input
$y_{of(r)}$	vehicle front (rear) wheel input
$y_{2f(r)}$	vehicle front (rear) suspension attachment point
$\hat{y}_{of(r)}$	vehicle front (rear) wheel inputs described in frequency domain
$\hat{y}_{of(r)}$	vehicle front (rear) suspension attachment point accelerations described in frequency domain
z	vehicle c.g. lateral displacement
Z_o	total lateral vehicle input due to guidewall irregularities
$\Delta Z_{fa(ra)}$	vehicle front axle (rear axle) lateral tracking errors
$\ddot{Z}_{fa(ra)}$	vehicle front axle (rear axle) lateral accelerations
δ	vehicle front wheel steering angle
δ_m	guideway surface roughness mid chord
ε	irregularity construction tolerance
ε_a	angular-fixed datum construction tolerance
ε_c	camber deviation construction tolerance
ε_o	joint offset construction tolerance
ε_{sr}	surface roughness construction tolerance
ε_{rw}	angular relative datum construction tolerance
λ	wavelength
λ_m	m^{th} span eigenvalue
$\bar{\lambda}_m$	m^{th} normalized eigenvalue, $\lambda_m \ell_s$
ω_m	undamped natural frequency of the mth mode of beam vibration
ω_p	vehicle pitch cancellation frequency
ω_n	vehicle unsprung natural frequency

ω_v	vehicle sprung mass natural frequency
$\hat{\omega}_i$	i^{th} non-dimensional Fourier frequency, $\frac{2\pi i V}{\ell_b \omega_v}$
Ω	wavenumber, $\frac{2\pi}{\lambda}$
Ω_c	cutoff wavenumber for surface roughness irregularity
π	3.14159...
ϕ	phase angle between front and rear axle inputs
ϕ_m	m^{th} mode beam shape function
ψ	vehicle yaw angle
ρ	beam mass density
σ	standard deviation
σ_a	angular-fixed datum irregularity magnitude standard deviation
σ_c	camber deviation irregularity magnitude standard deviation
σ_o	joint offset irregularity magnitude standard deviation
σ_{rw}	angular-relative datum irregularity magnitude standard deviation
$\sigma_{\delta m}$	mid chord deviation from straight edge standard deviation
ξ_b	beam damping ratio
ξ_m	beam damping ratio for m^{th} mode
ξ_v	vehicle secondary suspension damping ratio

SUMMARY

This study has developed a methodology for relating cost to ride quality in elevated guideway design for automated guideway transit systems. The methodology consists of (1) a guideway configurational analysis in which structural design and costing techniques are used to identify promising guideway configurations and baseline construction tolerance levels, (2) a ride quality analysis in which guideway construction tolerance levels and structural properties are used directly with vertical and lateral plane vehicle models to compute ride quality as a function of operating conditions, and (3) a ride quality - cost sensitivity tradeoff study in which results of the two separate analyses are applied iteratively to determine system design tradeoffs.

This methodology has been applied to elevated guideways constructed from precast concrete beams 60 - 100 feet in length supporting small 10,000 lb or large 20,000 lb group rapid transit (GRT) vehicles.

The GRT system designs have illustrated that guideway cost is particularly sensitive to the following factors:

1) The superstructure which represents 70% of the total structural cost:

   a) Span Configuration

      Precast box type beam construction results in a structure which is 75% of the cost of a similar structure employing standard AASHTO I beam sections.

b) Span Length

As span length increases from 60 to 100 feet, camber, deflection, and cost increase. Thus a 100 foot span is 10% more costly than a 60 foot span.

c) Guideway Size

The guideway design for the 10,000 lb vehicle cost 75% of that for 20,000 lb vehicle

2) The support pier design showed that cast-in-place round piers were less than 60% of the cost of pre-cast trapezoidal piers

3) A spread footing foundation was 25% of the cost of a pile foundation. However, even when a pile foundation is required, pier plus foundation costs are only about 30% of the total structural cost.

Parametric cost-ride quality studies have shown:

1) The use of 3 and 6 span continuous beams reduces the effects of both live load deflection and camber to a point where construction tolerances are the primary factors influencing ride quality. Ride quality for the large vehicle is increased at 60 mph operation from 105 to 120 minutes in terms of ISO exposure time while the beam cost is decreased by 6% when 6-span continuous beams are used rather than simple spans.

2) For baseline values of construction tolerance, lateral ride quality was good, exceeding 150 minutes of ISO exposure time for 60 mph operation of the small vehicle.

Lateral ride quality can be improved by reducing joint offset tolerance from 1/4 to 3/16 inch to yield an improvement in ride quality by a factor of 1.3 at 30 mph and 1.1 at 60 mph in terms of ISO exposure minutes at a cost increase of $0.27 per foot. Reduction of angular errors in the lateral plane from baseline values was not found to improve ride quality. The cost of the lateral guidewall could be reduced with the use of lower quality forms. For a lower quality guideway in which the surface roughness is double the baseline value, a cost reduction of $2.67 per foot, 1.3% of total guideway structural cost, is

achieved with a 50% reduction in ride quality in terms of ISO exposure minutes.

3) For baseline guideway designs, vertical ride quality exceeded 55 minutes at 60 mph. The vertical ride quality can be improved by reduction of joint offset tolerance from 1/4 to 3/16 inch to yield an increase in ride quality by a factor of 1.4 at 30 mph and 60 mph in terms of ISO exposure minutes at a cost of $0.83 per foot. It can also be improved through the installation of a ceramic overlay which eliminates joint offset and reduces camber and which yields greater than a 60% improvement in ride quality at 30 mph and 60 mph at a cost of $22 per foot, 10% of the total structure cost.

This study has shown that multiple span guideways for GRT systems are cost effective. Ride quality for these structures is determined primarily by construction tolerances and is relatively insensitive to structural properties. For the large GRT vehicle these types of guideways can be constructed for approximately $1m per mile and provide a ride quality nearly equivalent to a 55 minute ISO exposure at 60 mph. The small GRT guideway can be constructed for approximately $800,000 per mile and provides a ride quality equal to a 90 minute ISO exposure at 60 mph. The ride quality in these systems can be improved by reducing construction-generated irregularities or by improving vehicle suspension characteristics. For vertical motion, a reduction in suspension natural frequency from 1.0 to 0.75 hertz, or the use of a ceramic overlay on the guideway, yielded factors of 1.5 in ride quality improvement in terms of ISO exposure. Thus changes in both vehicle characteristics and guideway characteristics may have significant influences on ride quality.

1. INTRODUCTION

1.1 Background

Group Rapid Transit (GRT) systems employing vehicles operated under automatic longitudinal and lateral control on dedicated guideways are under serious consideration for implementation in a number of areas [1].* Currently two GRT systems are in revenue service-the AIRTRANS and Morgantown systems which utilize small 10-20 passenger rubber tired vehicles operating along guideways with multiple stations. The potential for implementation of future GRT systems depends, to a significant extent, upon both the capability to provide safe, comfortable, timely and reliable service and also upon cost. For the two GRT systems in service the costs associated with guideways represent more than half the system total capital cost and in an assessment of these systems [1], identification of methods to achieve lower cost guideway-vehicle systems while achieving safety, reliability and acceptable levels of ride quality was identified as a high priority research task.

Guideway cost reductions for new types of systems such as GRT may be achieved by use of guideway specifications readily accepted and understood by contractors rather than research related specifications, relaxation of required construction tolerances and utilization of improved construction techniques, as well as by more efficient use of guideway materials and innovations in basic structure design. In

*Numbers in [ ] refer to references listed in Section 6.

a number of the advanced systems built to date, the use of stringent tolerances and specifications not commonly employed in construction have contributed to high costs [1,2]. Also potential reductions in cost have been limited directly by vehicle-guideway interactions, the loads produced on the guideway by vehicles and the associated vehicle ride quality requirements.

The development of reduced cost guideways for GRT systems can be guided, to a significant extent, by experience developed from construction of highways. However, for GRT systems several features must be specifically considered in design which are different from typical highway design, including:

(1) GRT vehicles are operated under automatic lateral steering and longitudinal control. Lateral steering control is typically achieved by measuring the vehicle lateral position with respect to a guiderail or sidewall and steering the vehicle to maintain a fixed lateral relative position, thus a sidewall reference is required. Also because vehicle safety must be assured under system failure conditions, positive retention of the vehicle, typically by a sidewall, is required.

(2) GRT vehicles operating on a guideway are relatively uniform in size and weight, thus design may be based upon a specific vehicle in contrast to highways which must accomodate a wide variety of vehicle sizes and weights.

(3) The vehicle-guideway system design is required to meet a specified level of passenger comfort in the lateral, vertical and longitudinal planes. Guideway characteristics coupled with the vehicle steering dynamics and the vertical suspension elements determine vertical and lateral ride quality while longitudinal control influences the longitudinal ride quality.

(4) Provision is required in the guideway for control and communication channels and for power pick-up by the vehicle.

These features require that GRT guideway design must address a number of factors in addition to those normally considered in highway design such as represented by AASHTO specifications [3]. Aspects of these factors, particularly the requirements on designs to meet ride quality specifications have been discussed in [4-8], while detailed analytical studies which provide methods of determining vehicle ride quality and the level of vehicle-guideway interactions are represented by [9-10].

In many urban areas, substantial portions of GRT guideways will be elevated to negotiate rights-of-way and to provide safety. To minimize the environmental impact of these elevated structures, small cross-section long spans are desired while to reduce cost simple construction methods, not requiring stringent tolerances are required. To achieve good ride quality, stiff, large cross-section spans built to minimize construction produced vertical support and lateral guidance surface irregularities are required. Thus, a fundamental tradeoff exists between ride quality and cost.

This report describes research to develop a methodology for relating guideway costs to ride quality and vehicle loading aspects of elevated, guideway construction and to identify, in detail, the cost sensitivities of critical vehicle-guideway parameters for GRT systems. The scope of the study is summarized in the following section.

1.2 Scope and Objectives of Study

The specific objectives of this study include:

(1) Establishment of a methodology which relates guideway cost to ride related factors

(a) Identification of the generic guideway parameters which influence ride quality.

(b) Identification of the incremental costs associated with changes in these parameters.

(c) Development of a design methodology for achieving a guideway design which minimizes ride comfort related costs while meeting specifications.

(2) Preparation of design data for typical prototype GRT vehicle-guideway systems

(a) Determination of the relative incremental costs associated with critical guideway parameters.

(b) Determination of the relative influence of critical guideway-vehicle parameters on ride quality.

(c) Synthesis of cost-guideway parameter ride-quality data into sets of trade-off curves relating costs for GRT systems directly to guideway parameters.

The first objective is to provide a general framework for cost effective design of automated guideway systems while the second objective is to apply the methodology to several specific GRT systems. While the methodology can be applied to a wide variety of systems, specific application has been focused on systems with the following characteristics:

VEHICLES

- Rubber tired automotive-type
- Under complete longitudinal control

- Automatically steered by controlling the front tires steering angle in response to a measurement of the lateral position error between the guideway sidewall and the vehicle
- Operating speeds of 30-60 mph

GUIDEWAY

- Elevated, mainline (straight) with 60-100 foot spans
- U-shaped interior profile to provide vertical support, a lateral guidance reference and containment should the system fail
- Constructed from concrete
- Constructed using simple or continuous spans

Specific design data have been developed for guideways to accomodate the small and large GRT vehicles whose general characteristics are summarized in Table 1.1.

TABLE 1.1: GROUP RAPID TRANSIT VEHICLE CHARACTERISTICS

		Small Vehicle	Large Vehicle
Length:	ft	15	22
Width:	ft	7	9
Weight:	lbs	10,000	20,000
Speed:	mph	30-60	30-60

The general methodology employed to relate guideway costs to ride quality is described in the following section.

1.3 Guideway Cost-Construction Tolerance-Ride Quality Relationships

The construction cost-construction specification-ride quality relationships for an elevated guideway system are summarized in Figure

1.1. Guideway design requirements and cost are influenced by:

(1) Parameters which directly influence ride quality through the guideway vertical and lateral surface.

(2) Parameters not influencing ride quality but which are required to determine cost and to insure that general strength and safety requirements are met as set by vehicle live load, dead load, wind loads and earthquake loads and soil conditions.

Guideway parameters which directly influence vehicle ride quality that are attributed to guideway construction methods are illustrated in Figure 1.2 for the lateral and vertical reference planes. Each of the parameters is assumed to be random, varying in value between levels established by construction tolerance specifications. The resultant guideway static profile is represented as a surface generated by the superposition of the individual random irregularity profiles.

In addition to the random construction tolerances, vehicle ride quality in the vertical plane* is influenced by deterministic camber and by guideway deflection due to vehicle loads. The dynamic deflections are a function of the beam cross-section properties-specifically the rigidity, area and span length-while deterministic camber is primarily a function of the detailed prestressing steel design. Ride quality constraints place requirements on and establish bounds for these structural parameters and construction tolerance related parameters. However, because ride quality is a composite specification, many possible combinations of guideway and

*The parapet walls are considered rigid with no camber.

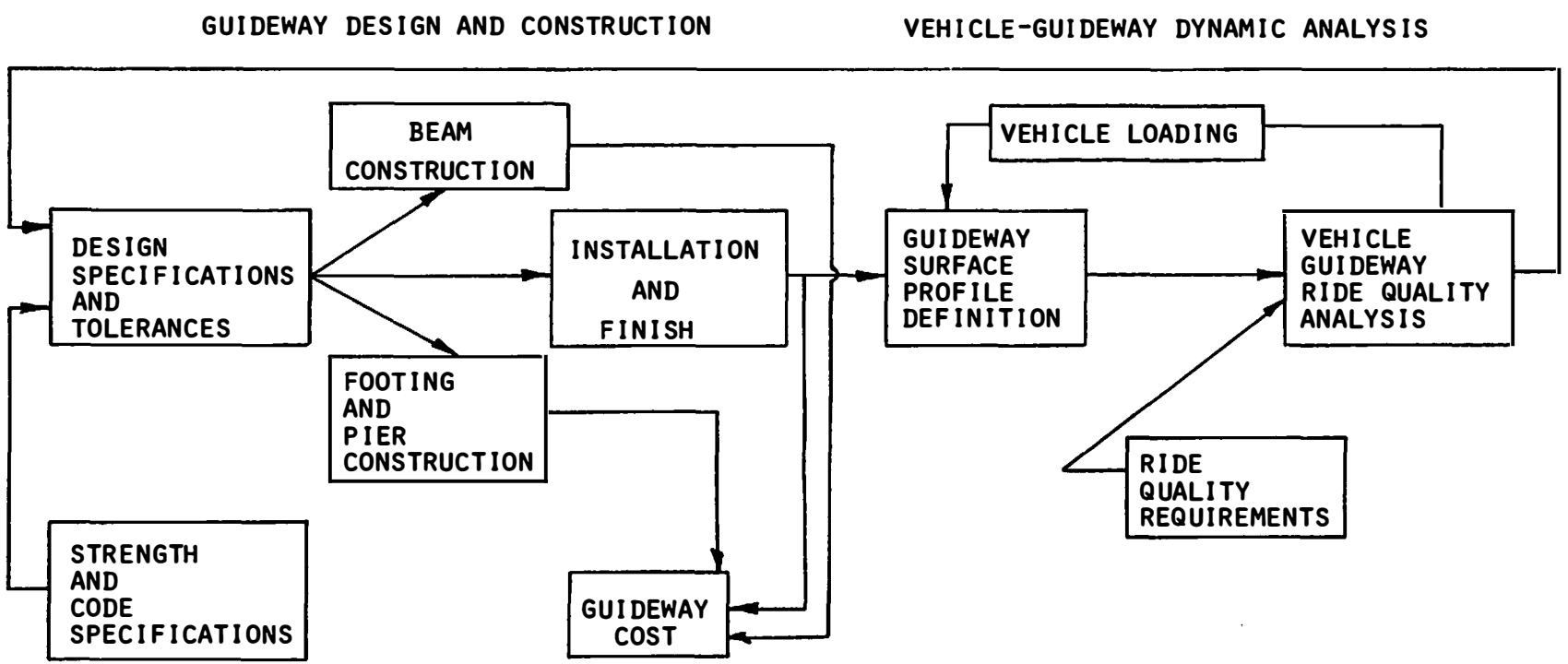

FIGURE 1.1: RELATIONSHIPS OF RIDE QUALITY, CONSTRUCTION TOLERANCE AND GUIDEWAY COST

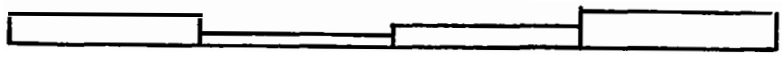

LATERAL AND VERTICAL
JOINT OFFSET

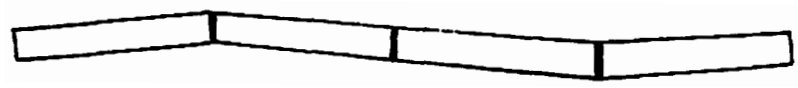

LATERAL AND VERTICAL
ANGULAR MISALIGNMENT

VERTICAL CAMBER

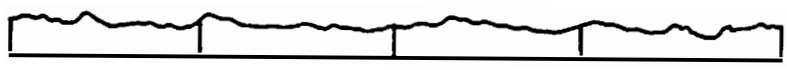

LATERAL AND VERTICAL
LOCAL SURFACE ROUGHNESS

FIGURE 1.2: CONSTRUCTION GENERATION SURFACE PROFILE IRREGULARITIES

vehicle parameters can result in a system which meets ride quality and a primary design goal is to develop a system design meeting these specifications in a cost effective manner.

A large number of detailed guideway design parameters do not directly influence ride quality but are required for specification of parapet walls, the main support beam, the pier and the foundation to insure that appropriate design codes are met and to compute guideway costs. Thus, to perform ride quality - cost tradeoff studies, essentially the structural design of a complete guideway must be considered.

1.4 Study Methodology

In order to systematically study cost-ride quality relationships the methodology illustrated in Figure 1.3 has been developed. The methodology consists of the following components.

(1) A Configurational Analysis in which the guideway superstructure, piers and footings are designed to accomodate a vehicle of given speed, size and weight. The detailed design is based upon engineering practice, codes, and economy. Cost data is based upon 1976 New England area unit labor and material costs related to span construction and transportation, earthwork, footing and pier construction and final installation, alignment and finishing.* This configurational analysis results in the definition of span structural properties and construction tolerance levels for span vertical support and lateral

*The cost does not include land acquisition, power and communication equipment installation or contractor profit.

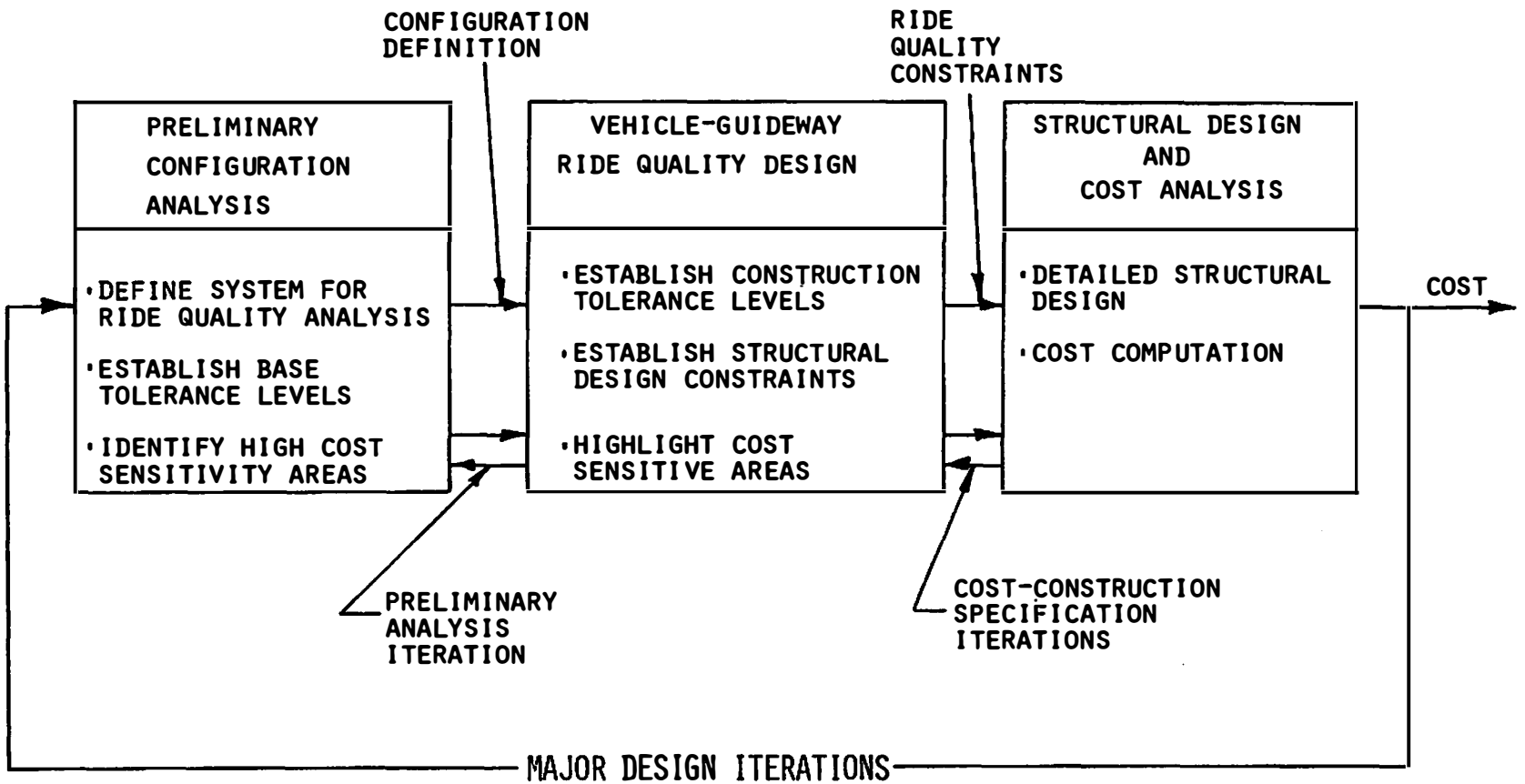

FIGURE 1.3: COST-CONSTRUCTION TOLERANCE - RIDE QUALITY DESIGN METHODOLOGY

guidance surfaces. The costs of construction and sensitivity of design alterations to cost are also identified. The detailed description of this configurational analysis is contained in Section 2.

(2) Vehicle-Guideway Ride Quality Analysis in which span structural properties (rigidity, natural frequency and length), camber and construction tolerances are used as inputs to vehicle vertical and lateral plane computer simulation dynamic models to compute ride quality. The construction tolerances are represented as producing random irregularities which excite a lateral plane two degree of freedom vehicle model and which together with guideway camber and dynamic deflection due to vehicle traveling weight excite a vertical four degree of freedom vehicle model. Ride quality is determined using these models by computing the total or one third octave band (ISO ride quality criteria) rms vehicle accelerations as the vehicle travels along a prescribed guideway. The detailed ride quality analysis results in determination of ride quality sensitivity to guideway and vehicle parameters. The analysis method and sensitivity study results are described in Section 3.

(3) Ride Quality-Cost Sensitivity Assessment in which results of the structural design-cost analyses are coupled with the ride quality analyses and through successive system design-cost computation-ride analysis iterations a "minimum" cost system is achieved which meets desired ride quality. These ride quality-cost tradeoff studies are summarized in Section 4.

2. GUIDEWAY STRUCTURAL DESIGN AND COST ANALYSIS

2.1 Configuration Definition

In this chapter the structural design and costing of guideway configurations is described. Single lane, elevated guideways consisting of precast, prestressed concrete beams ranging in span length from sixty to one hundred feet and erected as simple, three or six span continuous structures have been considered as shown in Figure 2.1. In the designs the guideway vertical support beam serves as the prime structural member. Parapet sidewalls, either cast-in-place or cast integrally with the beams, provide the sidewall reference surfaces to guide and restrain the vehicles. Straight sections of guideway with a nominal sixteen foot vertical clearance are considered for the detailed pier and footing design. Factors such as curvature, variation in topography, skewed crossings and variable soil conditions have not been considered.

2.2 Structural Design Basis

At present specific design codes and specifications have not been developed for GRT guideways. However, except for the factors listed in Section 1.1 concerning (1) sidewall guidance reference requirements (2) uniformity of vehicles, (3) design for passenger comfort and (4) provision for ancillary power pick-up, control and communication channels, GRT guideway design is similar to elevated highway structure design. A review of specifications cited in the American Associated of State Highway Transportation Officials (AASHTO) Standard

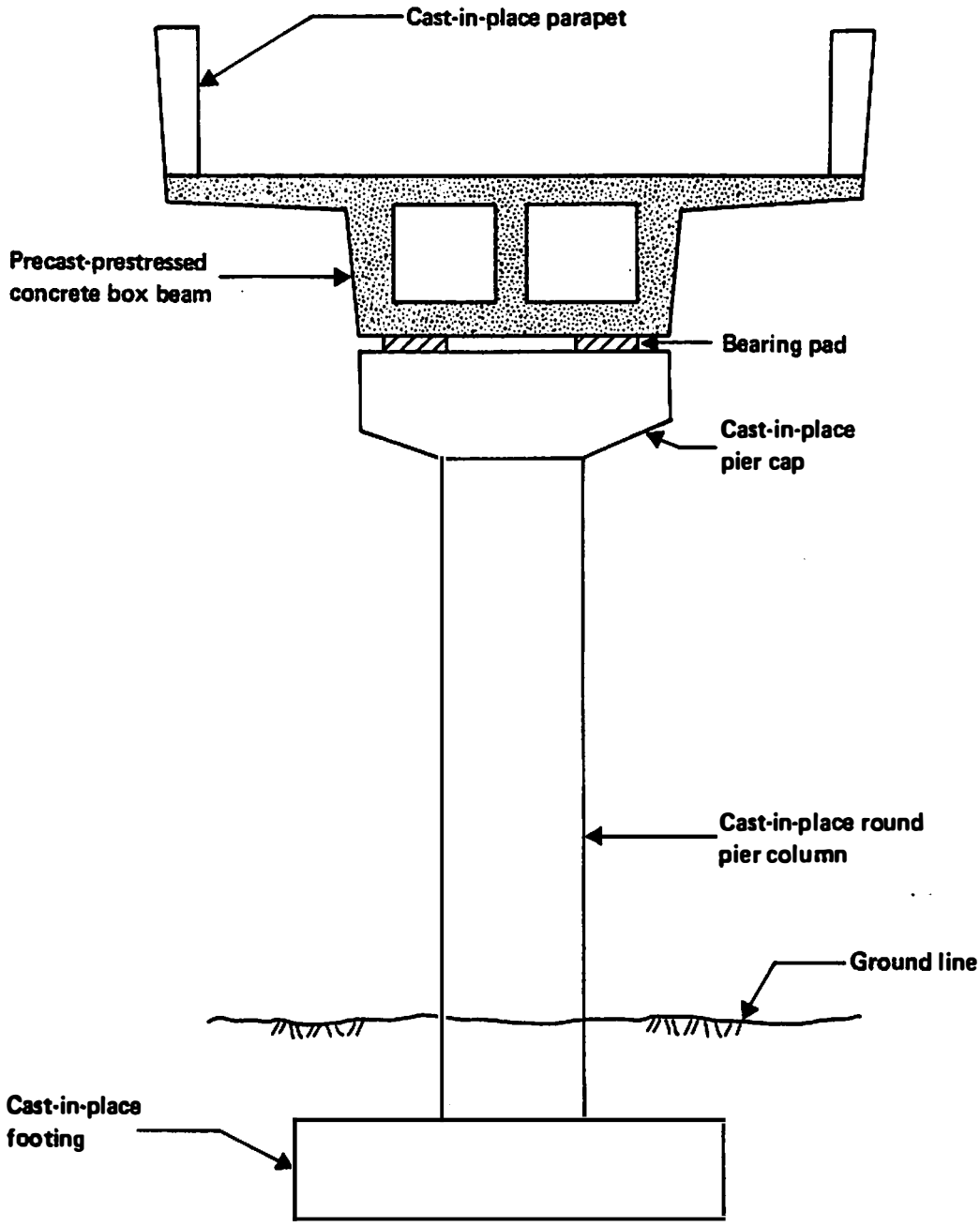

FIGURE 2.1: GUIDEWAY CONFIGURATION

Specifications [3] has indicated that the general design and material quality specifications are directly applicable to the design of elevated GRT structures. Because these specifications have evolved over a period of years and are familiar to engineers and contractors, they provide a well-understood basis for the design of a structure which can be built practically. A specific review of the codes was conducted to determine if for GRT structures, the utilization of the applicable parts of the code would lead to increased guideway cost in comparison to other design methods based upon sound engineering practice. No areas were found in which use of the codes would artificially increase costs.

The detailed design of the structure concrete members has been based upon the Load Factor Design Method [11]. Specific loads considered include the structure dead weight, the vehicle static and dynamic loads and environmental loads including wind, earthquake, ice, snow and thermal loads. In addition to these standard loadings, special conditions proposed for GRT vehicles have been considered:

(1) The span shall be capable of supporting a series of fully loaded vehicles parked end-to-end.

(2) The parapet sidewalls shall withstand a full speed crash of a fully loaded vehicle.

The parked vehicle condition was found in all design cases to be more restrictive than a single vehicle dynamic load and thus the parked vehicle condition limited all the design cases considered.*

*This parked vehicle condition increases the cost of the guideways considered in comparison to a single vehicle condition from $2.00 per linear foot for 60 foot spans to $7.50 per linear foot for 100 foot spans.

The major construction materials and the applicable stresses used in the structural design are listed below:

Reinforced Concrete:	3000 psi ultimate strength, with allowable compressive strength of 1200 psi.
Prestressed Concrete:	5000 psi ultimate strength, with allowable compressive strength of 2000 psi under design loads.
Prestressing Steel:	1/2" Dia., Grade 270 strands conforming to ASTM-A416 with a final effective stress after losses of 160,000 psi.
Reinforcing Bars:	Grade 60 conforming to ASTM-A615 with an allowable tensile stress of 24,000 psi.

These are standard construction materials and were selected after consideration of both light-weight and high strength concrete. Since a large portion of a beam load capacity is utilized by its self-weight, lightweight aggregate was evaluated for precast beam sections. The chief advantage of lightweight structural concrete is that a beam of reduced cross-section may be used to support the same live load as standard concrete. This advantage is useful when design is governed by stress rather than stiffness and has been employed economically in high-rise buildings where span lengths are relatively short and deflections do not limit design. For guideway spans in the sixty to one hundred foot range, no structural advantage is gained with the use of lightweight concrete and the increase in material unit cost by 30 to 50% in comparison to standard concrete does not justify the use of lightweight aggregates. In addition, the decreased modulus of elas-

ticity in lightweight aggregates results in increased deflections in comparison to standard concrete.

No justification was found to use high strength concrete in excess of 5000 psi ultimate strength, because the increase in unit material costs could not be balanced by decreases in other unit costs.

The influence of design load factors, material properties, construction tolerances and soil conditions on each of the guideway main structural elements in the design process is summarized in Table 2.1. The detailed design calculations which lead to the guideway structural definition are illustrated in Appendix A for simple and continuous span small vehicle guideway structures. Design procedures similar to those outlined were employed for all designs developed in this study. Basic designs have been developed to accomodate the envelopes and weights of the small and large GRT vehicles cited in Table 1.1. The specific designs were developed in parallel with guideway costs and in several cases, a number of design iterations were performed to achieve a minimum cost structure which could meet requirements.

2.3 Cost Basis

In addition to the structural design and construction materials, overall construction costs are also influenced by factors such as construction scheduling, erection techniques and required construction tolerances. Many factors which may have a substantial effect on guideway costs are site related such as sub-soil conditions, existing

TABLE 2.1: FACTORS WHICH INFLUENCE STRUCTURAL DESIGN

		PIER FOOTING	PIER COLUMN	BOX GIRDER	PARAPET
LOADS	WEIGHT (DEAD LOAD)	P	P	P	–
	VEHICLE LIVE LOAD	S	S	P	S
	WIND LOAD	P	P	–	–
	EARTHQUAKE	P	P	–	–
	THERMAL (EXP. & CONTR.)	S*	S*	P*	P*
MATERIAL STRENGTH	CONCRETE	–	P	P	–
	PRESTRESSING STEEL	–	–	P	–
	REINFORCEMENT	P	P	S	P
OTHER FACTORS	TOLERANCES & WORKMANSHIP	S	S	P	P
	SOIL CONDITIONS	P	–	S*	–

LEGEND:

P = PRIMARY INFLUENCE

S = SECONDARY INFLUENCE

* = CONTINUOUS SPANS ONLY

structures, streets, utilities, site accessibility and the availability of equipment, materials and manpower. In order to achieve a consistent basis for the evaluation of alternate guideway configurations the following tenets have been adopted.

1. Locality. The Metropolitan Boston Area has been selected as a basis for cost studies, thus setting local labor rates, material costs, and standard practices of construction. The assumption that a precast concrete plant is located within a radius of 20 miles from the site was made.

2. Time Factor. The second half of 1976 was chosen as a base for applying the various cost factors, such as labor rates, material prices, equipment costs and labor productivity. As the study progressed, cost escalation factors with time were not applied to maintain a constant basis for comparing the various designs.

3. Construction Finishes. Color additives, special concrete treatments or other aesthetic features which add to the cost have not been considered.

4. Soil Conditions. Standard dry earth excavation was computed in the cost but such other costs as rock excavation, removal of street paving, relocation of existing utilities, dewatering of excavation which are site related have not been considered.

5. Right-of-way, Land Acquisition and State or Local Permits have not been considered.

6. Contractor's General Conditions, Overhead and Profit are cost factors, however because of the great variation in these

factors for different localities and market conditions, they were not considered in the cost. Typically they may vary from 15% to 25% of the total construction cost.

7. Weather Conditions. Winter protection, heating of concrete, snow removal and similar factors were not considered in the computations.

8. Curvature has not been considered and only straight guideway costs have been computed.

9. Electrical and Mechanical Systems have not been considered in developing guideway cost.

The specific structure elements considered in the development of the costs include:

- Earthwork consisting of earth excavation and backfill and a one foot crushed stone base under the concrete footing.
- Cast-in-place concrete spread footing.
- Precast or cast-in-place concrete pier.
- Cast-in-place concrete cap over pier.
- Precast, prestressed concrete box beams.
- Cast-in-place concrete sidewalls.
- Elastomeric bearings under the superstructure.
- Joint sealer between units of superstructure.

The cost is based on estimated quantities and unit prices. The unit prices were derived by considering factors such as materials, labor productivity and rates, fringe benefits, equipment rental, transporta-

tion and erection.

In addition to in house construction cost data, local contractors, fabricators and suppliers have been consulted for up to date costs. References [12-16] are commonly used in our commerical cost estimations and have been used in this study to determine unit costs.

The manner in which detailed costs are computed for a guideway configuration is illustrated in Appendix B. This procedure was used in the computation of all costs reported in this study.

2.4 Configuration Parametric Studies

Parametric studies have been conducted to identify cost effective guideway candidates for ride quality analysis. The studies have considered (1) the superstructure and parapet sidewalls, (2) the pier supports and (3) the foundation. Since the major cost component of the guideway is the superstructure, major effort was focused on it.

2.4.1 Superstructure Studies

The basic superstructure configurations shown in Figure 2.2 have been considered. These configurations encompass the use of standard beam sections for vertical support with a precast U-shaped member to contain the vehicle as shown in (a) and (b) and a variety of precast box-type beams either with integrally cast or cast-in-place parapet walls. For guideways which extend in length over several miles, configurations which employ standard beams with a U-shaped section installed on top were found to be more costly than other sections be-

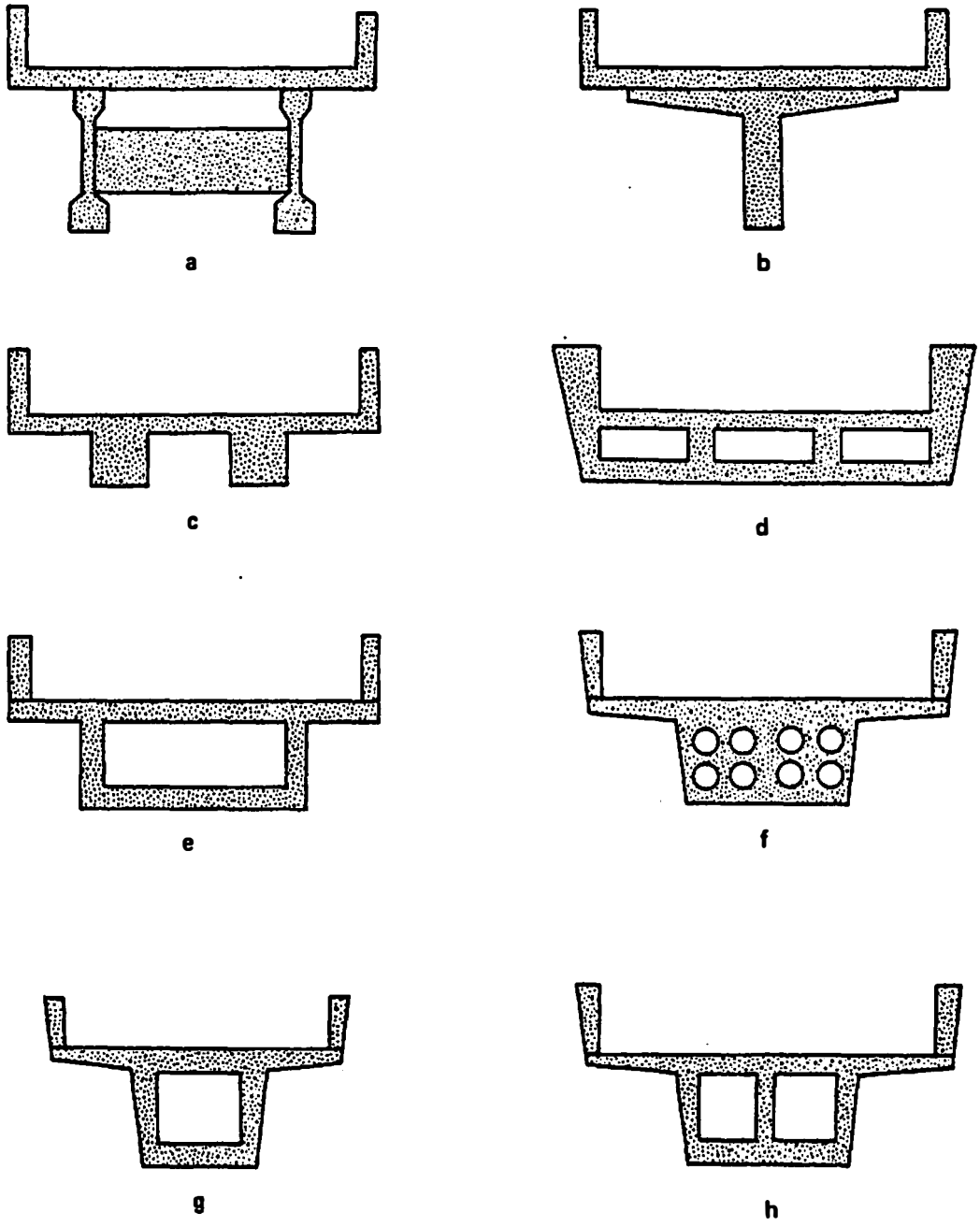

FIGURE 2.2: SUPERSTRUCTURE GUIDEWAY CONFIGURATIONS

cause of the field labor required to place the beams, the diaphragms connecting the beams and the U-shaped section. For example, configuration (a) was found to be 37% more expensive than configurations (g) and (h). Configurations (c) and (d) also were found to be inefficient in comparison to (e) through (g) because these sections have a relatively low ratio of inertia to area (I/A) which is a measure of efficiency of material utilization. The box type of beam with cast-in-place parapet walls was finally selected as most effective. The parapet walls were selected to be cast in place because casting them integrally with the beam for the size guideways considered resulted in an overall envelope which was difficult and costly to transport from the precast factory to the site. The basic box type of beam serves as both the prime structural member and the riding surface. It is a rigid structure with a high I/A ratio and has high resistance to a torsional moments, thus making it applicable to curved as well as straight sections of guideway.

The basic box beam and subsequent design refinements are represented as configurations (e) through (h). The final configurations selected for the small and large guideway designs are respectively configurations (g) and (h). These are a basic box with sloping exterior sidewalls. Sloping these walls permits the use of a permanent form for casting since the beam can be lifted out of the form without disassembly. In addition, these designs use fiber forms to shape the interior voids.* The sloping sidewalls and use of fiber forms in (g) and (h) result in

*The use of a fiber form requires the additional center interior vertical element in the large configuration of (h) compared to the small configuration (g).

a cost savings of approximately $22 per foot in comparison to the straight box of configuration (e) which is cast with removable plywood forms.

Using the generic box section, detailed designs were developed for 60, 80 and 100 ft simple span guideways for the large vehicle. As the span length is varied, the basic design parameters reduce to the section depth and the amount of prestressing steel. The distribution of prestressing steel in the 100 ft. span design is shown in Figure 2.3. Two types of designs were developed:

(1) For each span length, the design is developed to use the minimum section depth (minimum amount of concrete) permissible.

(2) The same section is used for each span length and the prestressing steel is reduced as span length decreases.

The structural characteristics and cost of the designs developed are summarized in Table 2.2. The data show that for the 60 and 80 foot span lengths, employing a larger section with a reduced number of prestressing cables results in a cost penalty which is less than 3% of the total superstructure cost, because while the cost is increased due to additional concrete, it is reduced by use of less steel. Since in an urban environment many different span lengths are required, the use of a constant section for a range of span lengths is advisable and very likely will result in a net cost reduction in comparison to using a different span depth for each length. Thus, the two basic cross-section shapes illustrated in Figure 2.4 have

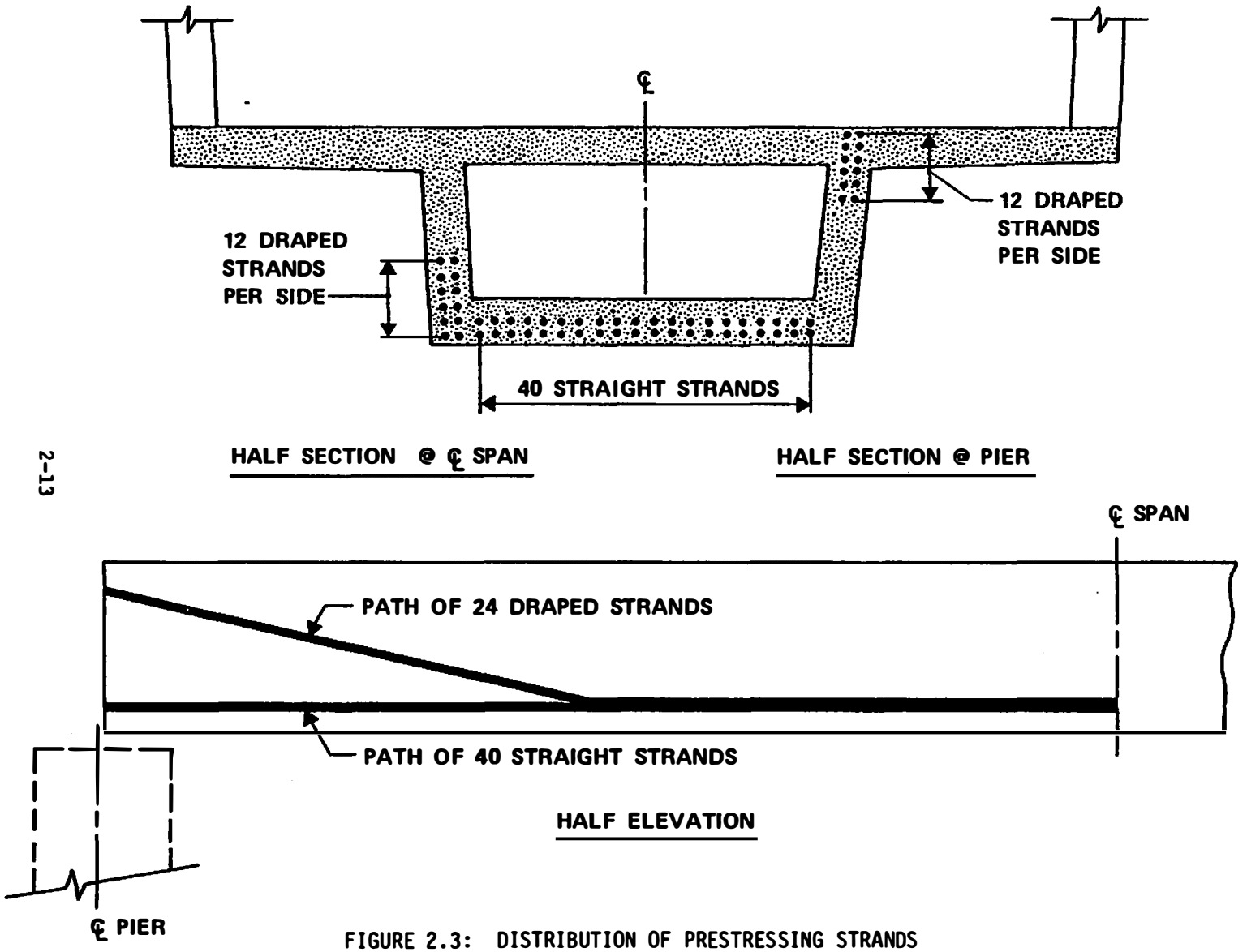

FIGURE 2.3: DISTRIBUTION OF PRESTRESSING STRANDS

TABLE 2.2: STRUCTURAL AND COST CHARACTERISTICS OF CONSTANT AND VARIABLE DEPTH SECTION SIMPLE SPANS

	SPAN LENGTH Ft	DEPTH Inches	AREA In^2	INERTIA In^4	NUMBER OF 1/2 INCH PRESTRESSING CABLES	BEAM COST DOLLARS PER FOOT
DESIGN 2A VARIABLE DEPTH	60	22	1333	80,044	40	111
	80	28	1399	148,919	52	124
	100	36	1524	287,766	64	139
DESIGN 2 CONSTANT DEPTH	60	36	1524	287,766	22	113
	80	36	1524	287,766	40	124
	100	36	1524	287,766	64	139

been adopted in this study for the small and large vehicle spans varying in length from 60 to 100 feet. These designs employ the tapered box sections with cast-in-place parapet walls. Structural design calculations for the sidewalls have indicated that a six inch thick parapet wall provides the strength to restrain the vehicle under crash conditions. However, to provide accommodation for the power pick-up and control hardware embedded in the sidewall, the wall has been designed with a seven inch width at the base and an eight inch width at the top.*

The final factor considered is the use of continuity at span joints. Both three and six span continuous beam systems have been studied. For GRT precast beam guideways the joints have been made live load continuous by extending reinforcing steel across the joints and filling the joints with concrete after assembly as shown in Figure 2.5.** This means of achieving continuity allows transfer of the moments generated by live loads across the joint and also eliminates expansion joints and one half of the bearings. The use of continuity also permits a reduction in prestressing steel when compared to simple spans and leads to a reduction in span camber. The disadvantage of continuous structures include the generation of secon-

*This added width allows better placement of the reinforcing bars connecting the wall to the support beams and thus should avoid a number of the problems encountered in current GRT system sidewalls.

**A preliminary analysis has indicated that complete continuity in which the dead load is carried across span joints is not cost effective for the GRT guideways considered in this study. It is primarily useful for long span cast-in-place monolithic structures.

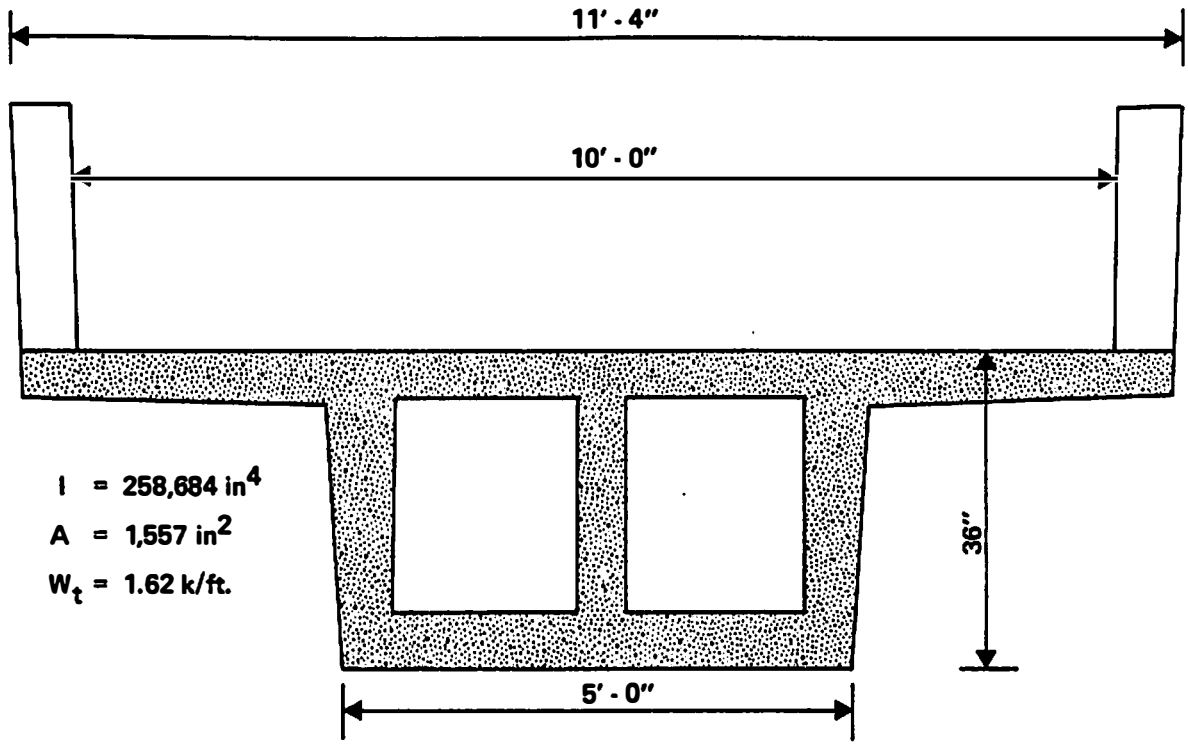

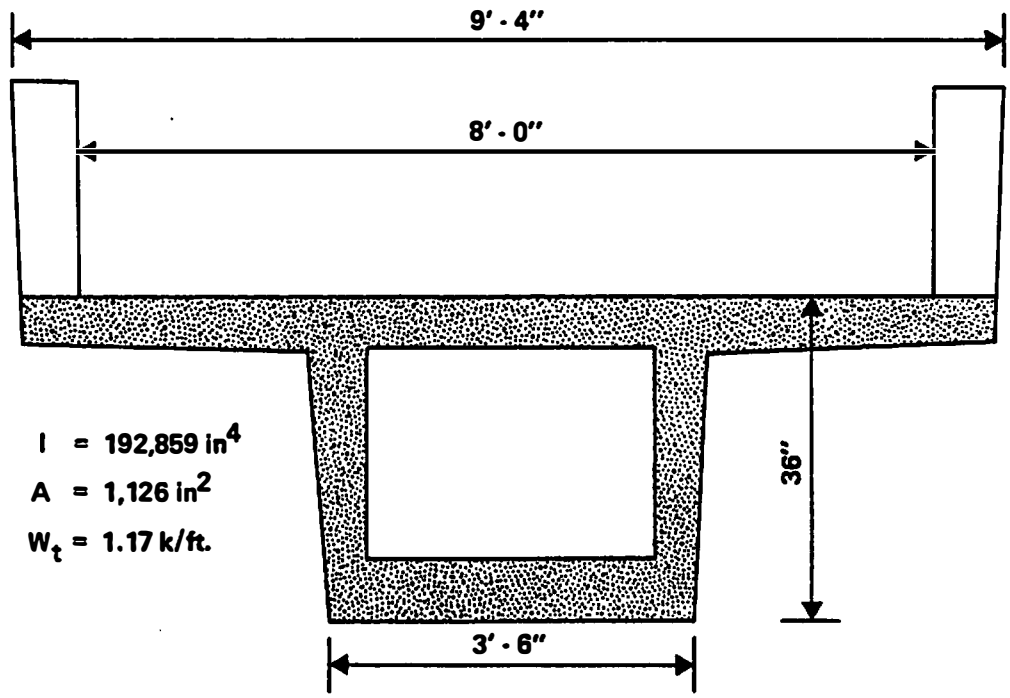

FIGURE 2.4: SMALL AND LARGE SUPERSTRUCTURE DESIGNS

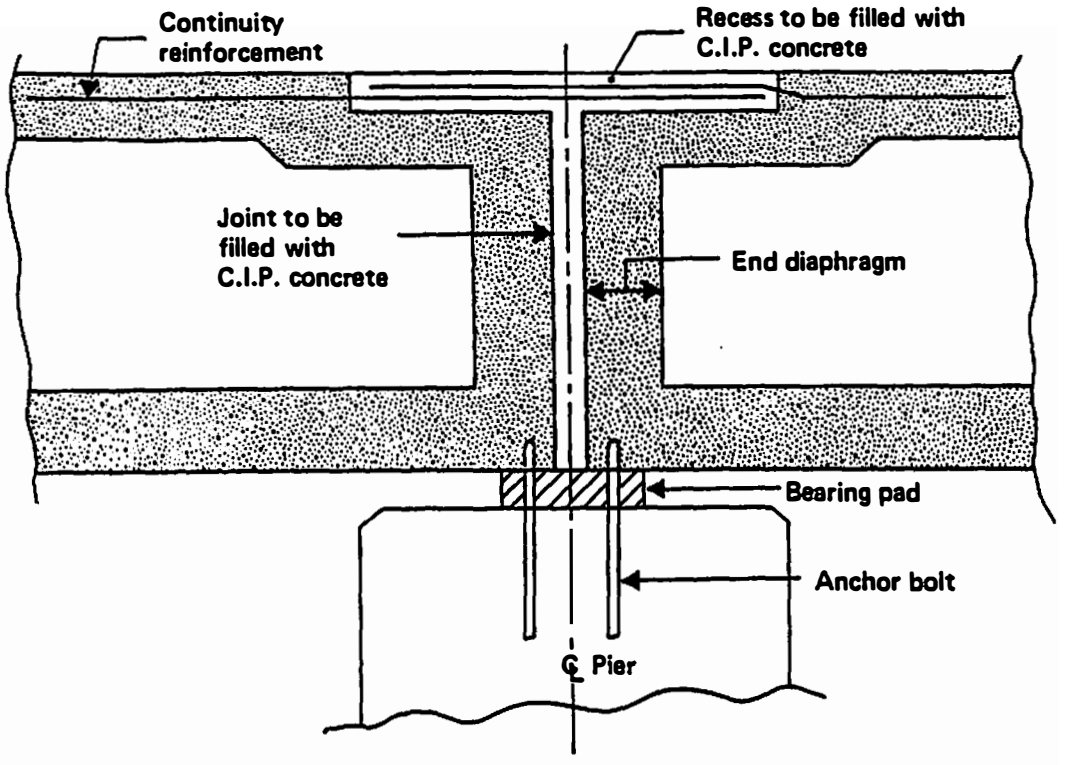

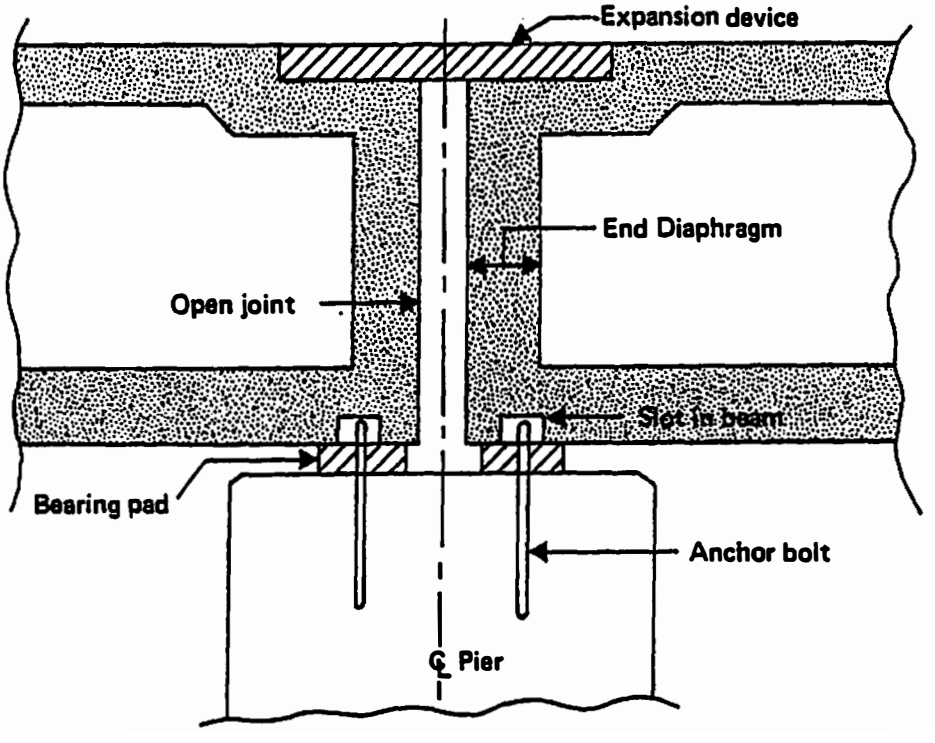

FIGURE 2.5: CONSTRUCTION OF CONTINUOUS SPANS

dary stresses due to shrinkage, creep, temperature and settlement of supports, as well as the additional labor required to achieve the continuous joint.

The costs of simple, three span continuous and six span continuous structures designed for the large GRT vehicle along with unit deflections and camber achieved are summarized in Table 2.3 for the 100 ft. span system. For this system the total superstructure costs of the continuous structures are less than that of the simple span because the decrease in prestressing steel required reduces the cost more than it is increased by the additional labor required to achieve continuity. The maximum end span unit deflections and cambers in the continuous structures are less than one half those of the simple span structure. Thus 3 and 6 span continuous guideways for this class of system can be constructed to reduce unit deflection and camber with no cost penalty in comparison to simple span guideways.

2.4.2 Support Structure Tradeoff Studies

In order to generate realistic cost estimates for the guideway system, studies of the support structure were conducted. Three parameters were considered which affect the substructure design and cost: (1) degree of restraint (connection) between beam and pier, (2) configuration of pier column and (3) foundation.

A rigid connection between the superstructure and supporting structure makes the whole structure behave as a unit which enhances the stability of the structure and also provides better resistance

TABLE 2.3: DEFLECTION, CAMBER AND COST FOR SIMPLE AND CONTINUOUS SPANS

	SPAN LENGTH Ft	UNIT DEFLECTION Inches		CAMBER: Inches		BEAM COST DOLLARS PER FOOT
		END SPAN	INTERIOR	END SPAN	INTERIOR	
DESIGN 3a SIMPLE SPAN	60	7.5×10^{-3}	7.5×10^{-3}	+ 0.20	+ 0.20	86
	80	19.8×10^{-3}	19.8×10^{-3}	+ 0.67	+ 0.67	97
	100	38.6×10^{-3}	38.7×10^{-3}	+ 1.62	+ 1.62	113
DESIGN 5 3-SPAN	60	3.3×10^{-3}	1.9×10^{-3}	+ 0.0	- 0.04	85
	80	8.5×10^{-3}	4.9×10^{-3}	+ 0.23	+ 0.02	95
	100	16.9×10^{-3}	9.7×10^{-3}	+ 0.82	+ 0.49	109
DESIGN 4a 6-SPAN	60	3.3×10^{-3}	1.9×10^{-3}	+ 0.0	- 0.04	85
	80	8.5×10^{-3}	4.9×10^{-3}	+ 0.23	+ 0.02	95
	100	16.9×10^{-3}	9.7×10^{-3}	+ 0.87	+ 0.49	109

against wind and earthquake loads. This type of monolithic construction is natural for cast-in-place concrete or structural steel, however it is not well suited for precast concrete elements since a cumbersome mechanical connection is required between the girder and pier. Therefore for the precast beams considered in this study, the beam is connected to the support pier by bearing pads and steel dowels.

Three types of 16 foot high piers were designed to support the superstructure. These designs and their resulting costs are summarized in Figure 2.6. The circular cast-in-place pier is the least expensive since with the use of fiber forms its labor and form costs are lower than the cast-in-place trapezoidal pier. The trapezoidal cast-in-place pier is somewhat more pleasing aesthetically than the circular pier, however, it requires the use of more extensive forms and thus costs more than the circular pier. The precast pier is almost twice the cost of the circular cast-in-place pier because the cost of transportation and erection are greater than the savings achieved from casting it in a plant. In addition, the mechanical connection of the pier to the foundation is relatively complex and allows the possibility for incomplete load transfer to the foundation. In the tradeoff studies cited in the following section the circular cast-in-place pier has been used since it is the most economical and provides a reliable pier-foundation connection.

For all of the design studies conducted in detail, it has been assumed that soil conditions permit the use of a cast-in-place concrete foundation. This type of foundation is commonly used for

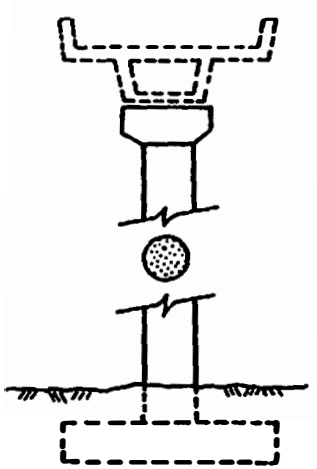

C.I.P. – ROUND COL.

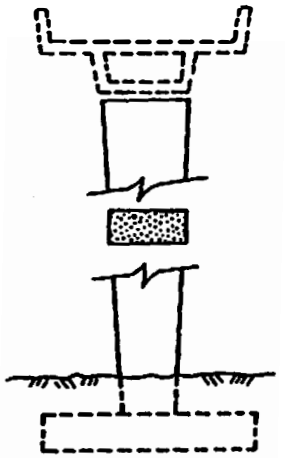

C.I.P. – TRAPEZOIDAL COL.

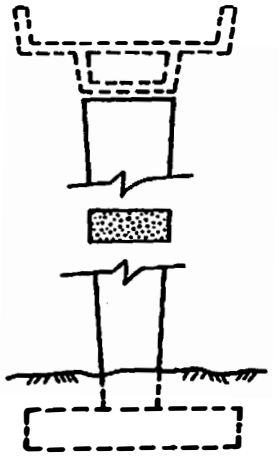

PRECAST – TRAPEZOIDAL COL.

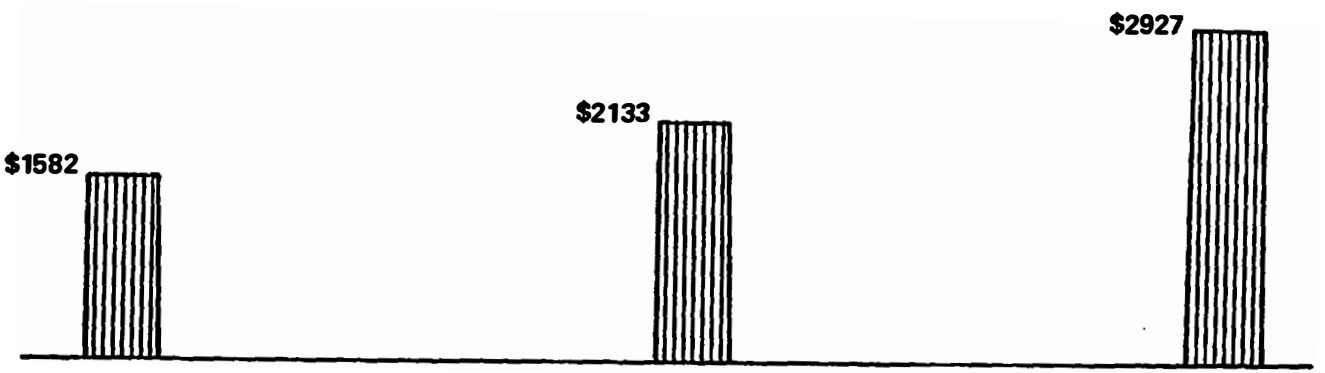

80 FT. SPAN – DESIGN 3 WITH SLOPING WALLS
(COST OF FOOTINGS NOT INCLUDED – CONSTANT)

FIGURE 2.6: PIER DESIGNS AND COSTS

good soil conditions.* If conditions are poor as is common with peat or clay, then a pile foundation may be required. The additional cost of employing a pile foundation and the fraction of foundation costs in comparison to superstructure costs are summarized in Figure 2.7. These data show that the pile foundation increases the cost by $47 per foot for the 80 foot simple span guideway in comparison to the concrete; however, foundation plus pier costs are only about 30% of the total cost and the superstructure represents the most significant cost item.

2.5 Baseline Designs and Cost Summary

Designs have been performed for simple and continuous 60, 80, and 100 foot spans to accommodate the small and large GRT vehicles. The designs include structures constructed from AASHTO beams (1) and straightsided box beams (2a) for which the section depth is increased as the span length increases from 60 to 80 to 100 foot in length as well as designs (2, 3a and 4-7) which use the same section depth for all span lengths but use a reduced number of prestressing cables for shorter spans. Designs 3a through 7 represent the tapered box beams constructed with permanent exterior and fiber interior forms which form the basis for the large and small guideway recommended designs. All designs are based upon a round cast-in-place pier and spread footing. The structural properties of the designs are summarized in Table 2.4.

The cost of these designs have been calculated assuming that standard construction tolerances are met in both plant and field fab-

*Prior to construction borings are taken and analyzed to determine soil properties such as bearing capacity.

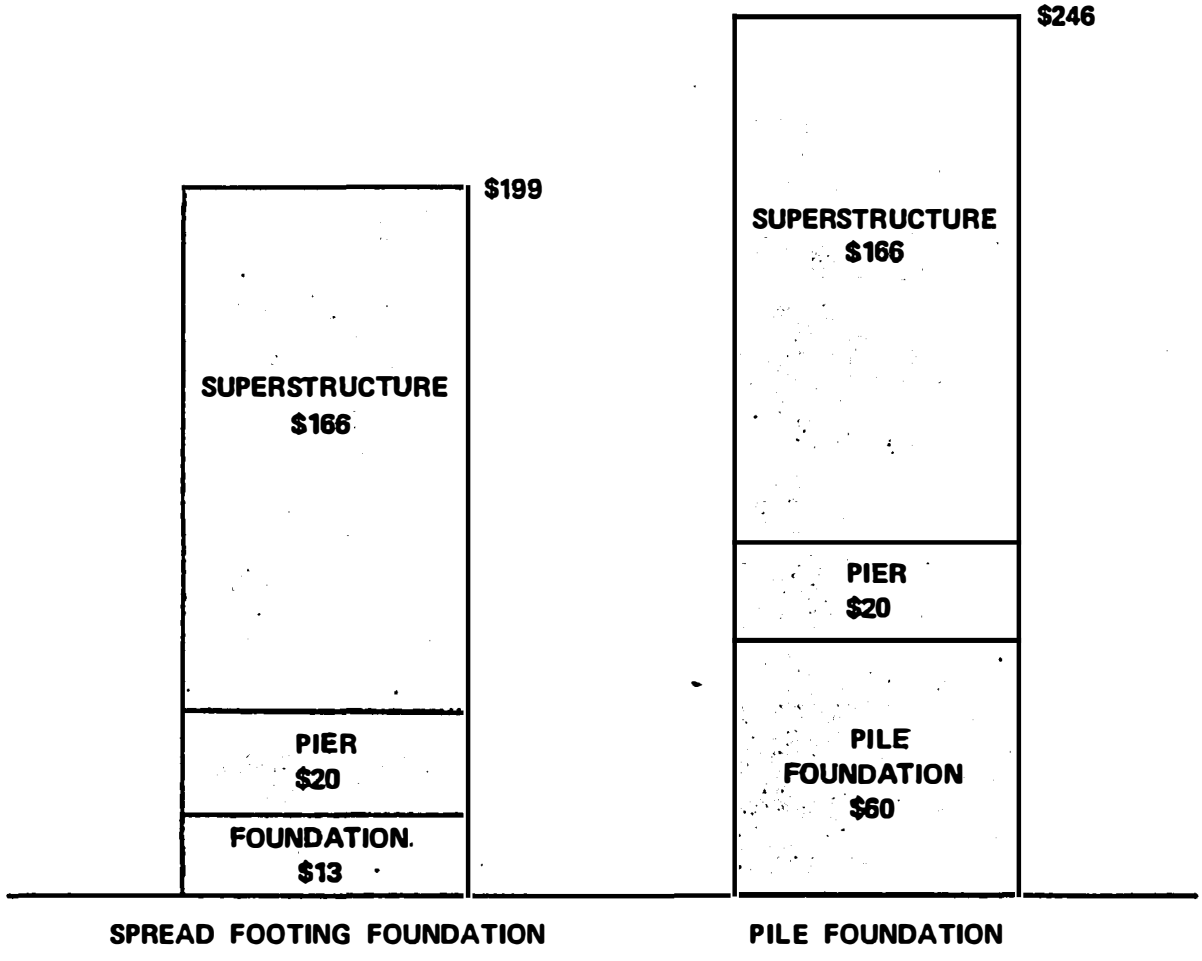

80 FT. SPAN – DESIGN 3 WITH SLOPING WALLS

FIGURE 2.7: COST BREAKDOWN BY STRUCTURAL COMPONENTS

rication. The standard levels of tolerance have been established by consulting field fabricators, prestressed concrete manufacturers and tolerance specifications of the Prestressed Concrete Institute [17]. The specifications are summarized in Table 3.2 of Section 3 in terms of guideway parameters which influence ride quality. Variations of tolerance levels from these baseline values are considered in Section 4.

The costs for the designs are summarized in Figure 2.8. These data show that:

(1) For every design, the costs increase with increasing span length. The superstructure cost, which represents more than 70% of the total structure cost, increases faster than the pier and foundation costs decrease as span length is increased. The minimum cost span length is the 60 foot span.* For the large guideway simple span design 3a, the 100 foot span design is a factor of 1.11 more expensive than the 60 foot span.

(2) For a given span length, the tapered box, using permanent exterior and fiber interior forms yields a minimum cost structure. For the 100 foot simple span large guideway, the straight box design 2 is a factor of 1.15 and AASHTO I-beam design 1 is a factor of 1.36 more expensive than design 3a.

(3) For a given span length, the cost of constructing a guideway with live load continuity varies very little from simple span construction, i.e., costs of a 3 or 6 span continuous structure are within 3% of the simple span costs.

(4) The small vehicle guideway design for any given span length is about 75% of the cost of the large vehicle guideway partially because of its reduced width and partially due to the lighter live load which must be accommodated.

---

*Structural costs would decrease somewhat below the 60 foot span cost, if spans were made shorter. However, as the span length is decreased further a point is finally reached for which costs begin to increase.

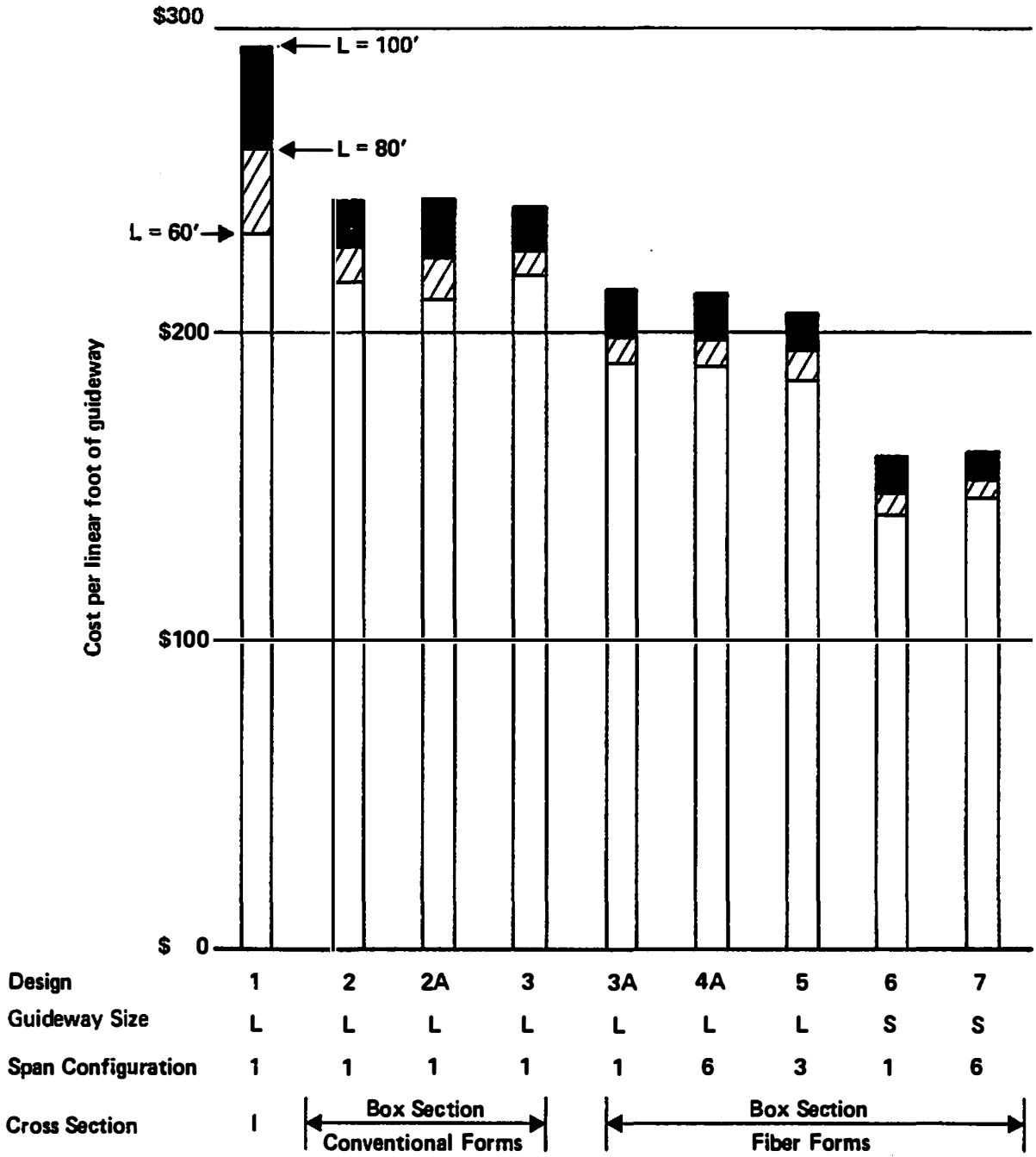

FIGURE 2.8: DESIGN COST SUMMARY

The distribution of costs for these designs is summarized in Figure 2.9 and indicates about 50% of the total cost is attributed directly to labor, while only 34% is attributed to material, with the remaining allocated to transportation and erection. Thus, the cost of installing a guideway is strongly dependent upon local labor costs.

The designs summarized in Table 2.4 and Figure 2.8 provide the definition of basic structures for ride quality analysis. These designs represent large guideways with structural costs of approximately 1.05 million dollars per mile and small guideways with structural costs of approximately $820,000 per mile.

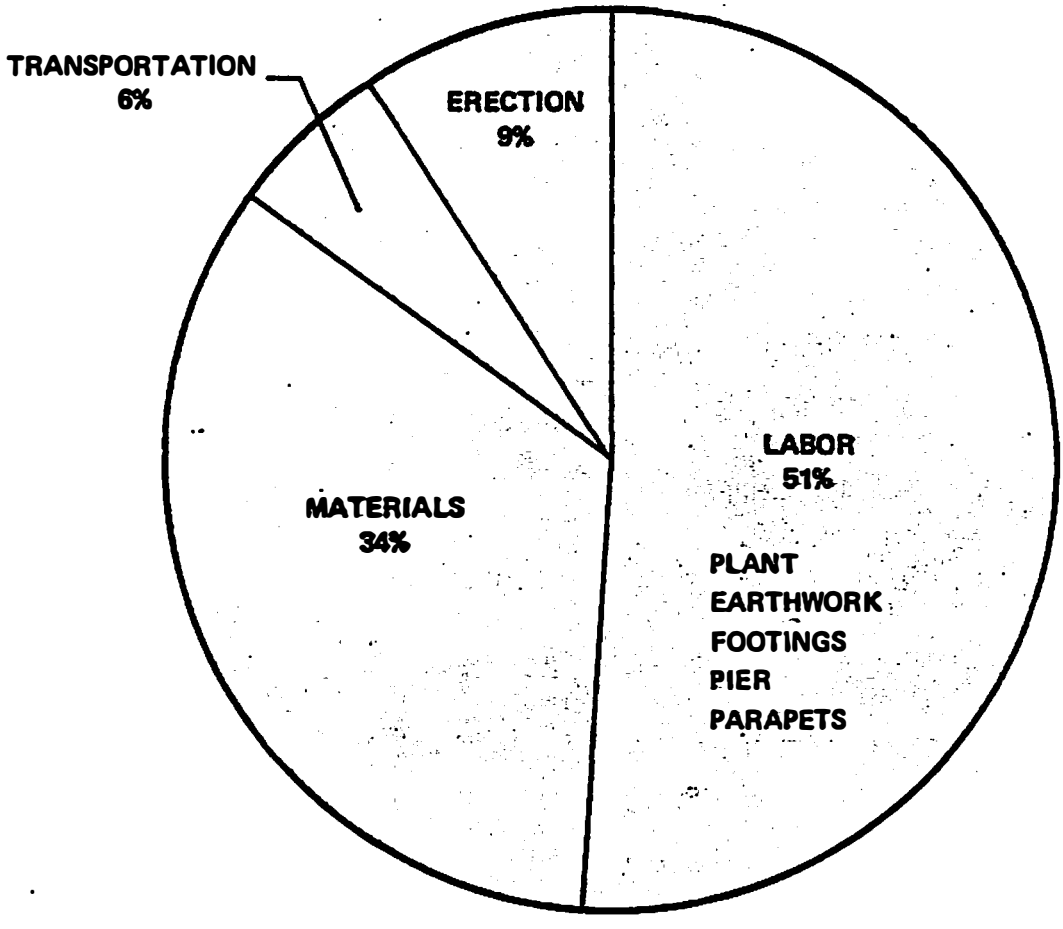

80 FT. SPAN – DESIGN 3 WITH SLOPING WALLS

FIGURE 2.9: DISTRIBUTION OF GUIDEWAY COSTS

TABLE 2.4: SUMMARY OF SPAN DESIGN STRUCTURAL PROPERTIES

DESIGN	SPAN LENGTH Ft	AREA In^2	INERTIA In^4	CAMBER: Inch	
				End Span	Interior
1	60	738	101,960	N.C.	N.C.
1	80	1120	250,780	N.C.	N.C.
1	100	1578	521,460	N.C.	N.C.
2	60	1524	287,766	+0.23	+0.23
2	80	1524	287,766	+0.81	+0.81
2	100	1524	287,766	+2.04	+2.04
2a	60	1333	80,044	+0.86	+0.86
2a	80	1399	148,919	+1.51	+1.51
2a	100	1524	287,766	+2.04	+2.04
3a	60	1557	258,684	+0.20	+0.20
3a	80	1557	258,684	+0.67	+0.67
3a	100	1557	258,684	+1.62	+1.62
4a,5	60	1557	258,684	+0.00	-0.04
4a,5	80	1557	258,684	+0.23	+0.02
4a,5	100	1557	258,684	+0.82	+0.49
6	60	1126	192,859	+0.19	+0.19
6	80	1126	192,859	+0.77	+0.77
6	100	1126	192,859	+1.58	+1.59
7	60	1126	192,859	+0.08	+0.03
7	80	1126	192,859	+0.36	+0.16
7	100	1126	192,859	+1.00	+0.69

N.C. = not calculated

Material Properties

Elastic Modulus = 4×10^6 lb/in^2 Unit Weight = 150 lb/ft^3

3. RIDE QUALITY ANALYSIS

3.1 Ride Quality Measurement

In this chapter the performance measures and specific vehicle-guideway models used to determine the ride quality performance of baseline vehicle-guideway systems are summarized.

While ride quality is difficult to define precisely and its quantitative definition is the subject of a number of current research efforts, many of the useful indices developed through past research [18] have measured ride quality in terms acceleration* perceived by a passenger in one or several orthogonal directions. One of the commonly used specifications has been issued by the International Organization for Standardization - the ISO ride quality specification for vertical, lateral and longitudinal motion [19]. In this study the ISO lateral and vertical specifications are used respectively as the principal means of assessing vehicle-guideway system ride quality in the lateral and vertical planes of motion.

The detailed ISO specifications are displayed in Figures 3.1 and 3.2. In the specification the acceleration time history at a point on the vehicle is analyzed to determine the rms accelerations in prescribed 1/3 octave frequency bands. These resultant accelerations are compared with the ISO reduced comfort criteria illustrated in the figures which are given as a series of curves with time in minutes as

*In some instances jerk, the first derivative of acceleration with respect to time has also been used.

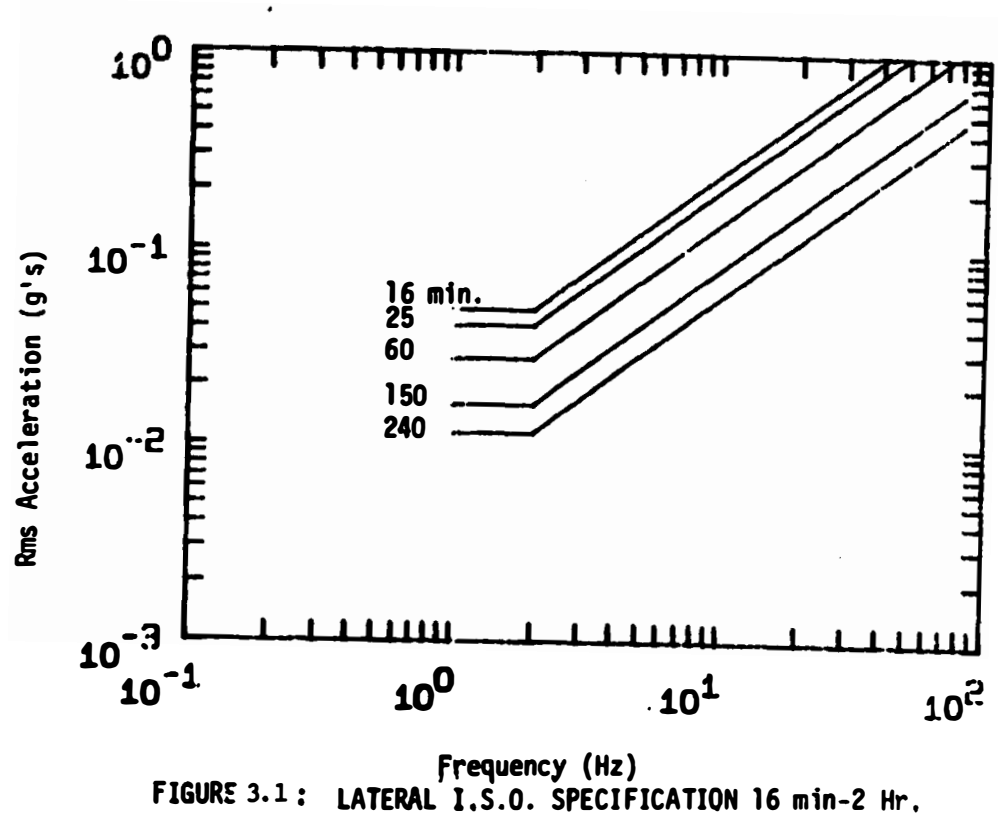

FIGURE 3.1 : LATERAL I.S.O. SPECIFICATION 16 min-2 Hr.

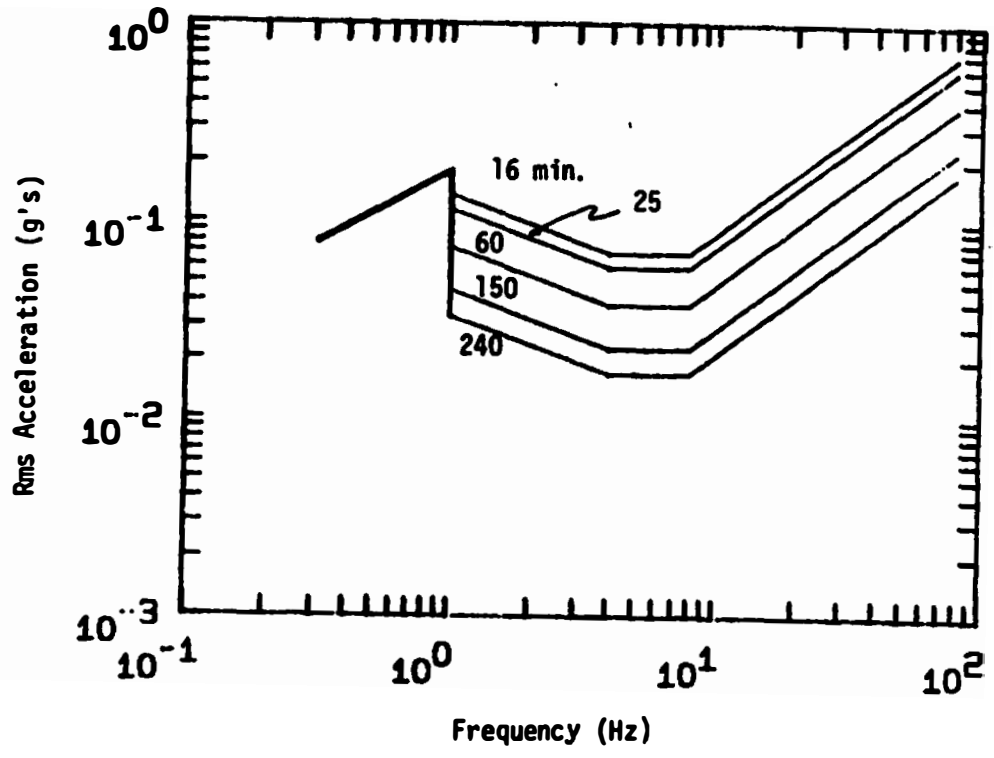

FIGURE 3.2: VERTICAL I.S.O. SPECIFICATION 16 min-2 Hr.

a parameter. If the vehicle accelerations lie just below the 16 minute curve then the vehicle is said to meet the ISO 16 minute reduced comfort criteria, while if they lie just below the 60 minute curve then the vehicle is said to meet the ISO 60 minute reduced comfort criteria. As the number of minutes in the criteria increases the general level of acceleration is reduced.

The reduced comfort curves for the lateral direction have a minimum in the 1-2 hertz range while the curves for the vertical direction have a minimum in the 4-8 hertz range to reflect the influence of frequency and direction upon the physiological aspects of discomfort. Also in the vertical direction, a low frequency extension curve for motions below 1.0 hertz is shown which has been proposed to limit the tendency for low frequency motion sickness.

In addition to the detailed ISO ride quality criteria, for a number of general parametric studies, total rms acceleration in either the vertical or lateral motion plane has been used to establish general trends.

3.2 Vehicle-Guideway Model

Vehicle-guideway analytical models have been formulated so that the lateral and vertical plane ride quality of a system may be computed from the guideway structural specifications, construction tolerances and vehicle specifications.

3.2.1 Guideway Representation

The guideway is represented as providing a vertical support surface and a lateral guidance surface to the vehicle. The vertical support surface is assumed to be uniform across the guideway width* and to be represented by the profile:

$$y_t(x,t) = y_s(x) + y_d(x,t) \tag{3.1}$$

where:
- y_t = total vertical profile
- y_s = static vertical profile
- y_d = dynamic vertical profile
- x = distance along guideway
- t = time

The lateral profile presented is assumed to consist only of a static component since deflection of the sidewall due to vehicle steering reference loads is negligible.

$$Z_o(x) = Z_s(x) \tag{3.2}$$

where:
- Z_o = total lateral profile
- Z_s = static lateral profile

The static profile of the guideway generated during construction may be decomposed into four basic types of irregularity which are related to construction practice as shown in Figure 3.3:

(1) Joint offset in which a discontinuity is generated between two adjacent spans.

(2) Angular misalignment in which the two end points of a span are offset from a straight datum.

---

*Vehicle roll motion is not excited.

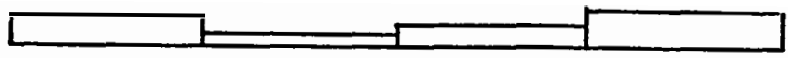

LATERAL AND VERTICAL
JOINT OFFSET

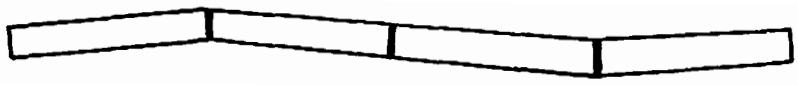

LATERAL AND VERTICAL
ANGULAR MISALIGNMENT

VERTICAL CAMBER

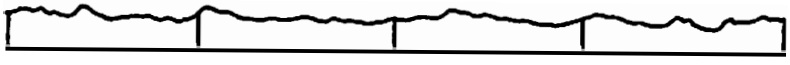

LATERAL AND VERTICAL
LOCAL SURFACE ROUGHNESS

FIGURE 3.3: CONSTRUCTION GENERATION SURFACE PROFILE IRREGULARITIES

(3) Camber deviation in which a span assumes a major camber curvature.

(4) Surface roughness in which local irregularities generate a rough local surface.

In the construction process, each of these four quantities varies from span to span. Thus, the guideway model assumes that each of the measurable quantities varies randomly and a model is adopted in which the vertical static plane is represented by:

(1) Vertical joint offset as a random variable with a uniform probability density contained between tolerance levels $\pm \varepsilon_o$.

(2) Span vertical angular misalignment is represented by pier height variation which is a random variable with a uniform probability density between tolerance levels $\pm \varepsilon_{\hat{n}}$. This irregularity may be considered from a fixed datum or from a datum in which each new value is referenced to the previous pier height.

(3) Surface roughness in which the local surface roughness amplitude is a Gaussian random variable whose amplitude is specified by measuring the maximum deviation under a ten foot straight edge laid along the guideway.

(4) Camber in which the midspan amplitude of the camber shown is represented by a random variable with uniform distribution between the tolerance levels $\pm \varepsilon_c$ with respect to a mean camber amplitude. The camber shape and mean camber amplitude are determined from structural analysis of the beam.

The lateral static plane profile is represented in a manner analogous to the vertical and consists of lateral joint offset, lateral span angular misalignment and lateral surface roughness.* The total vertical and lateral static profiles are generated by summing together the contributions of the random functions listed above as described in [7].

*Camber is not present in the lateral surface profile.

Guideway dynamic deflections in the vertical plane $y_d(x,t)$ are generated by the vehicle traversing a span. The guideway dynamic deflection is computed using a modal analysis technique described in Appendix C. In the analysis the assumption is made that the vehicle loads on the guideway are the traveling constant vehicle static axle loads and the vehicle inertial loads due to vertical accelerations are neglected compared to vehicle weight.*

3.2.2 Vehicle Representation

The motion of the rubber-tired GRT vehicle traveling along the guideway is represented as two independent, uncoupled vehicle motions - (1) a vertical plane motion excited solely by the guideway vertical profile $y_t(x,t)$ and a lateral plane motion excited solely by the guideway lateral profile $Z_t(x)$. The vertical motion vehicle model is a four degree of freedom model illustrated in Figure 3.4. The model includes vehicle sprung mass heave and pitch, unsprung front and rear suspension masses, and primary tire stiffness as well as secondary suspension stiffness and damping. The dynamic equations describing this model are summarized in Appendix C.

The lateral motion model is illustrated in Figure 3.5 where vehicle yaw and lateral motion are the two degrees of freedom represented. Vehicle roll motion induced by lateral steering (roll-steer effect) has been neglected since for prototype GRT vehicles it is desirable and practical to eliminate roll-steer effects by inherent

*For vehicles which meet good ride quality standards, the accelerations are typically less than 0.1g and vehicle inertia loads may be neglected in comparison to weight, in computing guideway deflections.

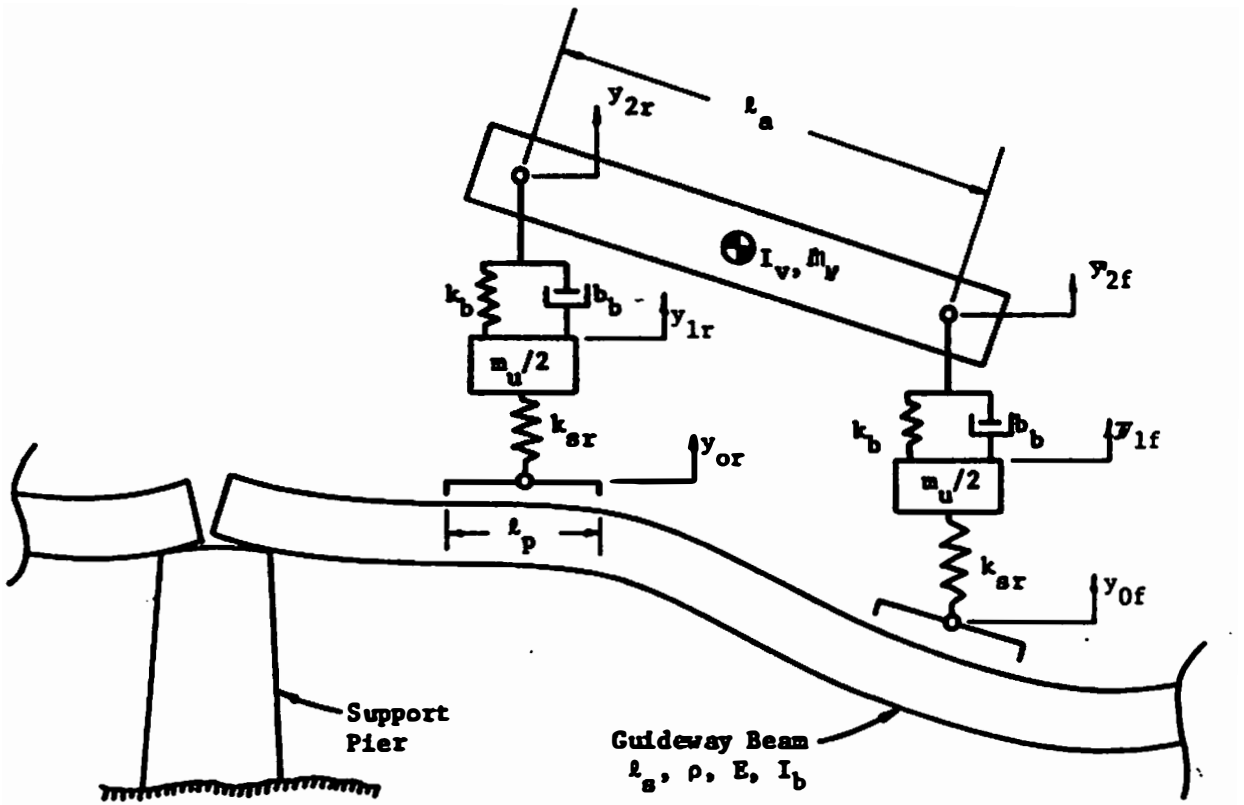

FIGURE 3.4: VERTICAL PLANE VEHICLE MODEL

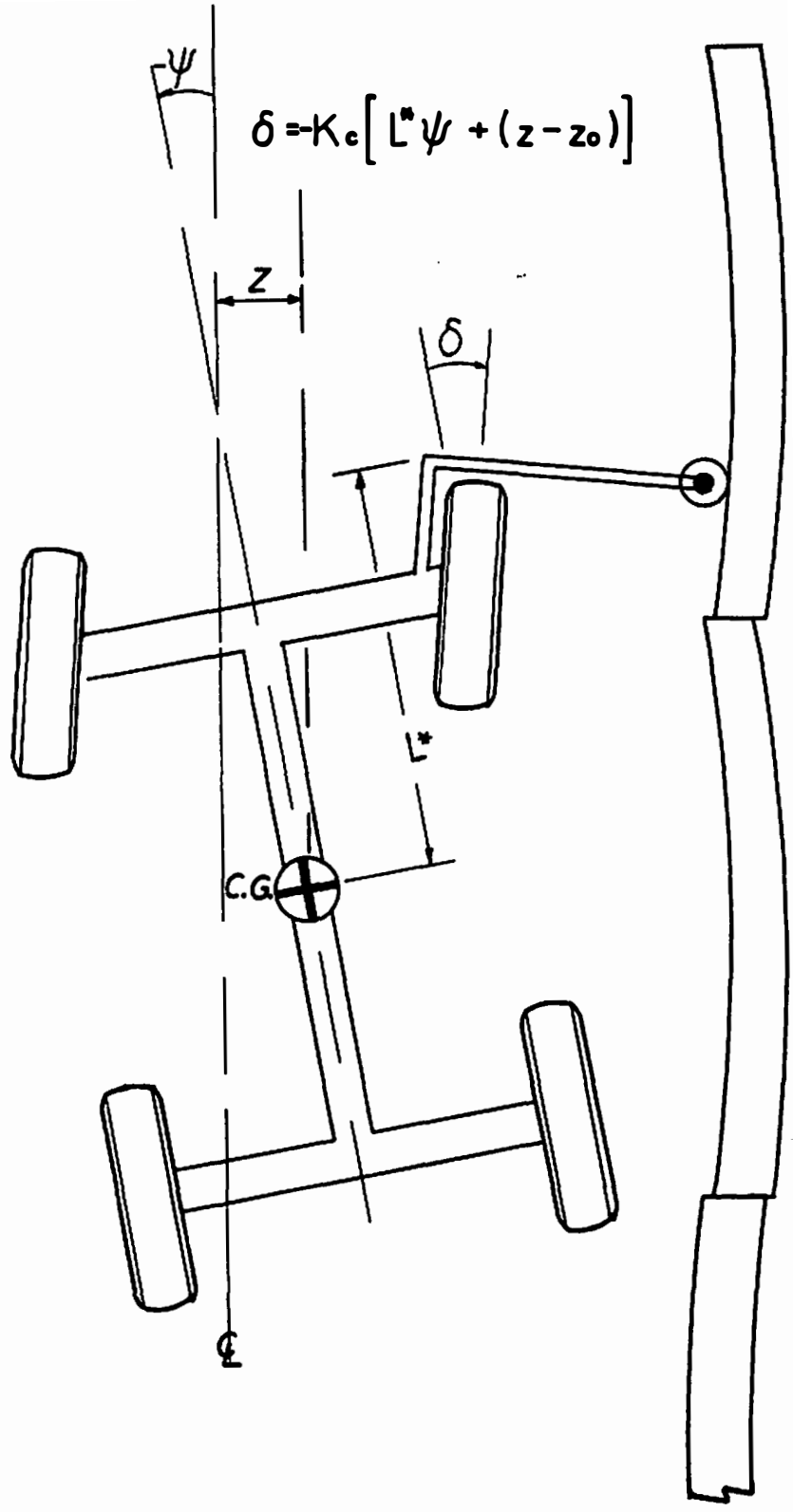

FIGURE 3.5: LATERAL PLANE VEHICLE MODEL

vehicle suspension design. In the model the vehicle restoring forces are generated by tire lateral forces which are assumed to increase linearly with tire slip angle. The vehicle is guided with a sensor arm which steers the front axle wheels with steering angle δ in response to the measured lateral error between a point on the vehicle and the guidepath:

$$\delta = -K_c[(L^* \psi + (Z - Z_o)] \tag{3.3}$$

where: δ = steering angle

K_c = steering gain

L^* = sensor location in front of vehicle center of mass

ψ = vehicle yaw angle

Z = vehicle lateral displacement

Based upon the detailed study of lateral vehicle dynamics summarized in Appendix C where the lateral dynamic equations are summarized, values of steering gain K_c and sensor location L^* have been selected to provide a good working compromise between ride quality and tracking error. As reference [20] has shown, when L^* is located at the front of the vehicle as K_c is increased the vehicle tracking error decreases and the rms lateral acceleration increases. Thus, a value of K_c must be selected which provides a good compromise between tracking error* and relative acceleration.

3.2.3 Summary of Ride Quality Computation Techniques

Two primary ride quality computation techniques may be

*Large tracking errors are undesirable since the guideway lane width would have to be increased to accomodate large vehicle lateral excursions from the nominal path.

developed from the guideway and vehicle analytical models described above-the time domain and direct frequency domain techniques illustrated in Figure 3.6. In the time domain technique, a static guideway profile is synthesized using a random number generator. This static profile is then superimposed on the guideway dynamic profile generated by a vehicle passage and input to the vehicle. The vehicle time history accelerations and other motions are computed simultaneously with the guideway dynamic motions through numerical integration of the vehicle-guideway system differential equations. The acceleration time histories, which are similar to the experimental time histories which would be recorded on a test vehicle, are then analyzed using Fast Fourier Transfer (FFT) techniques to determine the rms accelerations in 1/3 octave frequency bands as prescribed by ISO. This type of analysis is applicable to either linear or nonlinear vehicle-guideway models.

For systems which are linear and in which the guideway equations may be partially decoupled from the vehicle equations (as is the case when the influence of vehicle inertial acceleration forces are neglected in comparison to vehicle weight in computing guideway loads) a direct frequency domain computation of rms accelerations is possible. In this method, the guideway random irregularities are represented by spectral densities and the guideway mean camber and dynamic deflection profile, which are deterministic, by Fourier series. Then with the vehicle models represented in transfer function form, the output vehicle accelerations in each frequency band

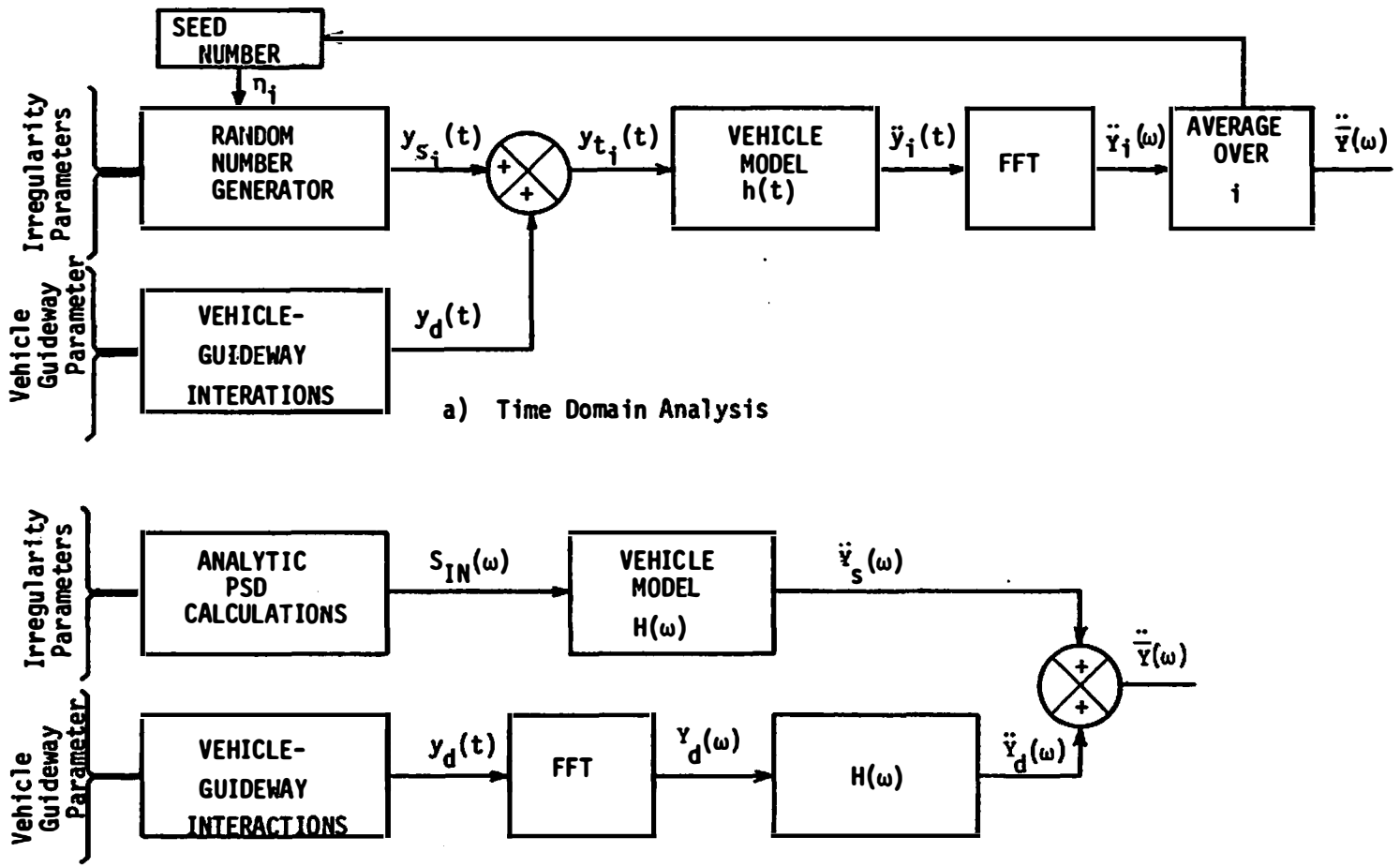

b) Frequency Domain Analysis

FIGURE 3.6: TIME AND FREQUENCY ANALYSIS TECHNIQUES

may be computed directly and the total rms acceleration computed by summing the contributions in an appropriate manner over all frequencies. This frequency domain analysis technique is described in Appendix C. Since it provides results in much shorter computation times than the time domain analysis technique, it is used in this study for computation of rms accelerations. In reference [7], the rms acceleration in 1/3 octave bands computed for the vehicles described above are shown to be equal when computed using either the time domain or frequency domain methods.

3.3 Summary of Baseline Vehicle-Guideway Parameters

A number of parameters require specification to define the vehicle-guideway system for ride quality analysis. The baseline small and large GRT vehicle parameters are summarized in Table 3.1, while the guideway construction tolerances are summarized in Table 3.2. These baseline vehicle-guideway parameters are used unless otherwise specified in the discussion of specific results.

3.4 Influence of Guideway Static Irregularities on Ride Quality

In this section the influences of vertical and lateral random guideway static irregularities on ride quality are determined, including the effects of vertical and lateral joint offset, angular misalignment and surface roughness as well as random vertical camber deviation.* First the vertical irregularities are considered in terms

*Beam deflection and deterministic camber are considered in a following section.

TABLE 3.1: BASELINE VEHICLE PARAMETERS

	PARAMETER	SMALL VEHICLE	LARGE VEHICLE
VERTICAL	Weight: lbs	10,000	20,000
	Length x Width: ft x ft	15 x 7	22 x 9
	Wheelbase: ft	12	19
	Sprung Mass Frequency: Hz	1.0	1.0
	Inertia Ratio, $\bar{I}_v$	1.0	1.0
	Unsprung to Sprung Mass Ratio, M_u	0.25	0.25
	Primary to Secondary Suspension Ratio	10.0	10.0
	Suspension Damping Ratio, ξ_v	0.25	0.25
LATERAL	C.G. to Front Axle Distance: ft	6.0	9.5
	C.G. to Rear Axle Distance: ft	6.0	9.5
	Yaw Moment of Inertia, I_y: lb-ft-sec^2	5065	20,900
	Front Axle Total Tire Stiffness: lb/rad	38,200	38,200
	Rear Axle Total Tire Sitffness: lb/rad	38,200	38,200
	Distance from C.G. to Sensor, L^*: ft	7.5	11.0
	Steering Gain: K_c, rad/ft	0.3	0.3

TABLE 3.2: BASELINE CONSTRUCTION TOLERANCES

		JOINT OFFSET	ANGULAR	DEVIATION UNDER 10 FOOT STRAIGHT EDGE	CAMBER
VERTICAL	CONSTRUCTION TOLERANCE ε: Inches	0.25	0.5	0.125	0.5
	STANDARD DEVIATION σ: Inches	0.144	0.289	0.042	0.289
LATERAL	CONSTRUCTION TOLERANCE ε: Inches	0.25	0.33	0.125	——
	STANDARD DEVIATION σ: Inches	0.144	0.289	0.042	——

of the amplitude power spectral density (PSD) of each individual irregularity.

VERTICAL PROFILE STATIC IRREGULARITY RESPONSE

The total static vertical irregularity power spectral density consists of four irregularity types. Camber variations are due to inaccurate prestressing techniques and are assumed to have a mid-span deviation of 0.5 inches or less from the mean camber shape. The camber deviation irregularity has a characteristic wavelength, ℓ_s, which is equal to the span length of the guideway and may be scaled as guideway span length is altered. Angular misalignment in the vertical plane is represented as a variation from one pier height to the next. The tolerance for the successive pier misalignment is assumed to be 0.5 inches and its characteristic wavelength is also equal to the span length. Surface roughess is assumed to be limited to an eighth inch under a ten foot chord as described in detail in Appendix C. Vertical joint offset occurs only at beam ends and therefore has a characteristic wavelength which is a function of the number of spans per beam. The construction tolerance for the joint offset is 0.25 inches.

The amplitude PSD of each irregularity for baseline construction tolerances on a 60 foot simple span system is plotted versus spatial frequency, $\Omega/2\pi = 1/\lambda$, (λ = wavelength) in Figure 3.7. These data show that at long wavelengths $\lambda > 150$ ft angular deviations dominate, while in the region $150 > \lambda > 25$ ft camber and joint offset dominate and for $\lambda < 25$ ft surface roughness and joint offset dominate.

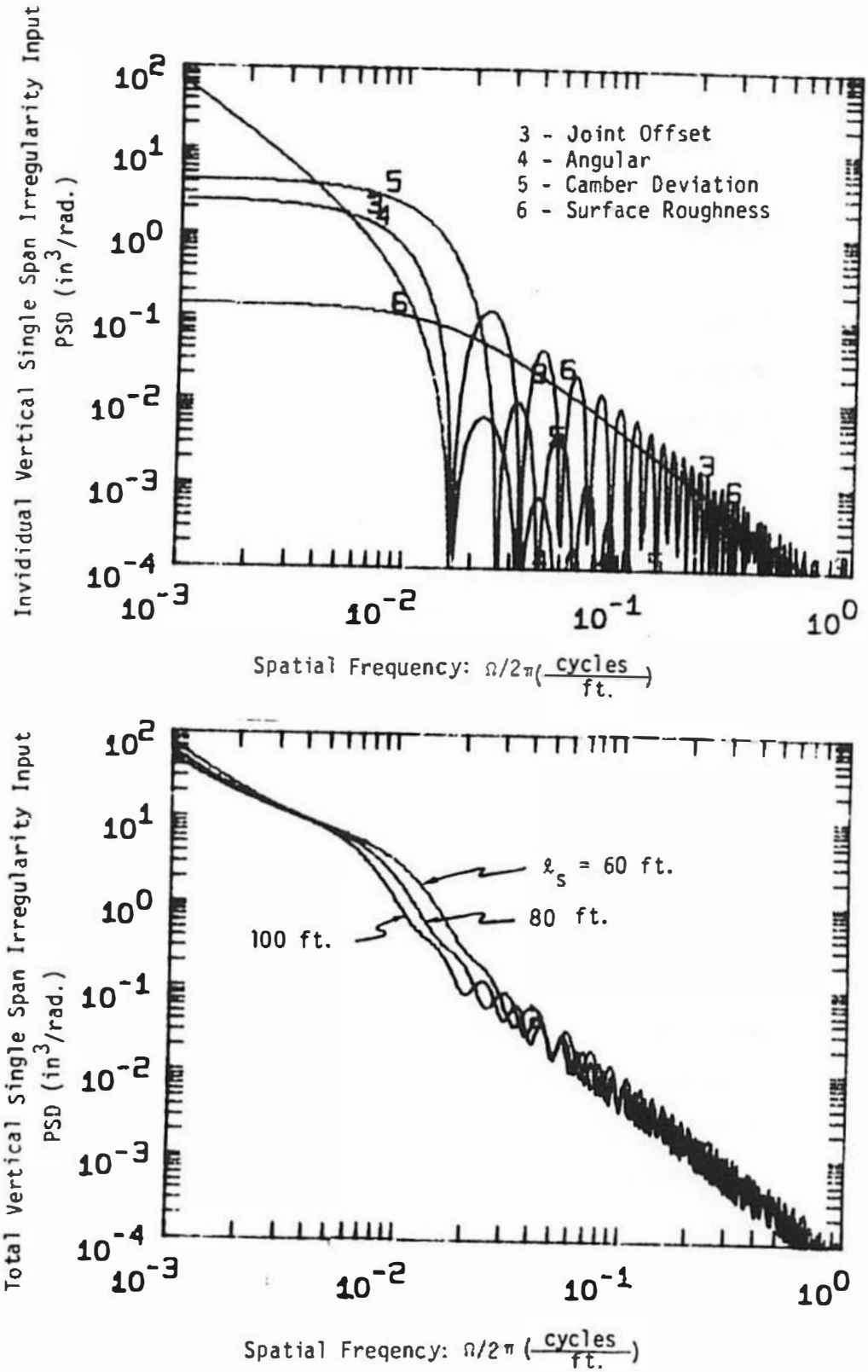

FIGURE 3.7: VERTICAL SINGLE SPAN DIMENSIONAL IRREGULARITY INPUT PSD

The total power spectral density due to the sum of irregularities is also plotted in Figure 3.7 for 60, 80 and 100 foot simple spans.

This plot shows that only in the range $150 < \lambda < 50$ feet do the PSD's for the three span lengths differ with the shorter spans having greater amplitude and that overall the PSD's for all three span lengths may be approximated by the form:

$$\phi_v = \frac{A}{\Omega^2} \tag{3.4}$$

where: ϕ_v = vertical static irregularity PSD

A = roughness factor $\simeq 1.2 \times 10^{-6}$ ft-rad*

Ω = wavenumber - radian/ft

To determine the relative influence of each irregularity to vehicle acceleration, the small and large vehicle front and rear vertical accelerations in 1/3 octave frequency bands were computed for the vehicle traveling at 60 mph across 60 ft simple spans. These data are compared in Figures 3.8 and 3.9 with the ISO 25 minute specification and show that in both cases, angular misalignment generates accelerations which are small compared to those generated by surface roughness, joint offset and random camber. The data also show for this speed that camber has a major contribution in the 1 hertz frequency range corresponding to the secondary suspension natural frequency for both vehicles while joint offset has a major contribution in 6-8 hertz range corresponding to the suspension unsprung mass natural frequency of both vehicles. Surface roughness has major con-

*This roughness level is equivalent to that measured on the tracked air cushion guideway in Pueblo, Colorado.

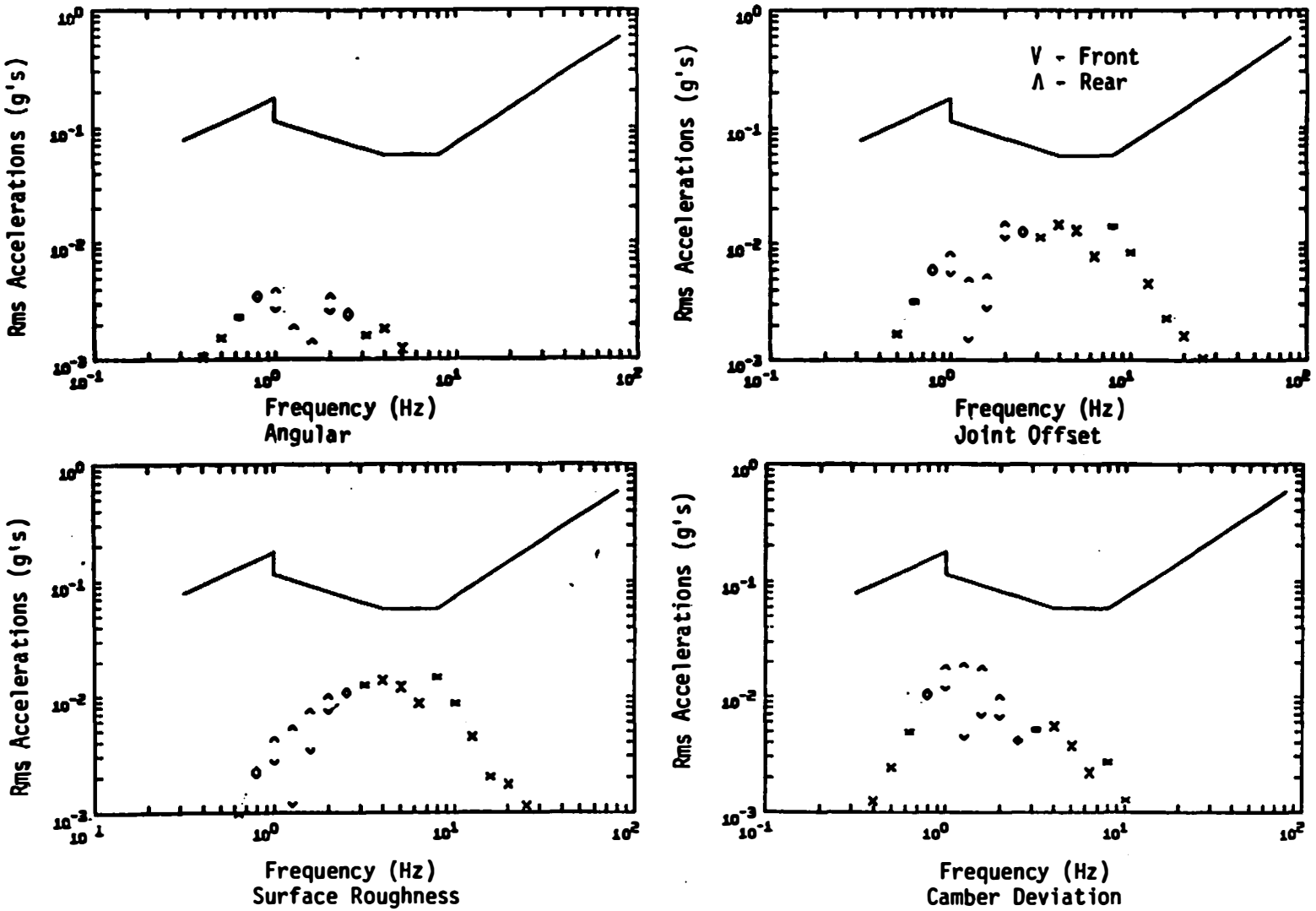

FIGURE 3.8: SMALL VEHICLE VERTICAL I.S.O. SINGLE SPAN RESPONSE TO SEPARATE IRREGULARITIES
60 FOOT SPAN LENGTH, 60 MPH

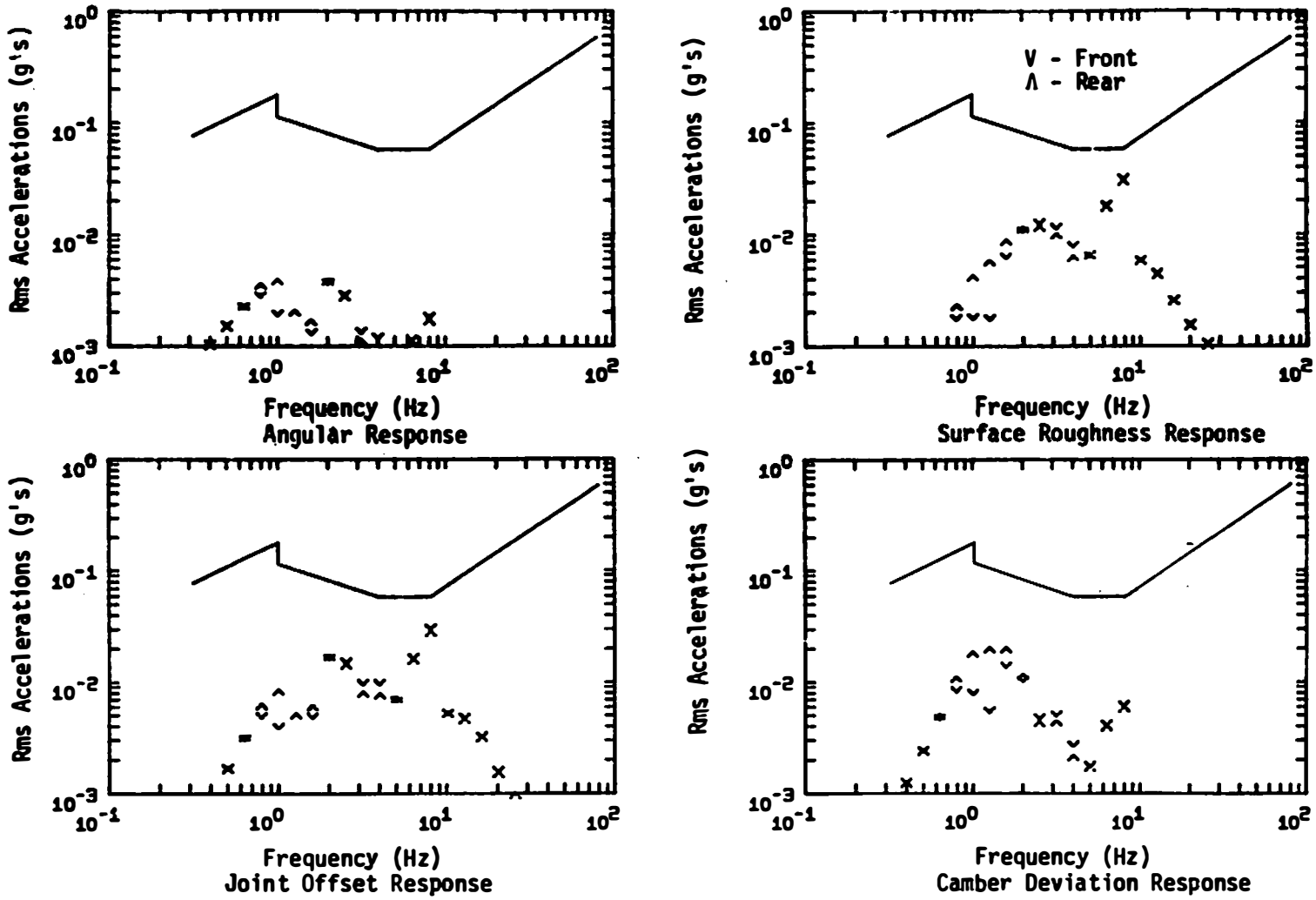

FIGURE 3.9: LARGE VEHICLE VERTICAL I.S.O. SINGLE SPAN RESPONSE TO SEPARATE IRREGULARITIES
60 FOOT SPAN LENGTH, 60 MPH

tributions in the 2-8 hertz range for the small vehicle and in the 6-8 hertz range for the large vehicles.

A summary of the individual irregularity results are shown in Figure 3.10 where for each irregularity the following are tabulated:

(1) The level of baseline tolerance used to compute vehicle accelerations

(2) The level of irregularity tolerance which can be used to meet a 25 minute ISO ride quality criteria for the small and large vehicles.

These data show that when each irregularity is considered individually, the angular and camber irregularity tolerance could be increased significantly while joint offset and surface roughness could be increased only moderately before the 25 minute ISO specification is exceeded. These data show that since the angular irregularity does not influence ride quality as strongly as the other types of irregularities, its baseline tolerance level could be increased with little degradation of ride quality.

Figure 3.11 summarizes response data of the small and large vehicles to a vertical static profile which is the sum of all the baseline static irregularities. Both vehicles meet a 25 minute ISO specification when operating at 60 mph. The large vehicle response is a maximum at 6-8 hertz which is a resonance due to unsprung mass vibration. In the small vehicle the unsprung mass natural frequency is identical to the large vehicle, however at 60 mph speed, the vehicle has a pitch cancellation frequency due to the length between the front

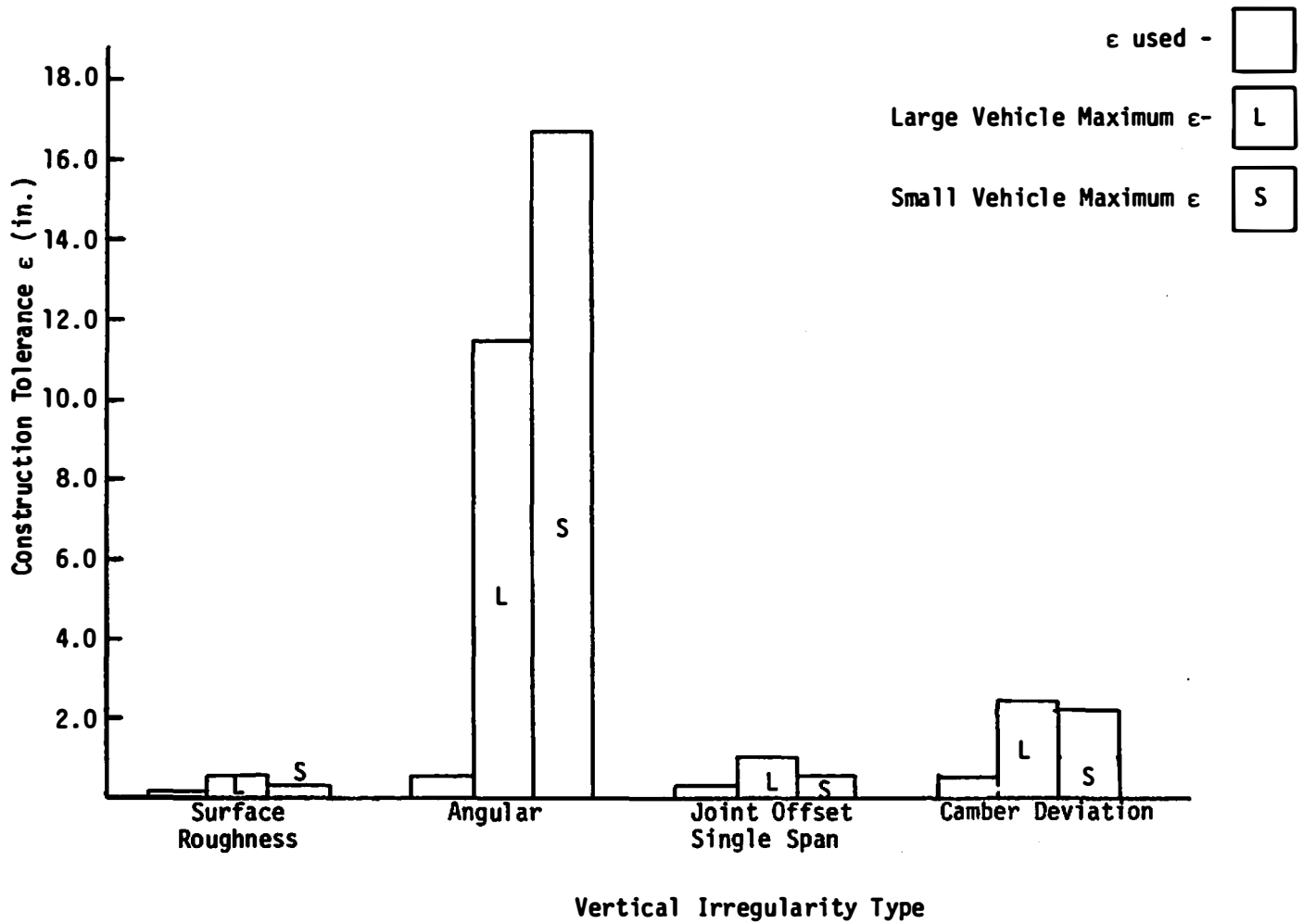

FIGURE 3.10: MAXIMUM VERTICAL CONSTRUCTION TOLERANCE TO MEET 25 MINUTE I.S.O. SPECIFICATIONS

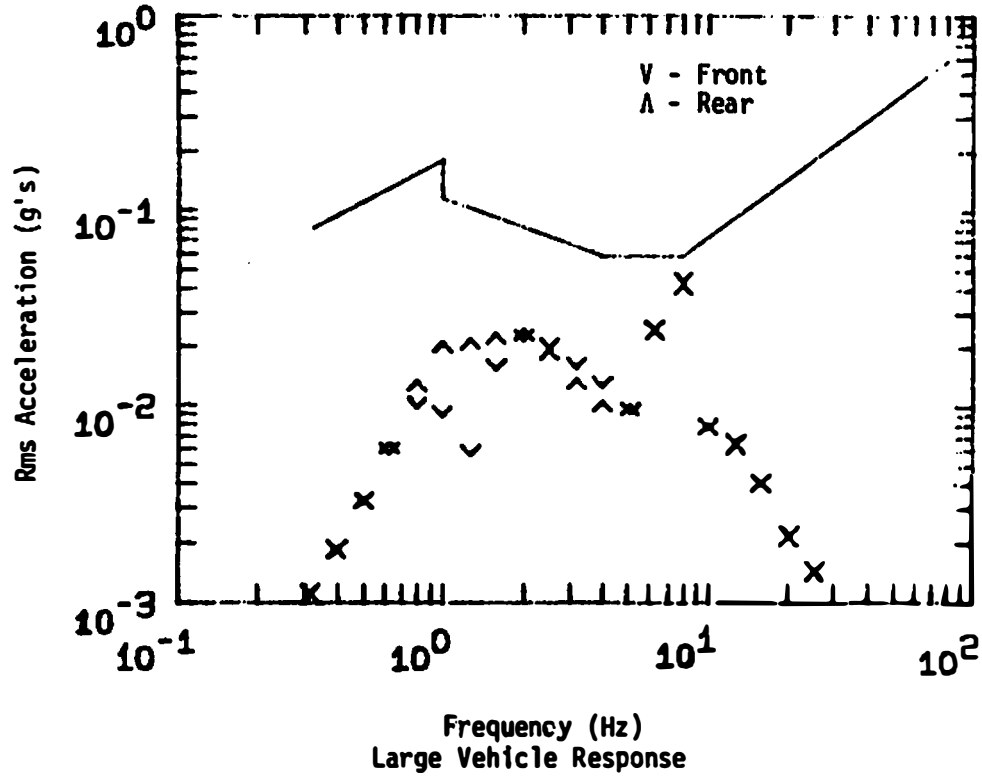

Large Vehicle Response

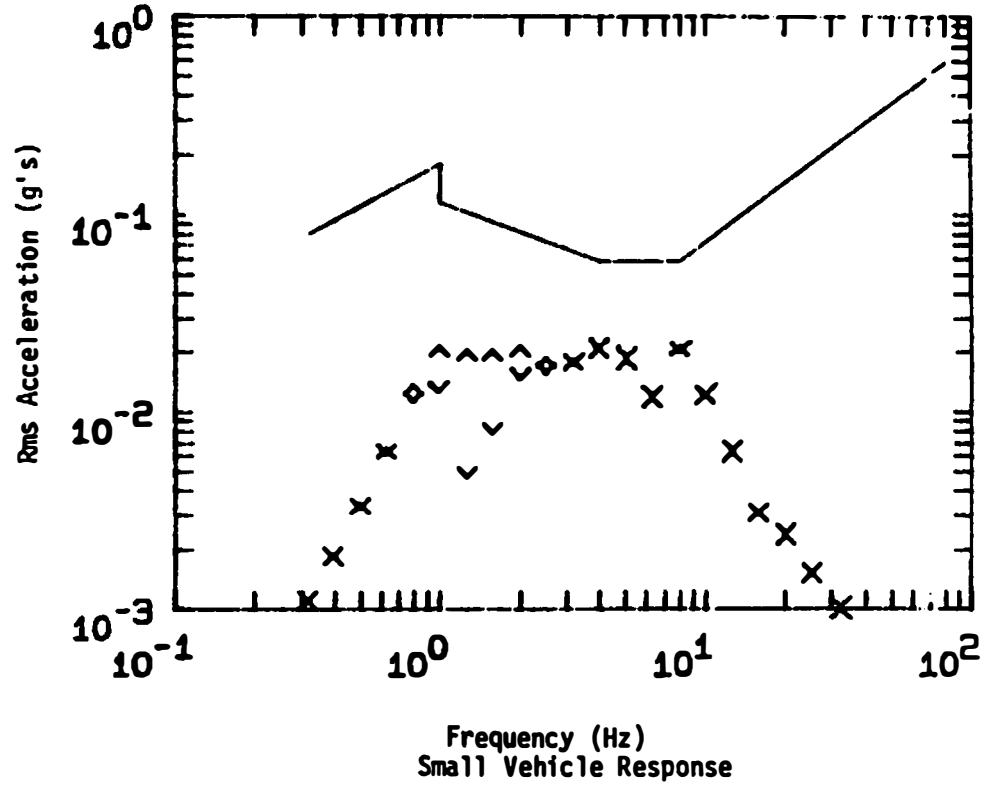

Small Vehicle Response

FIGURE 3.11: LARGE AND SMALL VEHICLE IRREGULARITY I.S.O. RESPONSE
60 ft. SPAN LENGTH, 60 MPH

and rear suspensions of $f_p = v\ell_a \simeq 8$ hertz which counteracts the unsprung mass amplification effect.

LATERAL PROFILE STATIC IRREGULARITY RESPONSE

In the lateral profile joint offset is assumed to be within $\pm$ 1/4 inch at beam joints while the maximum angular misalignment error allowed is one third inch, and is measured relative to the mean guidewall position, which is a fixed datum. Surface roughness measured by the midchord deviation from a ten foot straight edge is limited to an eighth of an inch.

The individual lateral irregularity PSD's are plotted in Figure 3.12, for baseline values of tolerance for a 60 foot simple span guideway. These plots show that for wavelengths above 150 feet angular misalignment has a major contribution to total irregularity and for wavelengths below 50 feet surface roughness and joint offset have major contributions to the lateral static profile. Data showing the total static irregularity profile PSD for 60, 80 and 100 foot spans are also plotted in Figure 3.12. The data for the three span lengths are similar and for wavelengths less than 50 feet may be approximated accurately with equation (3.3) used to represent the vertical profile where the roughness coefficient A is similar in value to the vertical case.

The response of the small and large vehicles to each individual irregularity are displayed in Figures 3.13 and 3.14 for 60 mph operation on 60 foot spans. These figures show for both vehicles

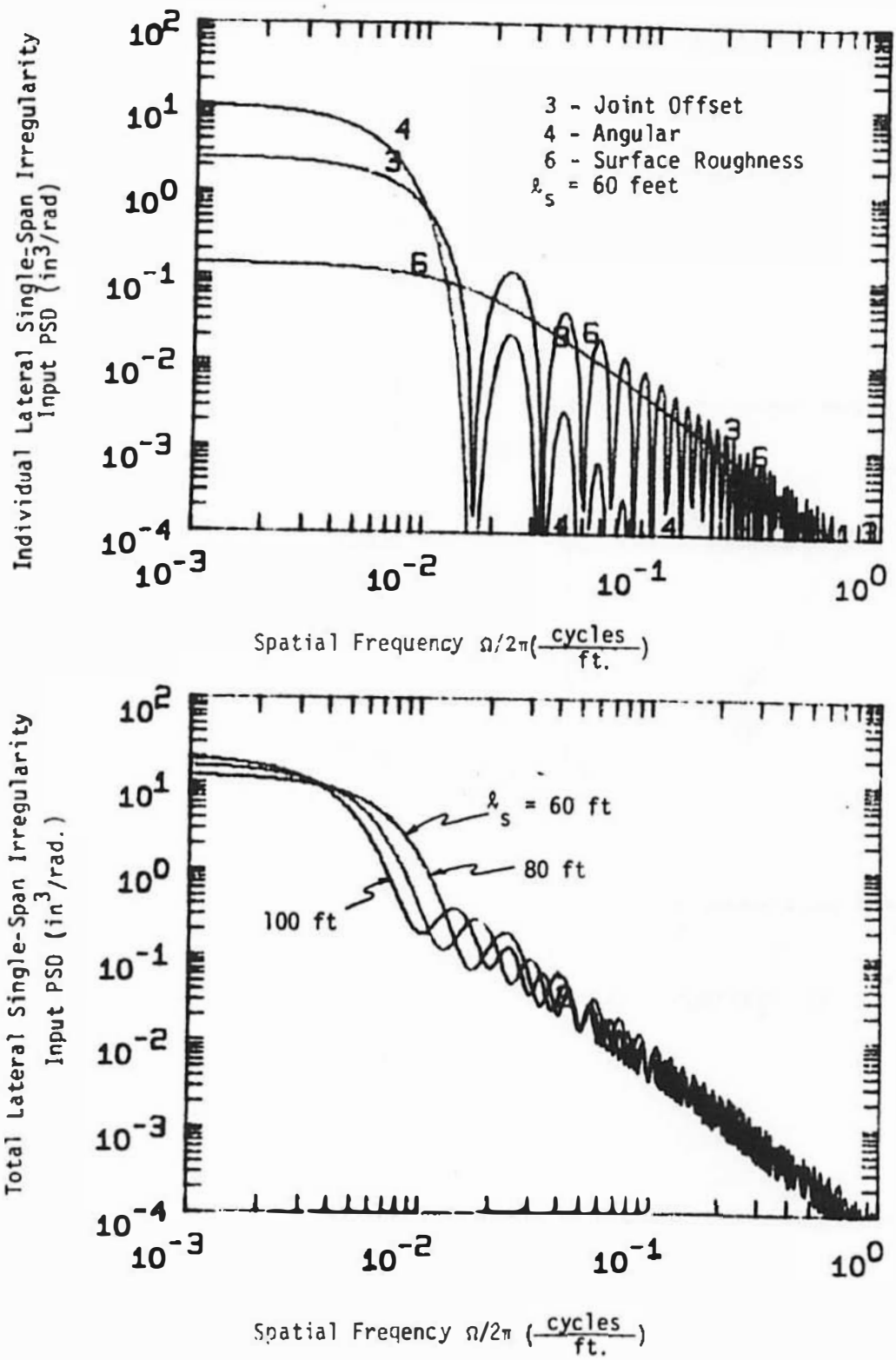

FIGURE 3.12 LATERAL SINGLE SPAN DIMENSIONAL IRREGULARITY INPUT PSD

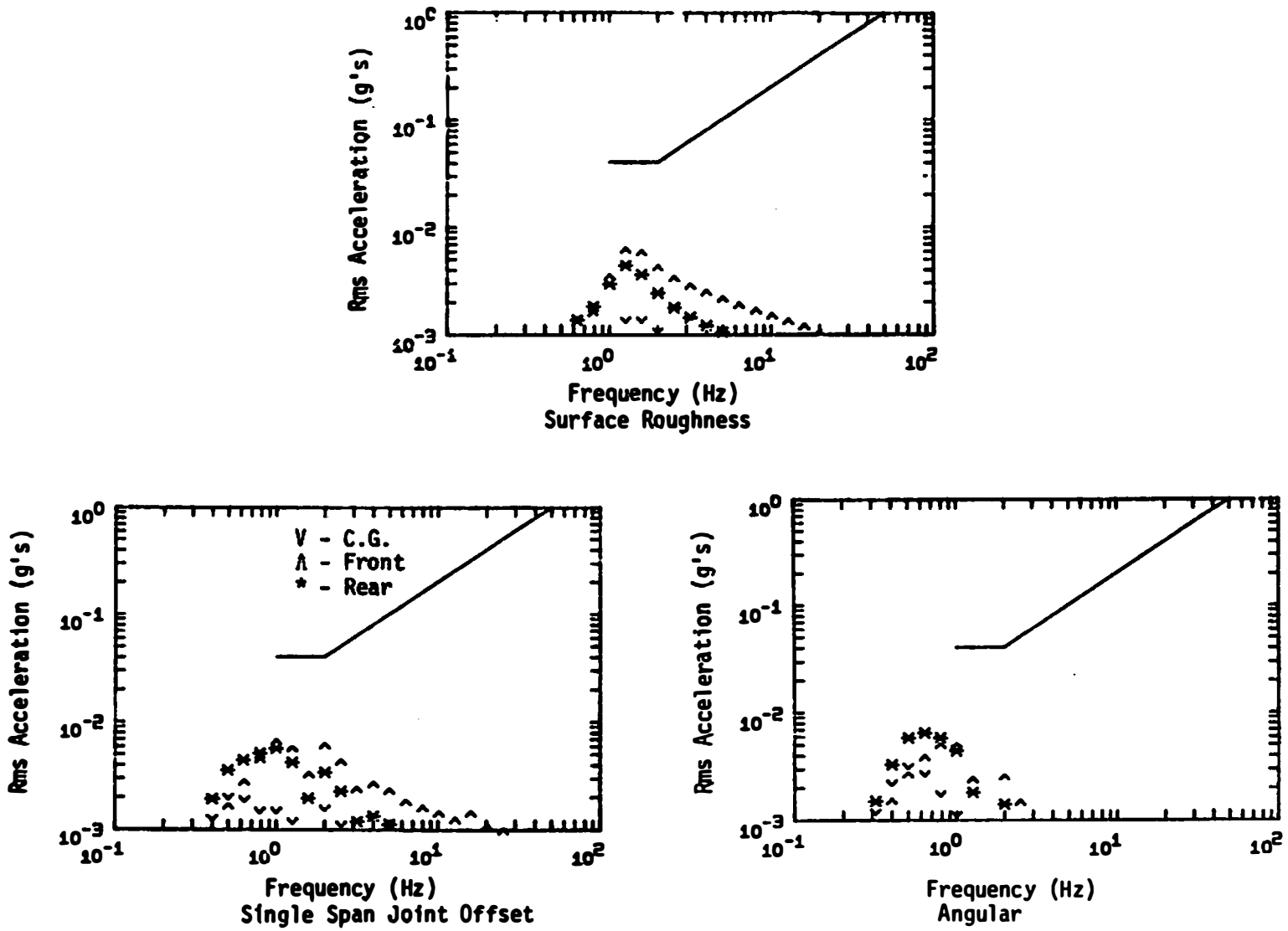

FIGURE 3.13: SMALL VEHICLE LATERAL I.S.O. SEPARATE IRREGULARITY RESPONSE
60 FT SPAN LENGTH, 60 MPH

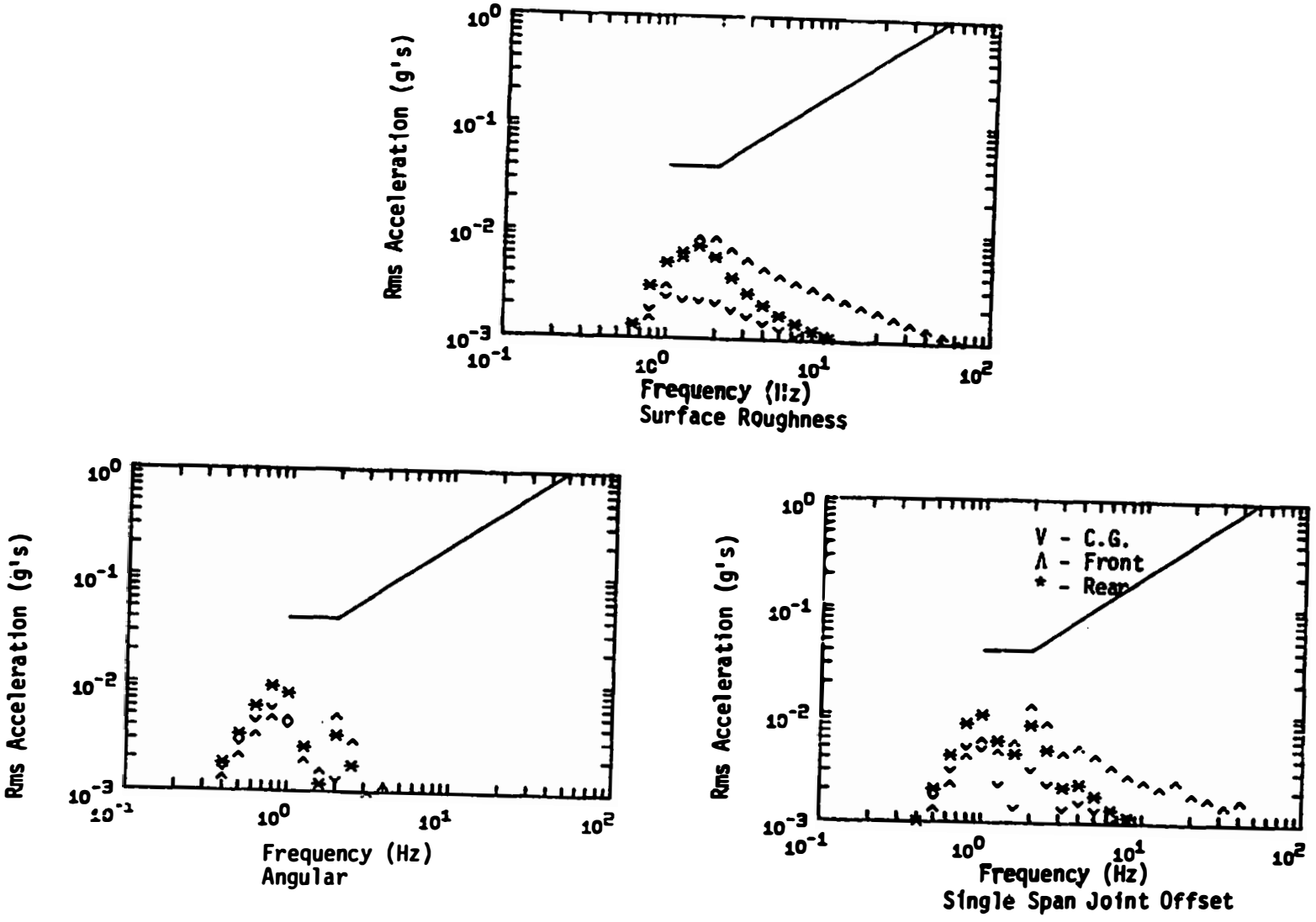

FIGURE 3.14: LARGE VEHICLE LATERAL I.S.O. SEPARATE IRREGULARITY RESPONSE
60 FT SPAN LENGTH, 60 MPH

that the maximum contribution of the surface roughness occurs in the 1-2 hertz range, the joint offset in the 0.7 - 3 hertz range and the angular response in the 0.3 - 1.0 hertz range. A summary of these data is contained in Figure 3.15 which displays the baseline tolerance levels and the maximum tolerance levels which could be used before the acceleration generated by each individual irregularity results in the small and large vehicles exceeding a 25 minute ISO specification. The data show that the angular tolerance level could be increased by a factor of almost eight before it would exceed the specification. The joint offset and surface roughness tolerances could be increased by factors of four before they exceed the specification; thus, in the lateral case, all baseline tolerance levels are considerably below values which would result in an individual irregularity exceeding the 25 minute ISO specification.

The responses of the small and large vehicle running at 60 mph along a 60 foot span guideway lateral profile consisting of the sum of the irregularities are displayed in Figure 3.16. Both the small and large vehicle lateral responses meet a very good ride quality specification, in excess of a 150 minute ISO specification. Thus, the lateral ride quality with baseline values of tolerance is quite good.

In lateral vehicle performance assessment, both ride quality and vehicle tracking error are important. The lateral rms tracking error* and total rms accelerations for the small and large vehicles running along the baseline guideways are summarized in Figures 3.17 and 3.18

*For these vehicles the maximum tracking error occurs at the rear of the vehicle.

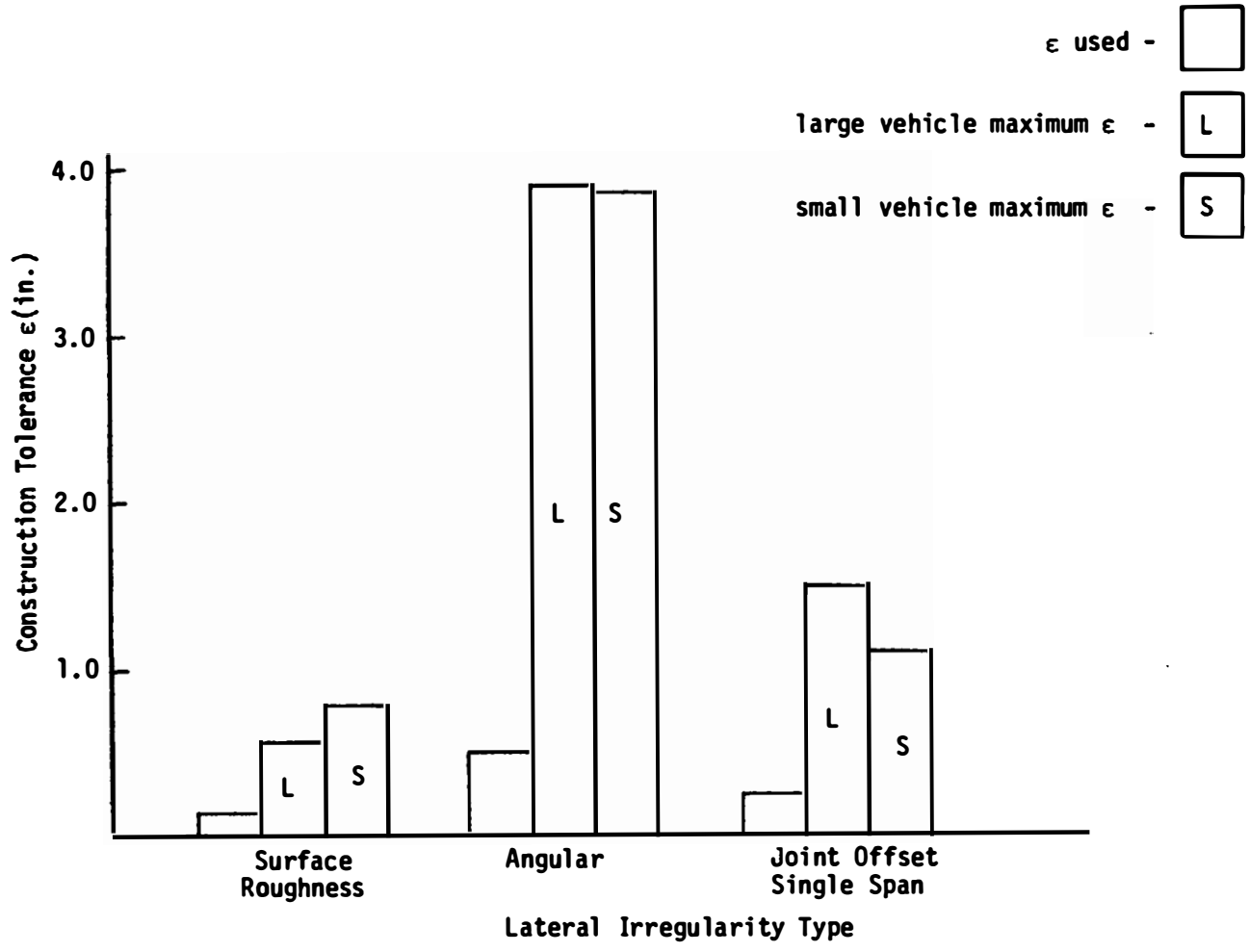

FIGURE 3.15: MAXIMUM LATERAL CONSTRUCTION TOLERANCE TO MEET 25 MIN. I.S.O. SPECIFICATIONS

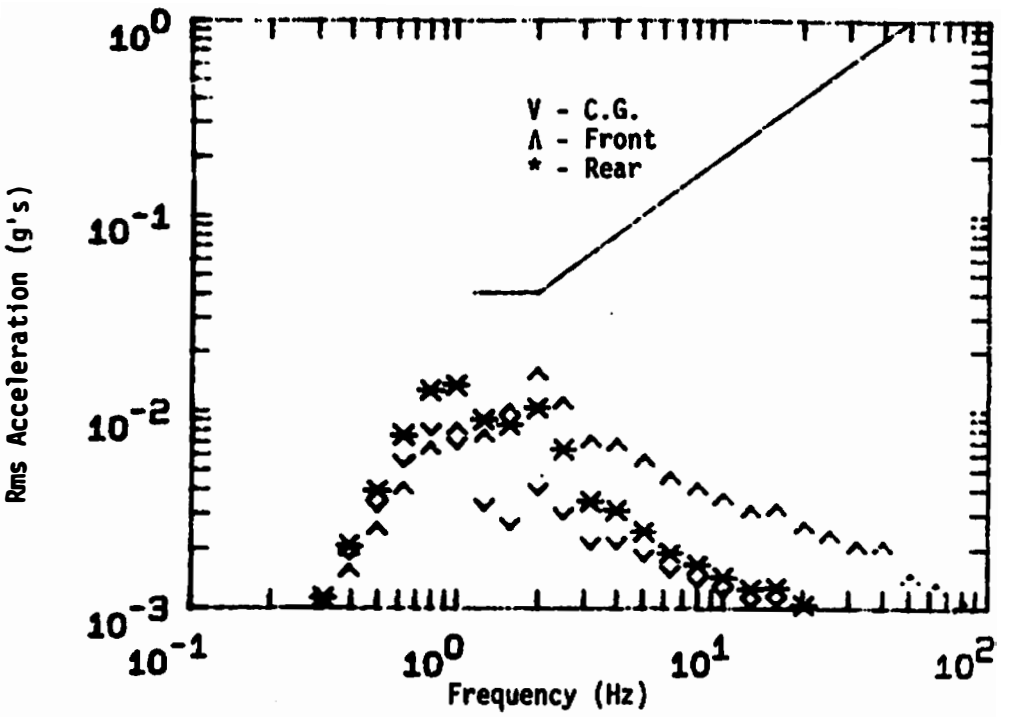

Small Vehicle Response

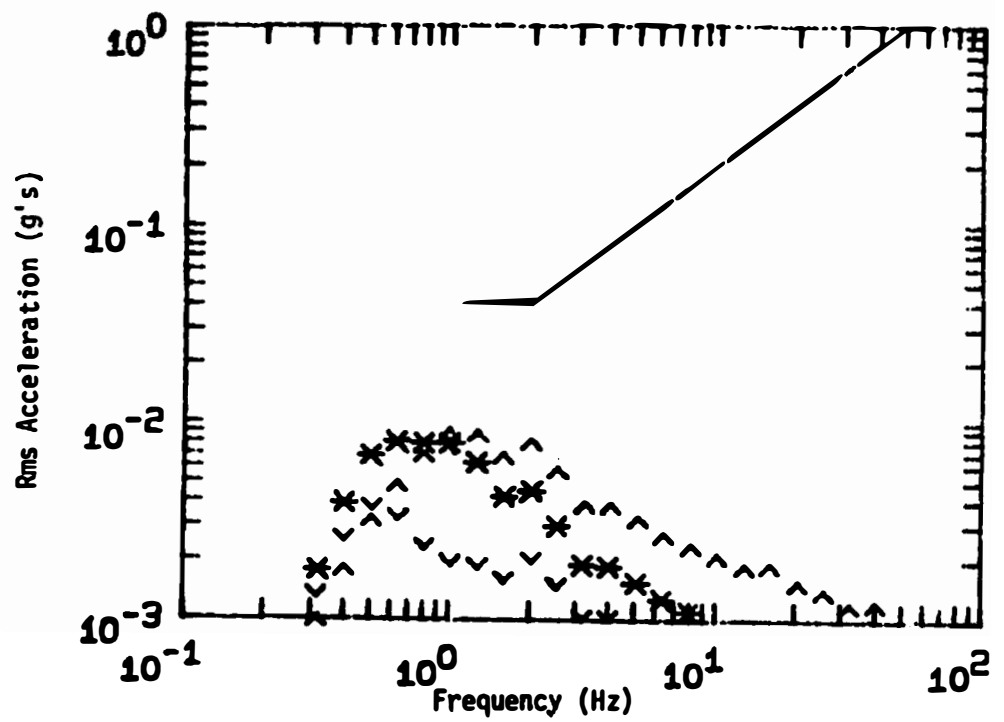

Large Vehicle Response

FIGURE 3.1G: LARGE AND SMALL LATERAL I.S.O. SINGLE SPAN RESPONSE 60 FOOT SPAN LENGTH AT 60 MPH

which show as vehicle speed is increased from 30 to 60 mph that the rms tracking errors increase nearly proportionally; however, the maximum rms tracking error is less than 0.36 inches. The rms accelerations also increase with speed with the large vehicle rms accelerations more than doubling and the small vehicle rms accelerations almost doubling as the speed is doubled. As span length is decreased, both rms tracking error and acceleration increase because of the increased number of joints per unit distance.

3.5 Influence of Simple Span Deflection, Mean Camber and Irregularities on Vehicle Response

The vertical response of vehicles on single span guideways with mean deterministic camber, dynamic deflections due to vehicle passage and surface profile irregularities are determined in this section. Mean camber for the baseline simple spans is upward while span deflection is downward, thus these two effects tend to cancel for the speed ranges and span configurations of typical GRT systems.

The vertical acceleration responses of the small and large vehicles running at 60 mph along 60 foot beam designs are summarized in Figure 3.19. The span crossing frequency is $v/\ell_s = 1.5$ hertz. The effects of guideway camber and deflection occur at this frequency and multiplies of this frequency. Comparison of this response with the response due to only irregularities illustrated in Figure 3.11 indicates that the influence of deflection and mean camber is strong only in the frequency range of v/ℓ_s to $2v/\ell_s$ and above this frequency irregularities dominate. For this 60 foot span the response in the 6-8 Hertz

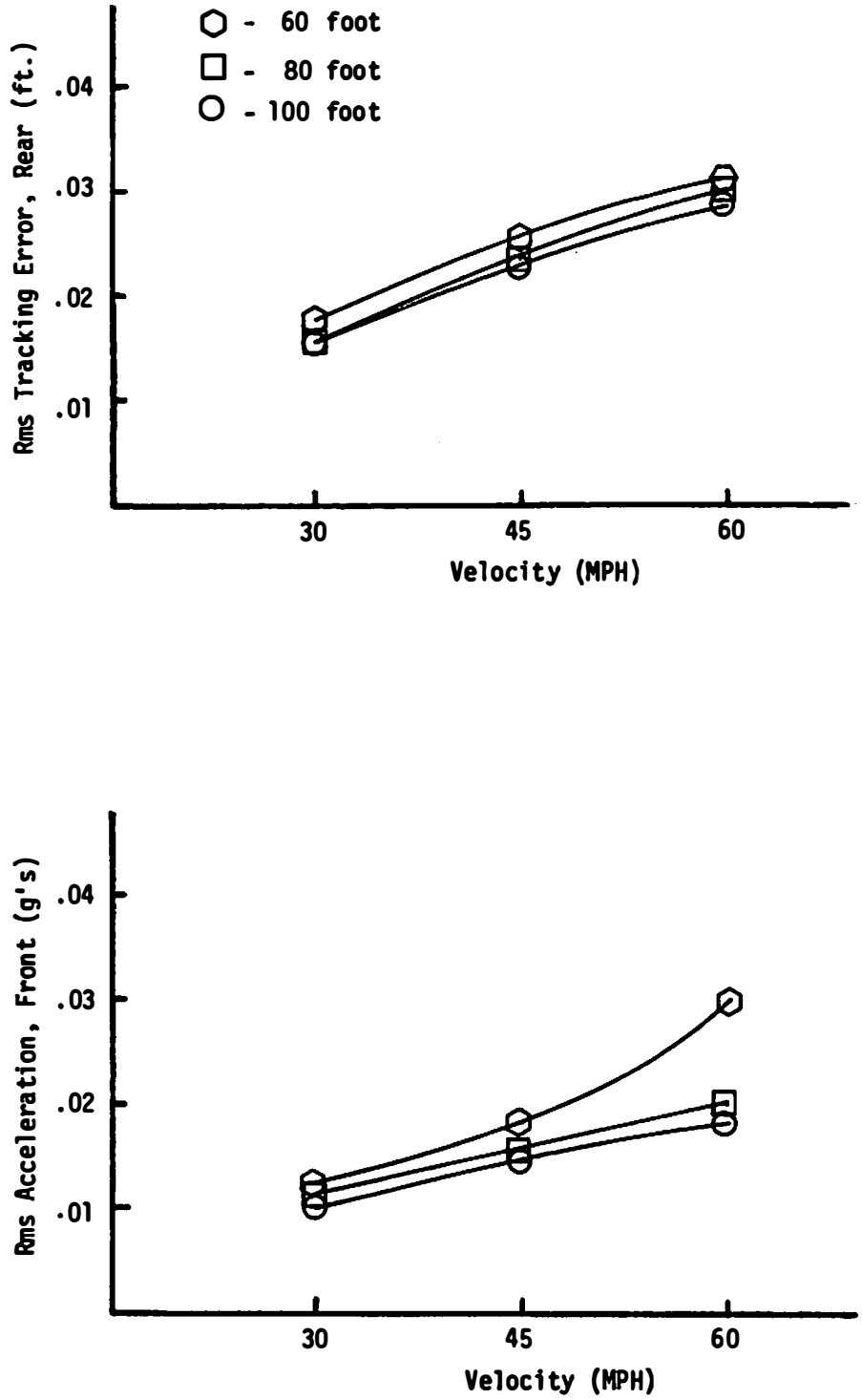

FIGURE 3.17: SMALL VEHICLE LATERAL TOTAL RMS RESPONSE AS A FUNCTION OF SPAN LENGTH AND VELOCITY

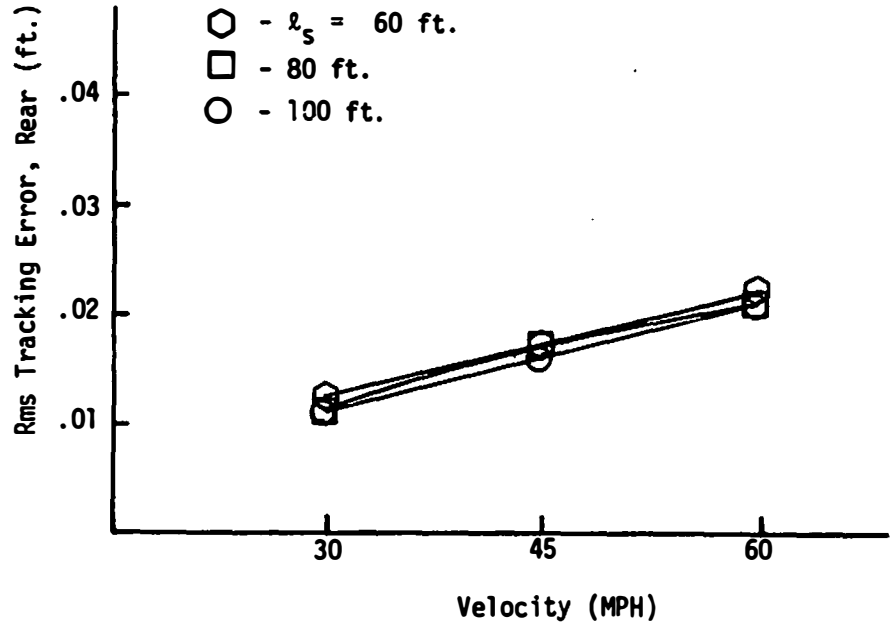

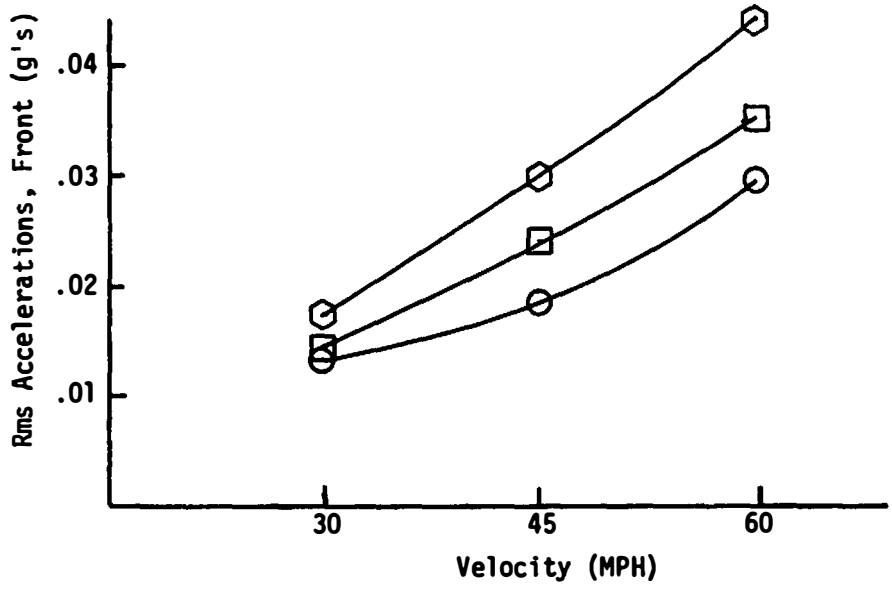

FIGURE 3.18: LARGE VEHICLE LATERAL TOTAL RMS RESPONSE AS A FUNCTION OF SPAN LENGTH AND VELOCITY

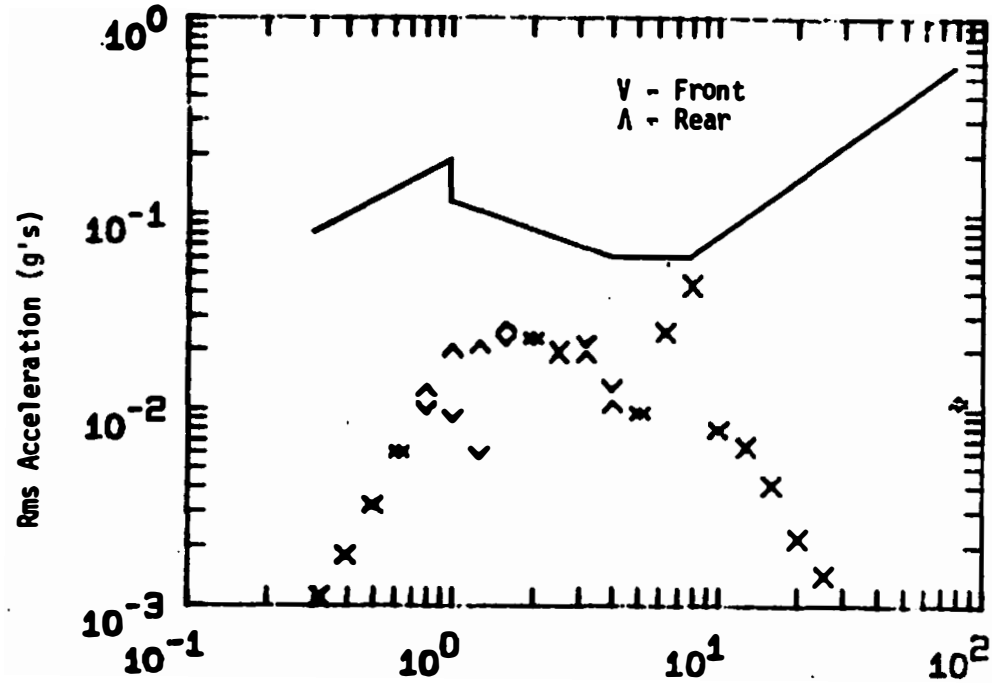

Frequency (Hz)
Large Vehicle Response

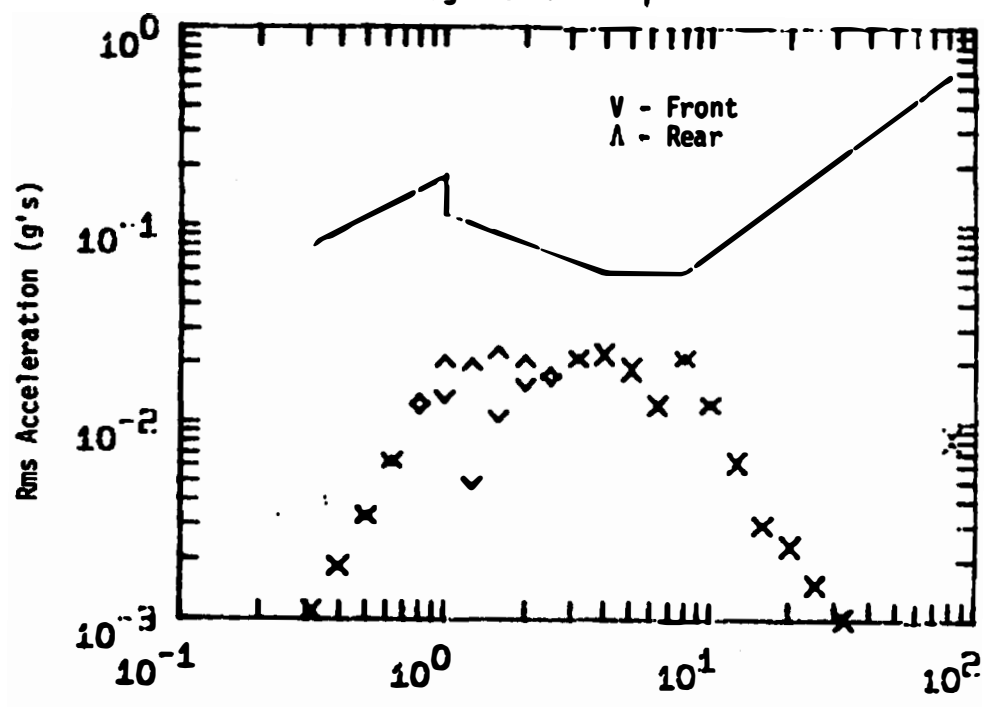

Frequency (Hz)
Small Vehicle Response

FIGURE 3.19 : LARGE AND SMALL VERTICAL SINGLE SPAN I.S.O. RESPONSE
60 FOOT SPAN LENGTH, 60 MPH

region is a maximum and thus the 60 foot span design ride quality is primarily limited by irregularities.

The ISO responses of the small and large vehicles for 60, 80 and 100 foot span lengths are summarized in Figures 3.20 and 3.21. These Figures show that as the span length increases, and the corresponding camber and deflection increase, the response due to camber and irregularity in the frequency range v/ℓ_s to $2v/\ell_s$, becomes increasingly significant in comparison to the irregularity response in the higher frequency range. For the 80 foot span the response at v/ℓ_s equals the maximum irregularity response, and for the 100 foot span the response at v/ℓ_s exceeds the higher frequency irregularity response.

Summaries of the rms vehicle accelerations on 60, 80, and 100 foot spans for 30, 45 and 60 mph are contained in Tables 3.3 and 3.4. These data show for the 60 foot spans the total vehicle acceleration is due primarily to the irregularities and as span length increases to 100 feet, the total rms acceleration is due about equally to the camber and deflection component and to the irregularity component. For all the cases, the beam maximum deflection is less than the mean camber. This tabular data shows that the camber and deflection associated with longer spans reduces ride quality. An increase in acceleration for 60 mph operation from 0.068 g's to 0.119 g's for the small vehicle and from 0.077 g's to 0.122 g's for the large vehicle occurs as the span length is incresed from 60 to 100 feet.

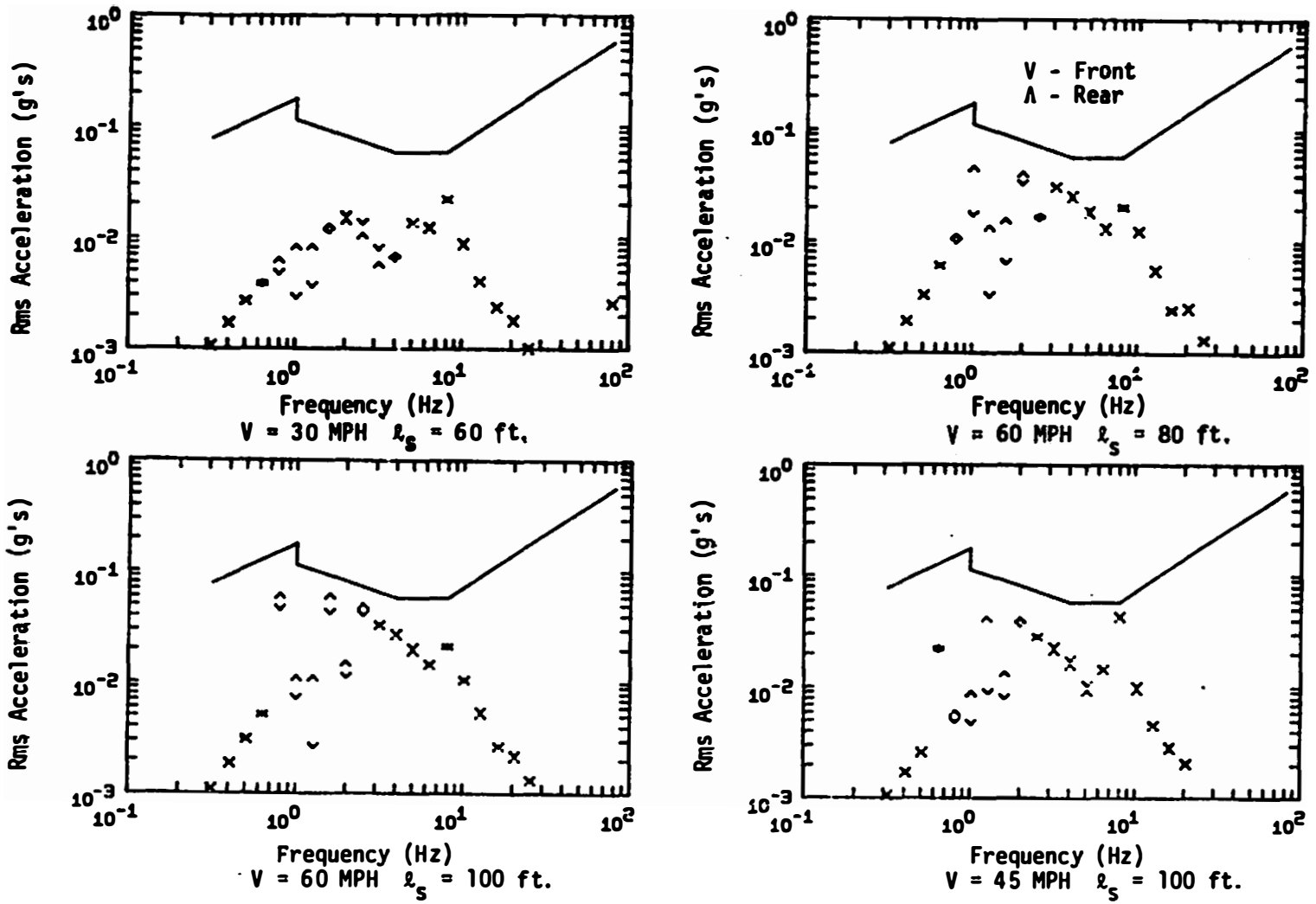

FIGURE 3.20: SMALL VEHICLE VERTICAL I.S.O. SINGLE SPAN RESPONSE AS A FUNCTION OF VELOCITY AND SPAN LENGTH

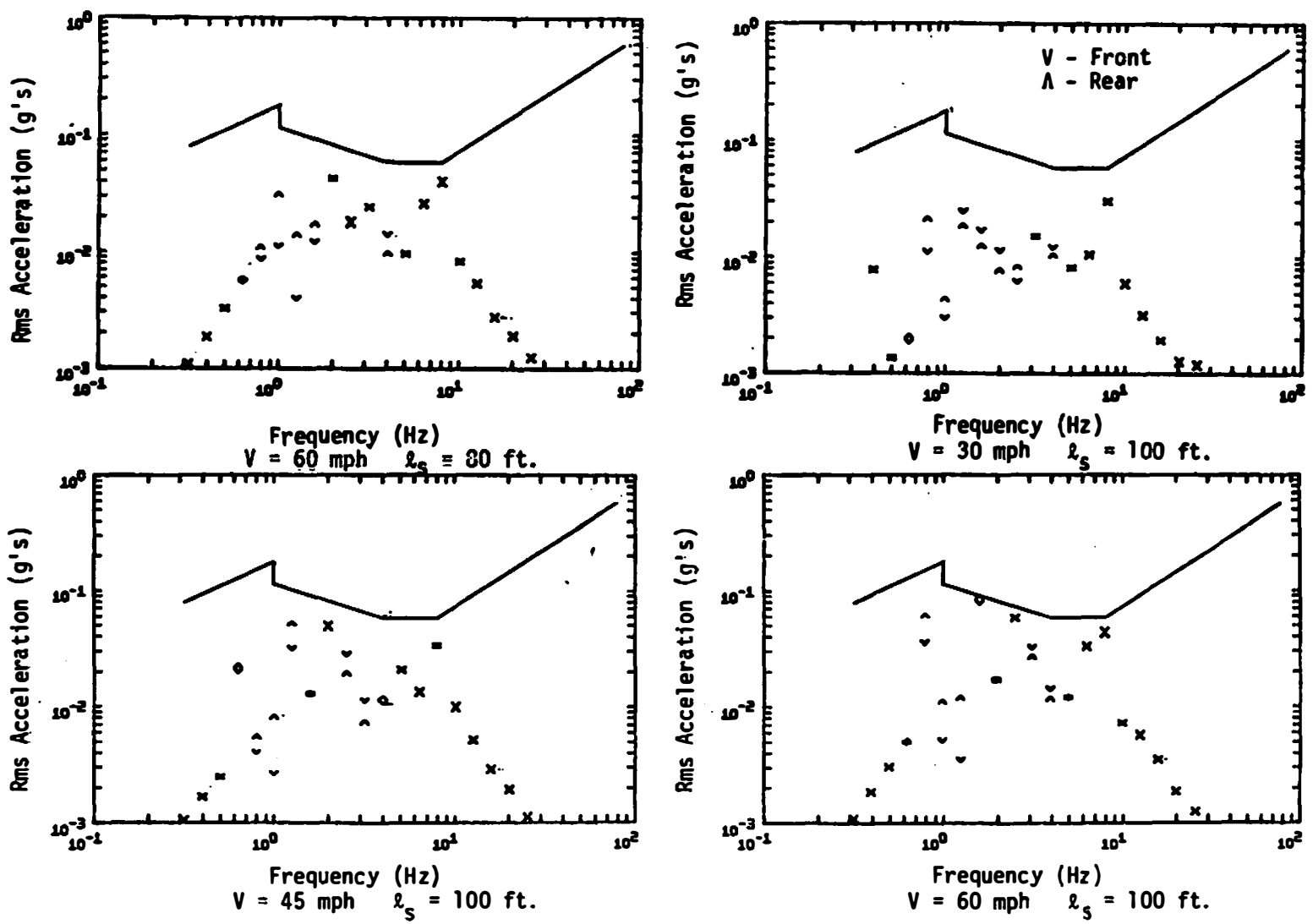

FIGURE 3.21: LARGE VEHICLE VERTICAL I.S.O. SINGLE SPAN RESPONSE AS A FUNCTION OF VELOCITY AND SPAN LENGTH

TABLE 3.3: SMALL VEHICLE RMS ACCELERATION ON SINGLE SPAN GUIDEWAY DESIGN 6

SPAN LENGTH Ft.	SPEED MPH	MAXIMUM DEFLECTION Inches	PEAK 1/3 OCTAVE BAND RMS ACCELERATION (g's) @ FREQUENCY (HZ)	RMS ACCELERATION: g's	
				IRREGULARITIES*	TOTAL
60	30	0.115	0.022 @ 8.0	0.041	0.042
	45	0.120	0.022 @ 8.0	0.061	0.063
	60	0.120	0.024 @ 1.59	0.065	0.068
80	30	0.564	0.019 @ 1.59	0.034	0.044
	45	0.550	0.042 @ 8.0	0.058	0.076
	60	0.550	0.046 @ 1.0	0.055	0.087
100	30	1.147	0.023 @ 0.79	0.034	0.053
	45	1.164	0.043 @ 8.0	0.055	0.091
	60	1.185	0.064 @ 1.59	0.050	0.119

*Value with Rigid Beam and Construction Irregularity

TABLE 3.4: LARGE VEHICLE RMS ACCELERATION ON SINGLE SPAN GUIDEWAY DESIGN 3a

SPAN LENGTH Ft	SPEED MPH	MAXIMUM DEFLECTION Inches	PEAK 1/3 OCTAVE BAND RMS ACCELERATION (g's) @ FREQUENCY (Hz)	RMS ACCELERATION: g's	
				IRREGULARITY	TOTAL
60	30	0.124	0.035 @ 8.0	0.046	0.047
	45	0.126	0.023 @ 8.0	0.041	0.043
	60	0.129	0.044 @ 8.0	0.074	0.077
80	30	0.430	0.022 @ 8.0	0.030	0.035
	45	0.449	0.031 @ 1.59	0.037	0.051
	60	0.425	0.039 @ 2.0	0.051	0.072
100	30	1.07	0.030 @ 8.0	0.039	0.057
	45	1.06	0.045 @ 1.26	0.036	0.076
	60	1.05	0.077 @ 1.59	0.058	0.122

3.6 Influence of Multiple Span Deflection, Mean Camber and Irregularities on Vehicle Response

Two multiple span guideway configurations have been analyzed- three and six continuous span systems in which live load continuity is achieved across interior joints. The primary features of the multispan case are:

(1) In multispan design, at all interior joints it is possible to essentially eliminate joint offset, thus it is only considered at end spans.

(2) The continuity across joints allows a reduction in prestressing steel which in turn results in reduced camber in multispan systems.

The rms one third octave frequency band acceleration responses of small and large vehicles running across a 6-span 80 foot span length guideway at 60 mph are illustrated in Figures 3.22 and 3.23 along with the beam deflections that occur under the front axles of the vehicles. The responses illustrate that with the reduced beam deflection and camber of these continuous spans, the maximum acceleration response amplitudes are primarily due to irregularities.

Summaries of the rms acceleration responses for small and large vehicles to crossing three and six span guideways are contained in Tables 3.5 and 3.6. These results show that except for 100 foot and 80 foot 60 mph cases, the maximum 1/3 octave band acceleration occurs in a frequency range where only irregularities contribute to the response. Comparison of multispan rms accelerations with those generated solely by irregularities indicates that in all cases less

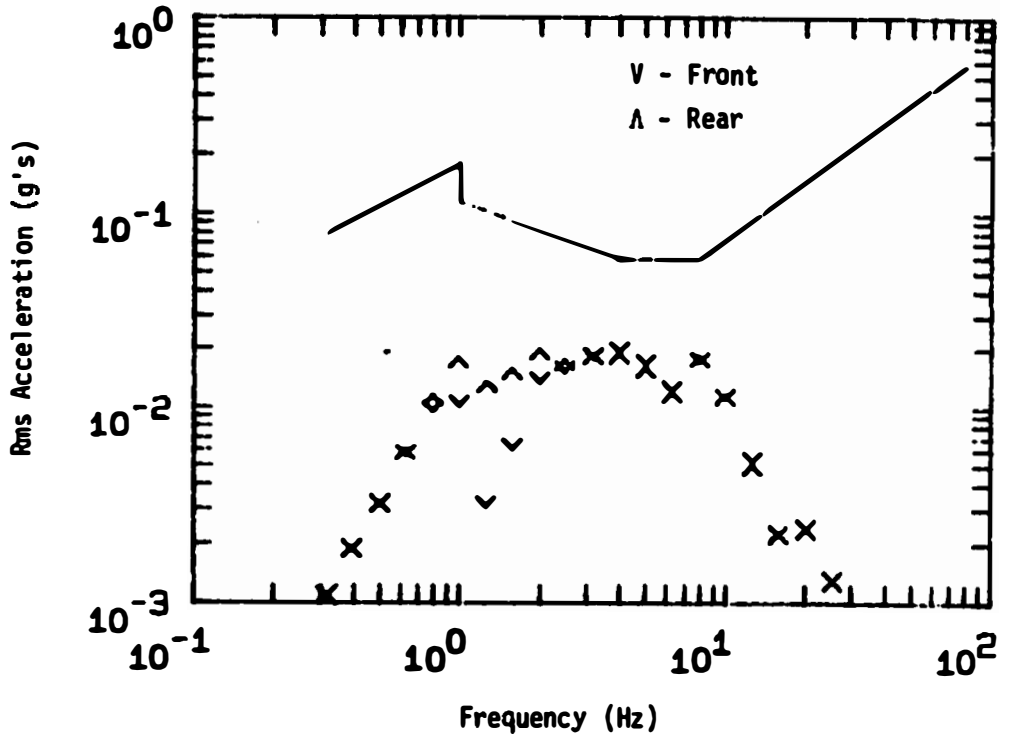

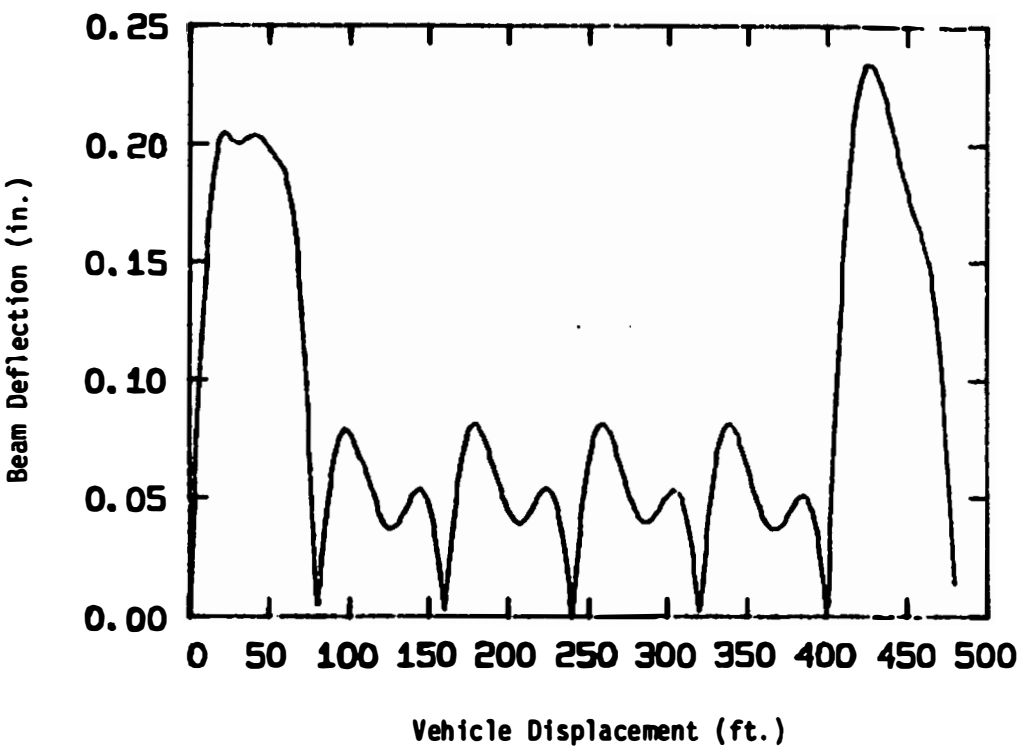

FIGURE 3.22 : SMALL VEHICLE SIX SPAN I.S.O. AND DEFLECTION RESPONSE OF 80 FOOT SPAN LENGTH AT 60 MPH

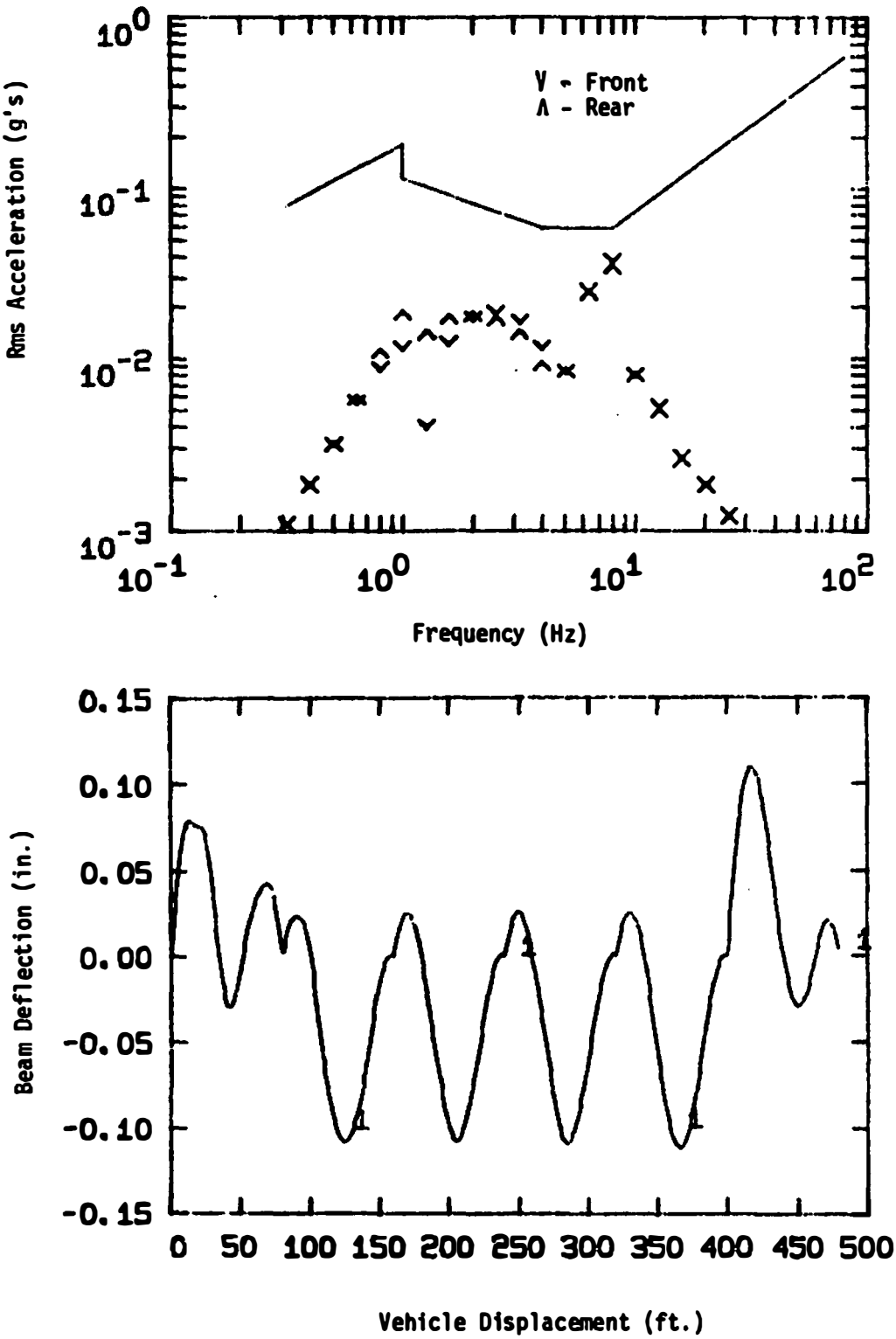

FIGURE 3.23: LARGE VEHICLE SIX SPAN I.S.O. AND DEFLECTION RESPONSE OF 80 FOOT SPAN LENGTH AT 60 MPH

TABLE 3.5: RMS VEHICLE ACCELERATIONS FOR THREE SPAN CONTINUOUS GUIDEWAYS

VEHICLE GUIDEWAY	SPAN LENGTH Ft	SPEED MPH	PEAK 1/3 OCTAVE BAND RMS ACCELERATION (g's) @ FREQUENCY (Hz)	TOTAL RMS ACCELERATION (g's)
LARGE DESIGN 4A	60	30	0.035 @ 8.0	0.046
		60	0.043 @ 8.0	0.075
	80	30	0.022 @ 8.0	0.035
		60	0.037 @ 8.0	0.064
	100	30	0.029 @ 8.0	0.041
		60	0.041 @ 1.59	0.074

TABLE 3.6: RMS VEHICLE ACCELERATIONS FOR SIX SPAN CONTINUOUS GUIDEWAYS

VEHICLE-GUIDEWAY	SPAN LENGTH Ft	SPEED MPH	PEAK 1/3 OCTAVE BAND RMS ACCELERATION (g's) @ FREQUENCY (Hz)	TOTAL RMS ACCELERATION (g's)
SMALL DESIGN 7	60	30	0.022 @ 8.0	0.041
		60	0.022 @ 8.0	0.068
	80	30	0.015 @ 8.0	0.035
		60	0.020 @ 4.0	0.058
	100	30	0.018 @ 8.0	0.040
		60	0.036 @ 1.59	0.074
LARGE DESIGN 5	60	30	0.035 @ 8.0	0.047
		60	0.043 @ 8.0	0.076
	80	30	0.022 @ 8.0	0.035
		60	0.037 @ 8.0	0.064
	100	30	0.029 @ 8.0	0.040
		60	0.039 @ 8.0	0.070

than 15% of the total rms acceleration is attributed to camber and deflection. Thus, use of multispan guideways essentially reduces the influence of guideway camber and deflection on vehicle ride quality to a small effect in comparison to the baseline static surface profile effects.

3.7 Influence of Vehicle Suspension Properties on Ride Quality

The influence of changing vehicle suspension sprung and unsprung natural frequencies on ride quality is summarized in Figure 3.24 for the large vehicle crossing a 100 foot simple span system at 60 mph. As the suspension sprung mass natural frequency is reduced from 1.0 to 0.75 hertz the rms acceleration is reduced by 50% while as the suspension natural frequency is increased from 1.0 to 1.5 hertz the rms acceleration is increased by nearly 50%. This reduction of vehicle sprung mass suspension natural frequency directly reduces rms accelerations. In vehicle design sprung mass suspension natural frequencies are generally selected to be as low as possible within the limits of available suspension travel and limits imposed by vehicle body deflection and roll due to centrifugal, wind and cargo loading.

The influence of unsprung mass natural frequency on total rms acceleration is relatively weak and variations in frequency from 5 to 7.5 hertz change rms acceleration by about 15%. While for the baseline vehicles, variations in unsprung natural frequency over the range cited show a small influence on vehicle acceleration, in the

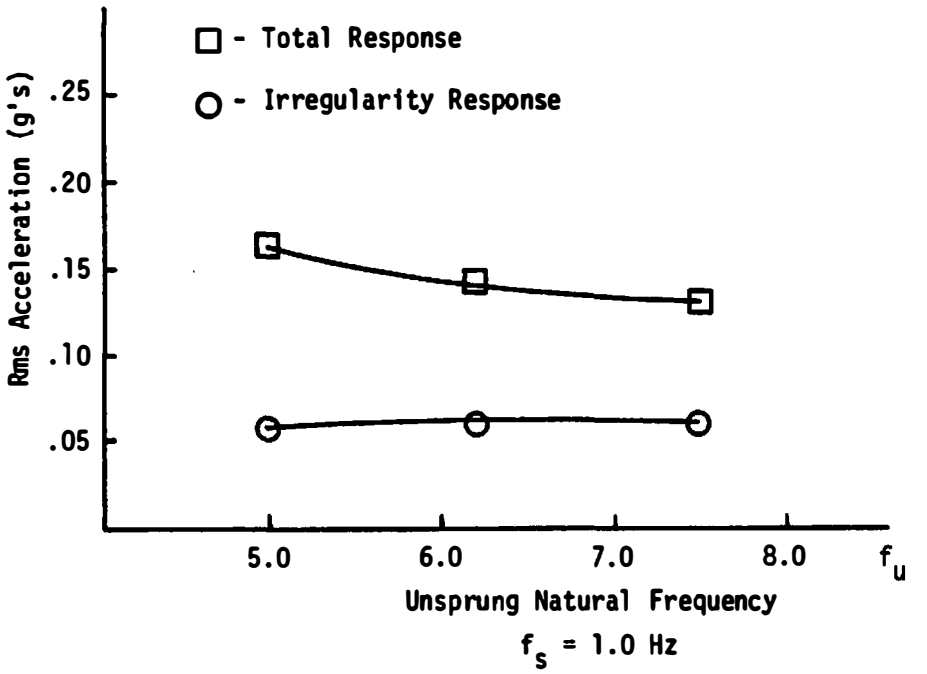

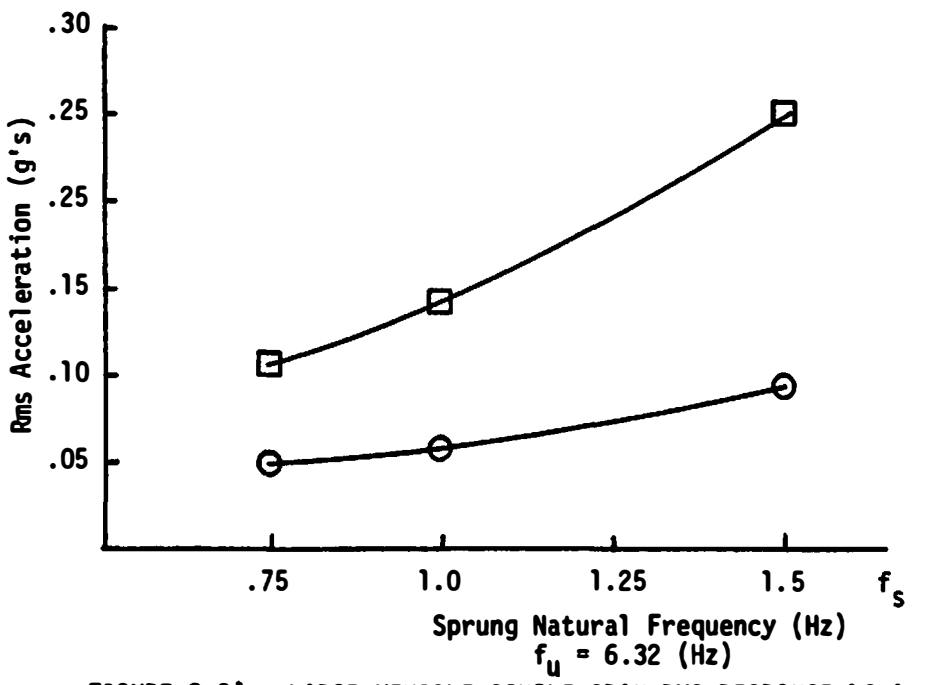

FIGURE 3.24: LARGE VEHICLE SINGLE SPAN RMS RESPONSE AS A FUNCTION OF SPRUNG AND UNSPRUNG NATURAL FREQUENCY

general case the unsprung suspension design, particularly the amount of unsprung mass can have a significant effect on vehicle performance [21]. For GRT vehicles with drive motors mounted on drive axles, the unsprung mass values are relatively high approaching and in some cases exceeding 25% of the sprung mass.

4. RIDE QUALITY COST TRADEOFF STUDIES

4.1 Scope of Tradeoff Studies

In this section the principal results of the structural design-cost analyses and the ride quality analyses are combined to generate ride quality-cost tradeoff data. While a large number of parameters influence both ride quality and cost, the detailed studies in Sections 2 and 3 have identified a number of parameters which are of primary importance, including the following parameters which are evaluated in this tradeoff study:

(1) Lateral surface profile irregularity parameters.

(2) Vertical surface profile irregularity parameters.

(3) Span continuity parameters.

4.2 Baseline Guideway Configuration

As a result of detailed design studies summarized in Section 2 baseline designs for tradeoff analyses have been developed. These baseline structures consist of a spread footing, cast-in-place pier, precast, prestressed concrete box beam and cast-in-place parapet side-walls. The round pier and box beam were selected primarily because they resulted in lower form costs when compared with other pier and beam shapes. The tolerance levels achieved in the fabrication of the guide-way using standard construction techniques are summarized in Table 3.2, while the structural properties of the designs are summarized in Section 2.5.

4.3 Lateral Ride Quality Cost Relationships

The lateral ride quality-cost relationship are influenced for a fixed vehicle configuration only by lateral sidewall construction tolerances which are represented in terms of (1) surface roughness with respect to a ten foot straight edge, (2) lateral joint offset and (3) angular misalignment of the side panels. The lateral ride quality achieved when the large vehicle is run over the 60 foot span guideway constructed with the standard tolerances has been summarized in Section 3.3 in terms of the ISO lateral acceleration limit which is met in terms of minutes for a reduced comfort level. To determine the sensitivity of ride comfort to parapet wall construction and cost, the following modifications to construction tolerance have been considered:

(1) Modification of lateral joint offset.

A practical modification of lateral joint offset from 1/4 inch to 3/16 inch tolerance level can be achieved by selectively grinding down sections of the parapet wall at which joint offsets are greater than 3/16 inch. Based upon the assumption that as a result of normal construction practice all joints are within 1/4 inch and that every third joint exceeds 3/16 inch, it is estimated that 4 hours per joint are required to grind each joint in excess of 3/16 inch. Labor and material costs for this job result in a charge of $48 per joint and for 60 ft spans represents a cost of $0.27 per foot. It is not considered practical to reduce the lateral offset significantly below 3/16 inch by grinding methods.

(2) Modification of angular offset.

A practical modification of angular offset, reducing it from 1/3 inch to 1/4 inch, can be accomplished by grinding selective portions of the parapet wall. Under the assumption that every third span requires grinding of 40 sq. feet of area to reduce the angular offset, a total of 21.3 hours is required which results in a total labor and material cost of $256 per span modified or $1.42 per foot for 60 foot spans.

(3) Modification of Surface Roughness.

The standard construction tolerance of 1/8 inch deviation under a ten foot straight edge is considered to be the minimum practical with respect to common field measurement capabilities. However, by the use of reduced cost forms and less labor in installing forms, it is practical to produce a surface which meets a 1/4 inch under a ten foot straight edge requirement. Relaxing this tolerance is estimated to reduce form related labor costs by 20% and material costs by 50% with a net cost reduction of $2.67 per foot.

(4) Modification of Surface by Ceramic Insert.

One of the problems associated with existing GRT guideways is the degradation of the parapet wall due to steering guidance wheel contact. A method recommended to reduce wear in guideways by the study "Advanced Technology Materials Applied to Guideways, Highways and Airport Runways" [22] is to use a ceramic strip along the parapet side wall. The cost of this strip using a one inch thick by six inch width

strip along both sidewalls is estimated to be $10 per foot with 80% of the cost associated with the material. Use of this strip should eliminate joint offset and reduce angular offset of 1/4 inch as well as provide a highly durable surface. It is not anticipated that the surface roughness is reduced below 1/8 inch in 10 feet.

The effects of each of these modifications upon the large vehicle ride quality are summarized in Table 4.1 and the level of ride quality achieved represented in equivalent minutes as a function of cost is summarized in Figure 4.1.

Figure 4.1 shows the increased cost and corresponding increases in ride quality as joint offset and angular errors are reduced and due to the ceramic overaly. Reduction of joint offset from 1/4 to 3/16 inch results in a cost increase of $0.27 per foot and yields an increase in ride quality at 30 mph by a factor of 1.3 and at 60 mph by a factor of 1.4 in terms of ISO exposure minutes. Reduction of angular error produces essentially no improvement in ride quality since its overall effect on ride quality is small. The use of the ceramic insert increases the cost by $10 per foot and yields an increase in ride quality at 30 mph by a factor of 1.6 and at 60 mph by a factor of 1.5 in terms of ISO exposure minutes in comparison to the baseline case. Since all levels of ride quality are good, relaxation of construction standards to allow a 1/4 inch deviation under a ten foot straight edge has been considered. For this case a savings of $2.67 per foot, about 1.3% of the total structure cost, is obtained with a decrease in ride quality to approximately 50% of the

TABLE 4.1

LARGE VEHICLE LATERAL RIDE QUALITY FOR SELECTED CONSTRUCTION TOLERANCE LEVELS

SPEED MPH	TOLERANCE: inches			ACCELERATION: g's*				ISO LIMIT IN MINUTES
	JOINT OFFSET	ANGULAR	SURFACE ROUGHNESS	PEAK IN 1/3 OCTAVE BAND	@	FREQUENCY HZ	RMS	
30	1/4	1/3	1/8	0.005	@	1.26	0.012	720
60	1/4	1/3	1/8	0.009	@	1.26	0.022	360
30	3/16	1/3	1/8	0.005	@	1.26	0.011	960
60	3/16	1/3	1/8	0.008	@	1.26	0.020	390
30	0	1/4	1/8	0.003	@	1.6	0.008	1200
60	0	1/4	1/8	0.007	@	1.26	0.014	540
30	1/4	1/4	1/8	0.005	@	1.26	0.012	700
60	1/4	1/4	1/8	0.009	@	1.26	0.020	360
30	3/16	1/4	1/8	0.004	@	1.26	0.011	960
60	3/16	1/4	1/8	0.008	@	1.26	0.018	400
30	1/4	1/3	1/4	0.008	@	1.26	0.109	400
60	1/4	1/3	1/4	0.014	@	1.26	0.031	180

*Accelerations at front of vehicle. These are greater for all cases considered than those at the vehicle rear or center of mass.

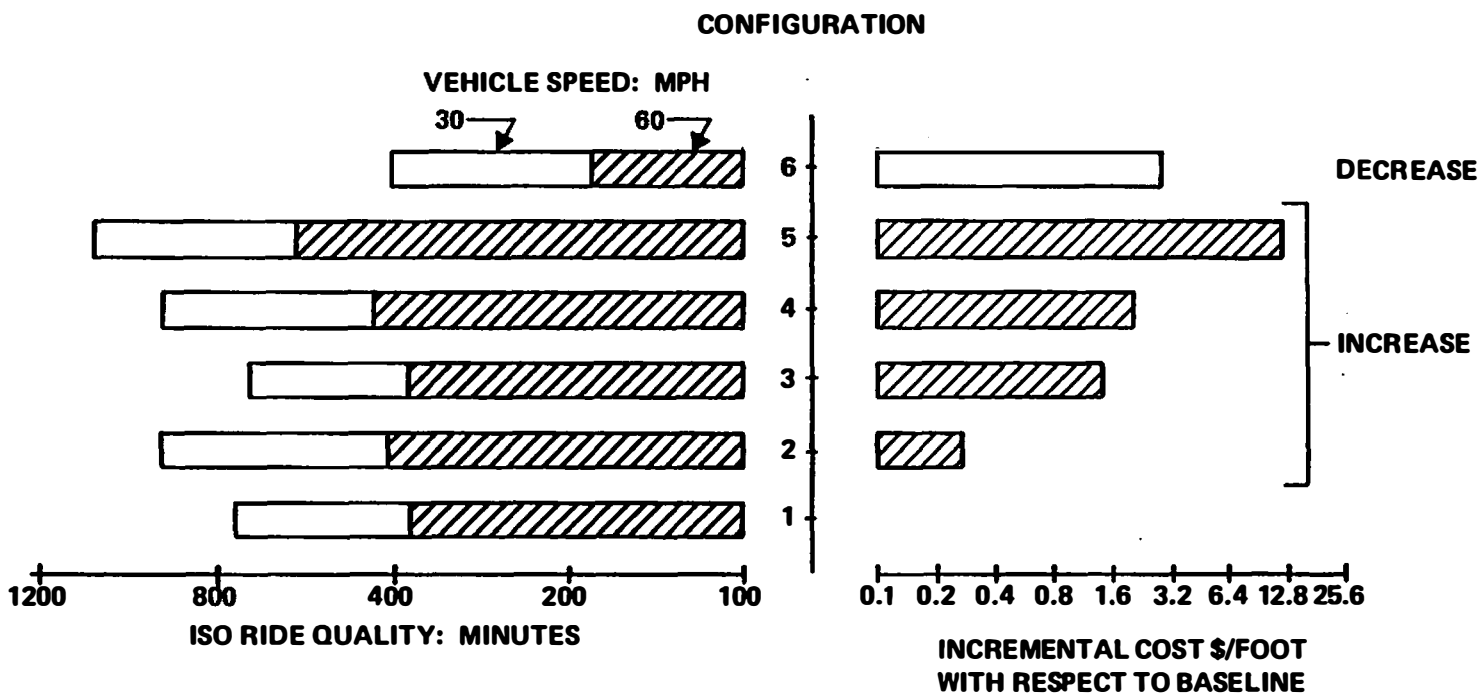

CONFIGURATION:

1: Baseline 60 ft., simple span, large guideway

2: Reduction of Joint Offset from 1/4 to 3/16 inch

3: Reduction of Angular Error from 1/3 to 1/4 inch

4: Reduction of Joint Offset from 1/4 to 3/16 inch and Angular Error from 1/3 to 1/4 inch

5: Use of Ceramic Insert to eliminate Joint Offset and reduce Angular Error from 1/3 to 1/4 inch

6: Increase of Baseline Surface Roughness from 1/8 to 1/4 inch

FIGURE 4.1: COST LATERAL RIDE QUALITY TRADEOFF FOR LATERAL SURFACE PROFILE MODIFICATIONS

baseline values at 30 and 60 mph. However, even with these reduced levels of ride quality, the ISO 3 hour exposure limit is met.

As shown in Section 3, the small vehicle response to guideway lateral irregularities is similar to those of the large vehicle, thus the trends and general levels of ride quality reported for the large vehicle above are expected to be similar for the small vehicle.

4.4 Vertical Ride Quality Cost Relationships

Vertical plane ride quality - guideway cost relationships are influenced both by the guideway structural design and construction tolerance levels. The structural design sets the beam rigidity and deterministic camber. These quantities are essentially determined by the beam cross-section properties and amount of prestressing steel used. As the cross-section depth is increased, for a span of a given length carrying a given load, the span is made stiffer and more concrete is required; however, less prestressing steel is required and the camber is decreased. The influence on stiffness, unit deflection, camber, and cost of varying the section depth for a 60 foot simple span design for the large vehicle is summarized in Figure 4.2. As the section depth is increased from 22 inches to 36 inches, the stiffness increases by a factor of 2.5, the camber at midspan decreases by a factor of 3. The total cost to manufacture the beam increases from $110 per foot to $112 per foot since the increase in materal cost is nearly balanced by the decrease in prestressing cost. The ride quality

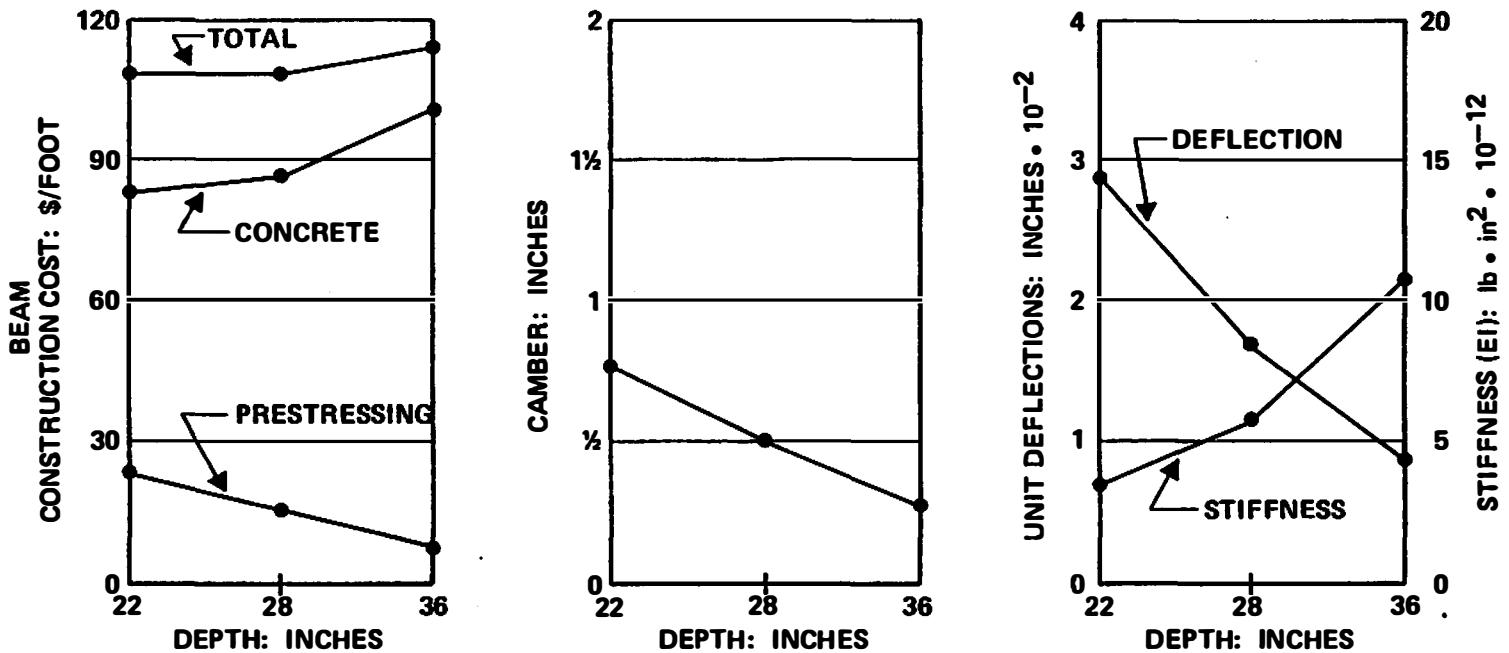

FIGURE 4.2: BEAM COST, CAMBER, UNIT DEFLECTION AND STIFFNESS FOR A 60 FOOT SIMPLE SPAN LARGE GUIDEWAY

achieved on these three beams for the large vehicle when the beams are erected to achieve the standard levels of construction tolerance is summarized in Table 4.2. The data show that as the beam depth is increased from 22 to 28 inches the ride quality increases at 60 mph from 25 to 50 minutes and at 30 mph from 75 to 90 minutes. The cost increase is about $2 per foot. Increasing the depth from 28 to 36 inches produces negligible further increase in ride quality since for this beam, the construction tolerance irregularities generate most of the acceleration rather than the beam deflection and camber. The cost increase from 28 to 36 inches if $4 per foot.

These results show that because span cost is relatively insensitive to section depth when designed for a given load, the use of increased section depth to improve ride quality, primarily because of the reduction in camber, is feasible. When it is noted that installation of a guideway in an urban environment requires a large variety of span lengths, and that for economic production of beams a common cross-section for all spans is desired, then the follwoing procedure is recommended.

> Select the span cross-section based upon the longest feasible span length requirement. For all shorter spans use the same cross-section but reduce the number of prestressing cables.

This design procedure results in both economy and good ride quality.

TABLE 4.2

LARGE VEHICLE

VERTICAL RIDE QUALITY FOR BASELINE LEVELS OF CONSTRUCTION TOLERANCE
AS A FUNCTION OF BEAM DEPTH FOR 60 FOOT SIMPLE SPANS

SPEED MPH	BEAM DEPTH INCHES	ACCELERATION: g's					ISO LIMIT IN MINUTES
		Peak in 1/3 Octave Band		@	RMS		
		FRONT	REAR	FREQ: Hz	FRONT	REAR	
30	22	0.035	0.036	8.0	0.058	0.055	75
60	22	0.060	0.06	1.56	0.119	0.121	25
30	28	0.035	0.035	8.0	0.05	0.05	90
60	28	0.049	0.048	8.0	0.084	0.097	50
30	36	0.034	0.035	8.0	0.047	0.046	90
60	36	0.044	0.043	8.0	0.071	0.079	55

The second major structural feature of guideways, is the use of continuity across span joints to construct continuous span systems. Continuity allows moment transfer across span joints and results in reduced deflection due to a given load. Properties of the 100 ft. span large guideway for simple, 3 span and 6 span continuous structures are summarized in Figure 4.3. The unit deflection and camber for the two continuous span systems are nearly identical and are less than half those corresponding to the simple span. The cost of the continuous span systems is slightly less than that of the simple span, because the additional cost of providing continuity is less than the decrease in cost associated with reduction of prestressing steel.

The ride quality achieved with the simple and continuous span systems is summarized in Figure 4.4 for the large vehicle run over a guideway constructed with the standard tolerance levels.

The data show that ride quality is increased for the continuous spans in comparison to the simple span at 30 mph from 55 to 60 minutes and at 60 mph from 105 to 120 minutes while the cost decreases from $114 per foot for simple spans to $107 per foot for six span continuous beams; thus, the use of continuity both increases ride quality and reduces cost.

The following modifications to vertical plane construction tolerances have been considered in assessing a ride quality-cost tradeoff.

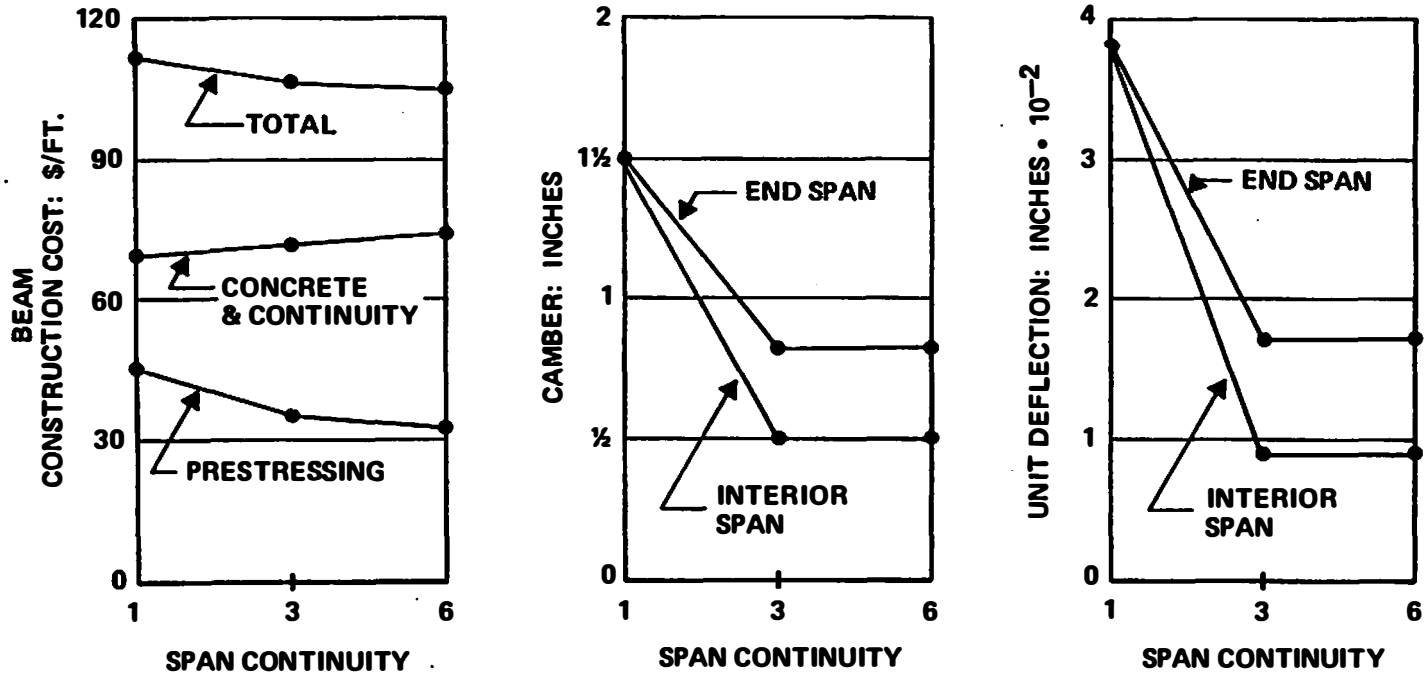

FIGURE 4.3: BEAM COST, CAMBER AND UNIT DEFLECTION AS A FUNCTION OF CONTINUITY FOR A 100 FOOT SPAN LARGE GUIDEWAY

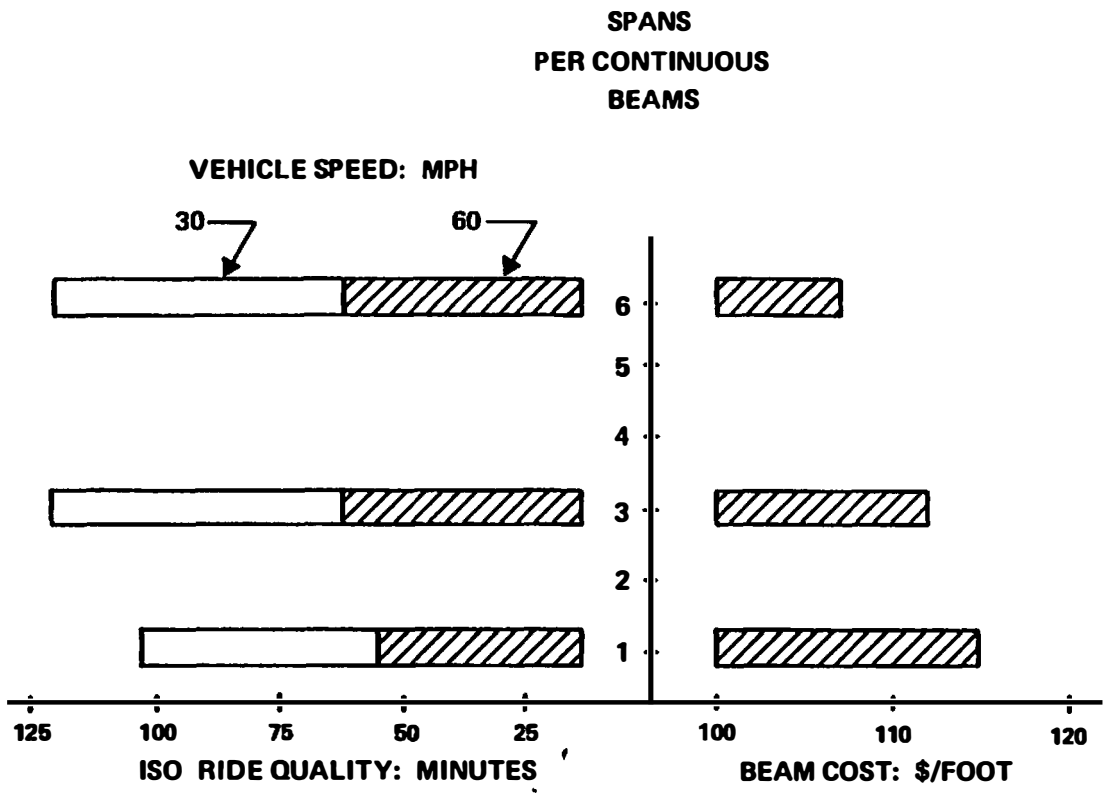

FIGURE 4.4: COST-VERTICAL RIDE QUALITY TRADEOFF AS A FUNCTION OF CONTINUITY FOR A 100 FOOT SPAN LARGE GUIDEWAY

(1) Modification of the Vertical Joint Offset

The value of vertical joint offset, achieved using standard construction techniques, 1/4 inch, can be reduced to 1/8 inch by more accurately shimming the guideway beams on the pier supports. This shimming operation involves use of a crane to support the beam while shimming is performed, a crane operator, part of a foreman and additional labor. If this operation is performed during normal construction then it is estimated to take an extra 30 minutes per joint to achieve the reduction in offset. The cost is $50 per joint or $0.83 per foot for a 60 foot span. If the reduction in offset were made after initial construction is completed then because of crane set up time the cost would increase to $2.83 per foot.

(2) Modification of Pier Height Misalignment

The nominal 1/2 inch pier height adjustment can be reduced to 1/4 inch by using additional shims on low piers and by bush hammering piers which are too high. Under the assumption that every one out of six piers needs additional shimming and one out of every six piers needs bush hammering, the cost of these operations is $522 for every six joints or $1.45 per foot for 60 foot spans.

(3) Modification of the Running Surface with a Ceramic Overlay

Ceramic materials have been recommended for guideways because of their durability. The installation of two ceramic strips, each one foot wide by approximately one inch deep on the guideway has

been studied. The cost of installing these strips of material is $22 per linear foot with $16 per foot associated with the material and the remainder for labor and the cost of light weight concrete to fill in between the strips. With the installation of these strips, the vertical joint offset can be reduced to zero and the random camber component in the guideway reduced from 1/2 to 1/4 inch.

The effects of these modifications on guideway ride quality have been determined for the 60 foot simple span large guideway and summarized in Figure 4.5 with costs for the modification.

The data show that reduction of joint offset from 1/4 to 1/8 inch increases the ride for the baseline guideway at 80 mph from 90 to 130 minutes and at 60 mph from 55 to 80 minutes at an incremental cost of $0.83 per foot if performed at the time of installation. Reduction of the pier height misalignment from 1/2 to 1/4 inch in combination with the joint offset reduction increases the cost with respect to the baseline by $2.28 per foot but does not increase the ride quality in comparison to the case of joint offset reduction. The vertical pier height misalignment does not have a significant influence on ride quality.

The installation of ceramic strips provides a more durable running surface and increases the ride quality with respect to the baseline at 30 mph from 90 to 150 minutes and at 60 mph from 55 to 90 minutes. The cost of this improvement is $22 per foot which represents an incremental cost of the total structure of about 10%. Since

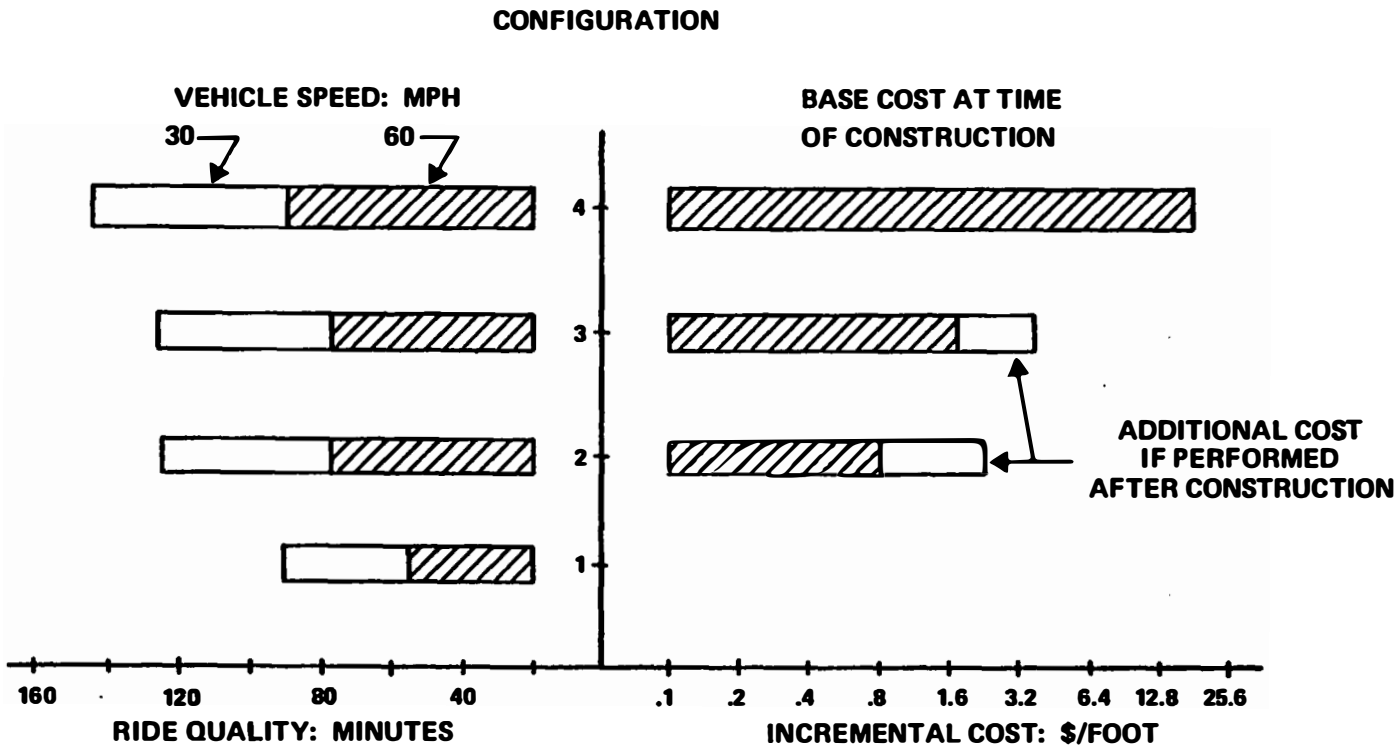

CONFIGURATION

1: Baseline 60 Ft., simple span, guideway

2: Reduction of Joint Offset from 1/4 to 1/8 inch

3: Reduction of Joint Offset from 1/4 to 1/8 inch and of pier height from 1/2 to 1/4 inch

4: Ceramic Overlay to eliminate Joint Offset and reduce random camber from 1/2 to 1/4 inch

FIGURE 4.5: COST-VERTICAL RIDE QUALITY FOR MODIFICATION OF VERTICAL SURFACE PROFILE ON THE 60 FOOT SIMPLE SPAN LARGE GUIDEWAY

much of this incremental cost is due to the cost of the ceramic material, an equivalent reduction in construction tolerances could be achieved at lower cost with the use of a less costly material.

While these cost-ride quality tradeoff results have been determined only for the large vehicle, it is expected that the trends for the small vehicle are similar.

5. SUMMARY AND CONCLUSIONS

This study has developed a procedure for assessing ride quality-construction cost tradeoffs for automated guideway transport elevated guideway systems. The study methodology consists of (1) a guideway configuration analysis in which structural design and costing techniques are used to identify promising guideway configurations, baseline construction tolerance levels, structural parameters and cost sensitivites, (2) a ride quality analysis in which the candidate guideway-vehicle systems are analyzed to determine ride quality levels as a function of operating conditions and (3) a ride quality-cost sensitivity tradeoff study in which the results of two separate analyses are applied iteratively to determine the tradeoffs in system design between ride quality and cost.

This methodology has been applied to a guideway constructed from concrete, prestressed spans of 60-100 foot in length supporting a series of small 10,000 lb or large 20,000 lb GRT vehicles.

The configurational analyses of guideway structures resulted in the design of a series of superstructure-pier foundation structures at sufficient detail to provide for structural integrity and cost calculation. These designs illustrated that guideway cost is particularly sensitive to the factors cited below:

(1) Superstructure - The superstructure is the single most costly part of the overall structure representing 70% of total struc-

tural cost. The following factors have been analyzed for the superstructure:

(A) Basic Span Configuration

A comparison of main support beam configurations has shown that use of a precast, prestressed tapered box beam is cost effective in which the top surface provides the vertical support surfaces for the vehicle and for which permanent, steel forms may be used for exterior surface support and fiber forms for interior surface support during casting. This configuration for simple spans is approximately 76% of the cost of a configuration employing AASHTO standard I-beams.

(B) Section Depth

For a given span length, a minimum section depth exists which will meet structural requirements. The use of a single section depth span design for spans varying in length from 60 to 100 feet was found to be cost effective in comparison to use of a minimum section depth for each span length. This section depth was selected based upon the 100 foot span length. For shorter spans, less prestressing steel was used. This reduction in prestressing steel reduces the total steel costs so that the increased cost of the "excess" concrete is balanced. Thus, an increased depth section was shown to be cost effective and has less camber and is stiffer than a corresponding minimum section depth beam.

(C) Span Continuity

Structural designs for three and six span beams for the small and large guideways were performed. These continuous span designs have less camber, about 50%, and less deflection per unit load than corresponding simple spans. They have costs comparable to or slightly less than corresponding simple spans.

(D) Span Length

The designs for 60, 80 and 100 foot span lengths showed that as span length increases, the cost, unit deflection under load and camber all increase. The cost increases for simple span guideways by 10% as the span length is increased from 60 to 100 feet. Thus, shorter span guideways have both reduced cost and reduced deflection and camber so that ride quality is improved.

(E) Guideway Size

The guideway design for a 10,000 lb, 15 ft x 7 ft vehicle had a cost which was 75% of the design for a 20,000 lb, 27 x 9 foot vehicle. The cost increase for the large vehicle guideway is partially due to increased width and partially to increased weight.

(2) Support Piers - Support pier design for all cases considered in this study was not found to have a direct influence on ride quality.* Studies of pier design have shown a round pier cast-in-place with fiber forms to be cost-effective. It is less than 60%

*The piers are rigid.

of the cost of a precast trapezoidal pier.

(3) Foundation - A spread footing foundation was used as a basis for the study. If soil conditions are so poor that a pile foundation is required, foundation costs would increase by a factor of four, however even with a pile foundation, the foundation plus pier costs are only about 30% of the total structure cost.

Both lateral and vertical motion ride quality were assessed for the small and large vehicles. For baseline levels of construction tolerance, lateral ride quality is influenced weakly by angular panel deviation and strongly by joint offset and surface roughness. Vertical ride quality for baseline levels of construction tolerance is influenced weakly by pier height variations, moderately by joint offset and deflection and strongly by surface roughness and camber. For baseline simple 60 foot span length guideways the following values of ride quality are achieved.

BASELINE ISO RIDE QUALITY: MINUTES

		Lateral	Vertical
small	30 mph	360	150
vehicle	60 mph	150	90
large	30 mph	720	90
vehicle	60 mph	360	55

For the baseline vehicle-guideway systems, the lateral ride quality is very good, while the vertical ride quality exceeds 90 min-

utes at 30 mph and 55 minutes at 60 mph. The small vehicle has better ride quality in the vertical plane and poorer ride quality in the lateral plane than the large vehicle.* As speed increases the ride quality is reduced.

Parametric studies of simple and continuous span systems have shown that the three and six span continuous beams have levels of camber and deflection which are sufficiently small so that ride quality is determined primarily by the guideway construction tolerances and is essentially independent of structural properties.

The vehicle sprung mass suspension natural frequency was shown to have a significant influence upon ride quality. For a reduction in the large vehicle natural frequency from 1.0 to 0.75 hertz, rms acceleration levels were reduced by 50% for 60 mph operation on 100 foot simple spans. Thus, basic vehicle suspension design can have as significant an influence on vehicle ride quality as any of the guideway parameters studied.

Parametric ride quality-cost studies were conducted for the large vehicle to evaluate modifications of baseline construction tolerances on both cost and ride quality. These studies showed that lateral ride quality improvement could be obtained by:

Reduction of joint offset from 1/4 inch to 3/16 inch to yield an improvement in ride quality by a factor of 1.3 at 30 mph and 1.1 at 60 mph in terms of ISO exposure minutes at a cost increase

*The larger yaw inertia of the large vehicle results in its better lateral ride quality while unsprung mass motion results in its poorer vertical ride quality.

of $0.27 per foot.

The reduction of angular errors from the baseline values was not found to significantly change ride quality.

Since the lateral ride quality with baseline construction tolerance levels is very good, a lower quality guideway in which less costly forms are used was studied. For this guideway which has a surface roughness of 1/4 inch under a ten foot straight edge, double the baseline value, a cost reduction of $2.67 per foot, 1.3% of total guideway cost, is achieved yielding a reduction in ride quality by approximately 50% at 30 and 60 mph in terms of ISO exposure minutes compared to the baseline system. However, with this increased roughness an 180 minute ISO ride quality criteria is met at 60 mph operation of the large vehicle.

The parametric studies showed that vertical ride quality improvement may be obtained by:

(1) Reduction of joint offset from 1/4 to 1/8 inch to yield an increase in ride quality by a factor of 1.4 at 30 mph and 60 mph in terms of the ISO exposure limit in minutes at a cost of $0.83 per foot.

(2) Installation of ceramic strips to eliminate joint offset and reduce camber from 1/2 inch to 1/4 inch to yield an improvement in ride quality by a factor of 1.7 at 30 mph and 1.6 at 60 mph at a cost of $22 per foot which is 10% of the total structure cost.

Reduction of angular offset in the vertical plane did not lead to a significant increase in ride quality.

In conclusion, this study has shown that the use of multiple span guideways for GRT systems results in cost effective structures for which ride quality is determined primarily by construction tolerances and is relatively insensitive to structural properties.* For the large GRT vehicle these types of guideways can be constructed for approximately $1m per mile and provide a ride quality nearly equivalent to a 55 minute ISO exposure at 60 mph. The small GRT guideway can be constructed for approximately $800,000 per mile and provides a ride quality equal to a 90 minute ISO exposure at 60 mph. The ride quality in these systems can be improved by reducing construction generated irregularities or by improving vehicle suspension characteristics. For vertical motion a reduction in suspension natural frequency from 1.0 to 0.75 hertz or the use of a ceramic overlay on the guideway yielded factors of 1.5 in ride quality improvement in terms of ISO exposure. Thus changes in both vehicle characteristics and guideway characteristics may have significant influences on ride quality.

Finally, it is noted that the methodology developed in this study for establishing cost-ride quality tradeoffs in GRT systems can be used to establish these tradeoffs for other types of vehicle-guideway systems.

---

*The main structural constraint in beam design is represented by the end-to-end parked vehicle stress condition.

6. REFERENCES

1. "Automated Guideway Transit - An Assessment of PRT and Other New Systems", Office of Technology Assessment, Washington, D.C., 1975.

2. Bernard, D.A. and Houser, C.R., "Engineering Evaluation of the Tracked Air Cushion Research Guideway", FHA Report FHWA-RDDP-DC-400, 1973.

3. "Standard Specification for Highway Bridges", Eleventh Edition, American Association of State Highway and Transportation Officials, 1973.

4. Ravera, R.J. and Anderes, J.R., "Factors in Lightweight Guideway Design and Costing," MITRE Report MTR-6969, 1975.

5. "Steel Structures for Mass Transit", American Iron and Steel Institute, 1976.

6. Hedrick, J.K., Ravera, R.J. and Anderes, J.R., "The Effect of Elevated Guideway Construction Tolerances on Vehicle Quality", ASME Journal of Dynamic Systems, Measurement and Control, 1975.

7. Snyder, J.E. III, Wormley, D.N., and Richardson, H.H., "Automated Guideway Transit Systems: Vehicle Elevated Guideway Dynamics: Multiple Vehicle, Single Span Systems", Report UMTA-MA-11-0028-75-1, 1975.

8. Birkeland, et al., "Investigation of Reduced Cost Guideway Design for the Tracked Air Cushion Research Vehicle", TRW/TRW SYSTEMS/ABAM Report, 96030-L003-0, December 1975.

9. Richardson, H.H. and Wormley, D.N., "Transportation Vehicle/Beam Elevated Guideway Dynamic Interactions: A State of the Art Review", Journal of Dynamic Systems, Measurement and Control, Vol. 96, 1976.

10. Ravera, R.J. and Anderes, J.R., "Analysis and Simulation of Vehicle-Guideway Interactions with Applications to a Tracked Air Cushion Vehicle", MITRE Report MTR-6839, 1975.

11. Lin, T.Y., "Prestressed Concrete Structures", Second Edition Jonn Wiley and Sons, Inc. N.Y. 1963.

12. "1976 Means Construction Cost Data", Robert Snow Means Company, Inc., Duxbury, Mass.

13. "1976 Building Cost File-Eastern Edition", McKee-Berger-Mansueto, Inc., New York, New York.

14. "1976 Dodge Construction Systems Costs", McGraw-Hill Information Systems Co., New York, New York.

15. "1976-1977 The Richardson Rapid System General Construction Estimating Standards", International Construction Analysts, Solana Beach, California.

16. "27th Rental Compilation", Associated Equipment Distributors.

17. "P.C.I. Design Handbook", Prestressed Concrete Institute, Chicago, 1971.

18. Fearnsides, J., Hedrick, J.K., and Firouztash, H., "Specification of Ride Quality Criteria for Transportation Systems: the State-of-the-Art and a New Approach", High Speed Ground Transportation Journal, Vol. 8, 1974.

19. "Guide for Evaluation of Human Exposure to Whole Body Vibration", Draft International Standard ISO/DIS 2631, International Organization for Standardization 1972.

20. Shladover, S., Fish, R., Richardson, H.H., Wormley, D., "Analysis and Design of Steering Controllers for Automated Guideway Transit Vehicles", Report UMTA-RD-MA-11-0023-76-1, September 1976.

21. Wormley, D.N., Smith, C.C., and Gilchrist, A.J., "Multispan Elevated Guideway Design for Passenger Transport Vehicles", Report FRA-OR&D-75-43-1, April 1975.

22. Roy, D.N., "Advanced Technology Materials Applied to Guideways, Highways and Airport Runways", Report DOT-OS-40009, October 1974.

23. Sussman, N.E., "Statistical Ground Excitation Models for High Speed Dynamic Analysis", High Speed Ground Transportation Journal, Vol. 8, 1974.

APPENDIX A

SUMMARY OF STRUCTURAL DESIGN CALCULATIONS FOR SMALL GUIDEWAY

PROJECT Guideway Research ACC. NO. 1
SUBJECT Preliminary Structural Design SHEET NO. A OF
General Data & Assumptions DATE 17 June 1976
COMP. L.E. CHECK CONT. NO. 2791.200

STRUCTURAL DESIGN PARAMETERS

Prestressed Concrete per AASHTO Specifications

Assume $f'_c = 5000$ psi $f'_{ci} = 4000$ psi

Allowable Concrete Stresses:

Temporary Stresses at Transfer

Compression	$0.60 f'_{ci}$	=	+ 2400 psi
Tension	$3\sqrt{f_{ci}}$	=	− 190 psi

Stresses at Design Loads

Compression	$0.40 f'_c$	=	+ 2000 psi
Tension	$6\sqrt{f'_c}$	=	− 424 psi w/ bonded reinf

Prestressing Steel

Use ½"φ Grade 270 strands (ASTM-A416) Area = 0.153 in²
Weight = 0.520#/'

Ultimate Strength $f'_s = 270{,}000$ psi

At transfer $f_{si} = 0.70 f'_s = 189{,}000$ psi $= f^T$

Final effective (15% losses) $= 0.85\,(189{,}000) = 160{,}000$ psi

P_T (max. transfer) $= 0.153 \times 189 = 28.92^k$/strand

P_F (max. final) $= 0.153 \times 160 = 24.48^k$/strand

PROJECT Small Guideway ACC. NO. 2
SUBJECT Simply Supported Spans SHEET NO. 424 OF
DATE 21 March 19 77
COMP. L.E. CHECK CONT. NO. 2791.200

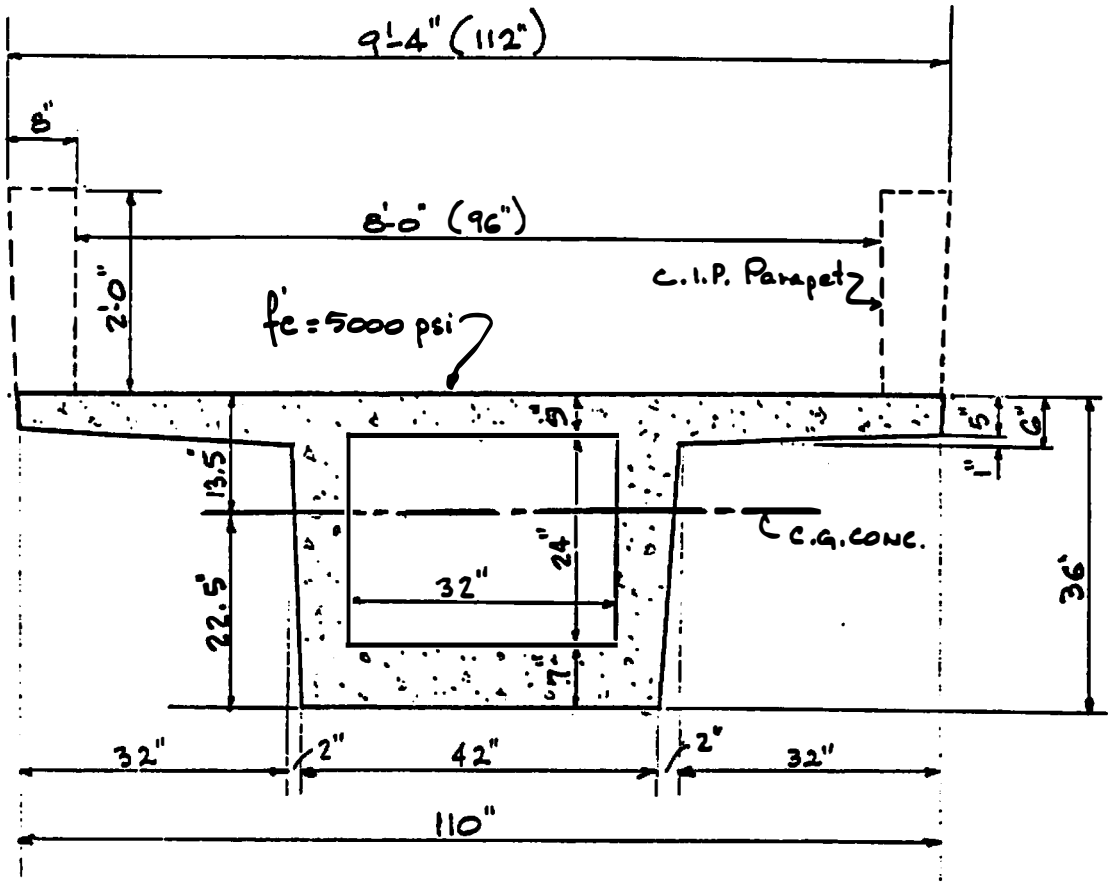

SMALL GUIDEWAY CROSS SECTION

Scale: 1" = 20"

Cross-sectional Area = 1,126 in^2

Moment of Inertia = 192,859 in^4

Weight = 1,173 lb/ft

PROJECT Small Guideway — ACC. NO. 3
SUBJECT Simply Supported Spans — SHEET NO. 403 OF
DATE 27 Dec. 1976
COMP. L.E — CHECK — CONT. NO. 2791.200

Section Properties

			Area	Dist.	Ad
Top Slab, 5" Const.	112 x 5	=	560	33.5	18,760
" " 2 ⊿	2 x 1/2 x 32 x 1	=	32	30.67	981.4
Bot. Slab	42 x 7	=	294	3.5	1029
Side walls	2 x 24 x 5	=	240	14.0	4560
			1126 in²		25,330.4

$y_b = \frac{25,330.4}{1126} = 22.50''$ $\qquad$ $y_t = 36 - 22.5 = 13.50''$

Moment of Inertia

Top slab	1/12 x 112 x 5³	+	560(11.0)²	=	1166.7	+	67,760
Top slab ⊿	2 x 1/36 x 32 x 1³	+	32(8.17)²	=	1.8	+	2,136
Bot. slab	1/12 x 42 x 7³	+	294(14.0)²	=	1200.5	+	106,134
Side walls	2 x 1/12 x 5 x 24³	+	240(3.5)²	=	11,520.0	+	2,940

$\Sigma I = 192,859 \text{ in}^4$

$S_b = \frac{192,859}{22.50} = 8572 \text{ in}^3$ $\qquad$ $S_t = \frac{192,859}{13.50} = 14,286 \text{ in}^3$

$k_b = \frac{14,286}{1126} = 12.69''$ $\qquad$ $k_t = \frac{8572}{1126} = 7.61''$

Weight of Box (excl. Parapets) $= \frac{1126}{144} \times 0.15 = 1.17$ K/ft

Shipping weight

100' Span	1.17 x 100 =	117 K	=	58.5 Tons
80' Span	1.17 x 80 =	93.6 K	=	46.8 Tons
60' Span	1.17 x 60 =	70.2 K	=	35.1 Tons

PROJECT SMALL GUIDEWAY ACC. NO. 4
SUBJECT Simply Supported Spans SHEET NO. 401 OF
DATE 23 Dec. 1976
COMP. L.E. CHECK CONT. NO. 2791.300

SMALL VEHICLE

Length = 15'-0"
Width = 7'-0"
Total Weight = 10,000# or 5,000# per axle

STATIC LIVE LOAD MOMENTS & REACTIONS

From large guideway analysis it was determined that the static live load condition governs structural design

Loading for Max. Pos Mom. @ ℄ of Span

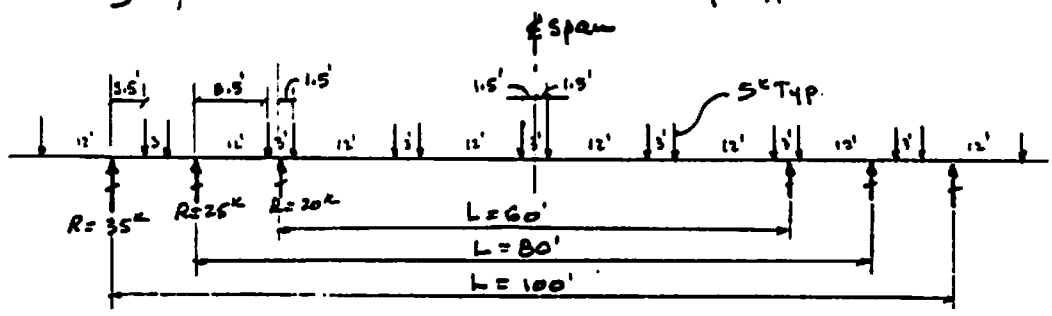

Max. Pos. LL Mom @ ℄ Span

L = 100' M = 35×50 − 5(1.5) − 10(15+30+45) = 842.5'k = 10,110 in-k
L = 80' M = 25×40 − 5(1.5) − 10(15+30) = 542.5'k = 6,510 in-k
L = 60' M = 20×30 − 5(1.5+28.5) − 10(15) = 300'k = 3,600 in-k

Loading for Max. Shear & Reaction

(Locate wheel over support)

L = 100' $\frac{53.5}{100} \times 14 \times 5^k$ = 37.5k
L = 80' $\frac{42}{80} \times 12 \times 5^k$ = 31.5k
L = 60' $\frac{31.5}{60} \times 9 \times 5^k$ = 23.7k

PROJECT SMALL GUIDEWAY ACC. NO. 5
SUBJECT Simply Supported Spans SHEET NO. 40 OF
DATE 27 Dec 1976
COMP. LE CHECK CONT. NO. 2791.200

100' Span

$M_{DL} = 1/8 \times 1.17 \times 100^2 \times 12 = 17,550^{\text{"k}}$

Parapets (For small guideway assume 2'-0" high x 7½" avg. thickness)

$w_{parapets} = 2 \times 2'0" \times \frac{7.5}{12} \times 0.150 = 0.375^k/'$

$M_{parapet} = 1/8 \times 0.375 \times 100^2 \times 12 = 5625^{\text{"k}}$

$\Sigma M = 10,110 + 17,550 + 5625 = \underline{33,285^{\text{"k}}}$

$R_{DL} = 1/2 \times 1.17 \times 100 = 58.5^k$

$R_{parapet} = 1/2 \times 0.375 \times 100 = 18.8^k$

$\Sigma R = 37.5 + 58.5 + 18.8 = \underline{114.8^k}$

Max. avail. $e_{\mathbb{C}} = 22.5 - 3.5 = 19"$

$P^F_{min} = \frac{33,285}{19 + 7.61} = 1251^k$

Try 46 - ½" ϕ strands $P^F = 46 \times 24.48 = 1126^k$

Midspan stresses due to final prestress (P^F)

$f^{PF}_{t,b} = \frac{1126}{1126} \mp \frac{1126(19)}{S_t, S_b} = 1.00 \mp \begin{matrix} 1.498 \\ 2.496 \end{matrix} = \begin{matrix} -0.498 \\ +3.496 \end{matrix}$

Midspan stresses due to external loads

		Top	Bot
DL Box Only	$\frac{17,550}{S_t, S_b}$	+ 1.228	− 2.047
Total Load	$\frac{33,285}{S_t, S_b}$	+ 2.330	− 3.883

PROJECT SHALL GUIDEWAY ACC. NO. 6
SUBJECT Simply Supported Spans SHEET NO. 405 OF
DATE 27 Dec. 19 76
COMP. LE CHECK CONT. NO. 279 1.200

100' Span – Cont'd

Combined Midspan Stresses

		Prestress	Ext. loads	Total
At transfer (DL Box only)	Top	− 0.588	+ 1.228	+ 0.640
	Bot	+ 4.130	− 2.047	+ 2.083 < 2.4 OK.
After transfer (DL Box only)	Top	− 0.498	+ 1.228	+ 0.730
	Bot	+ 3.496	− 2.047	+ 1.449 < 2.0 OK
All loads	Top	− 0.498	+ 2.330	+ 1.832 < 2.0 O.K.
	Bot	+ 3.496	− 3.883	− 0.387 < 0.424 O.K.

46-1/2"φ strands satisfy midspan requirements @ e = 19.0"

END SECTION

Max. e_{end} = tb = 12.69"

End stresses due to final prestress

$$f_{t,b} = \frac{P^F}{A} \mp \frac{P^F e}{S_t, S_b} \qquad P^F = 1126^k$$

$$f_{t,b} = \frac{1126}{1126} \mp \frac{1126(12.69)}{14286/8572} = 1.00 \mp \begin{matrix} 1.000 \\ 1.667 \end{matrix} = \begin{matrix} 0.0 \\ 2.667 > 2.0 \text{ N.G} \end{matrix}$$

Reduce e_{end} to yield a bottom stress under 2 ksi

$$e_{end} = \frac{(2.00 - 1.00) S_b}{P^F} = \frac{1.0 \times 8572}{1126} = \underline{\underline{7.61''}}$$

Check end stresses @ transfer ($P^T = 46 \times 28.92 = 1330.3^k$

$$f_{t,b} = \frac{1330.3}{1126} \mp \frac{1330.3(7.61)}{14286/8572} = 1.181 \mp \begin{matrix} 0.709 \\ 1.181 \end{matrix} = \begin{matrix} +0.472 \\ +2.362 < 2.4 \text{ OK.} \end{matrix}$$

46-1/2"φ strands satisfy end section with e = 7.61"

PROJECT Small Guideway — ACC. NO. 7
SUBJECT Simply Supported Spans — SHEET NO. 406 OF
DATE 27 Dec 1976
COMP. L.E. — CHECK — CONT. NO. 2791.200

100' Span - Cont'd.

Ultimate Flexural Strength

$$M_u \text{ reqd} = 1.3\left[(17,550 + 5625) + 1.67(10,110)\right] = 52,076''^k$$

$$p^* = \frac{A_s^*}{bd} = \frac{46 \times 0.153}{112(36-3.5)} = 0.00193$$

$$f_{su}^* = 270\left(1 - \frac{0.5 \times 0.00193 \times 270}{5}\right) = 255.93$$

$$M_u \text{ furn.} = A_s^* f_{su}^* d \left(1 - 0.6 \frac{p^* f_{su}^*}{f'_c}\right) =$$

$$= 46 \times 0.153 \times 255.93 \times 32.5\left(1 - \frac{0.6 \times 0.00193 \times 255.93}{5}\right) = 55,070'^k$$

$$M_u \text{ furn.} = 55,070''^k \quad > \quad M_u \text{ reqd} = 52,076''$$

Section adequate for ultim. load cap.

Note: No need to check ultimate capacity for the shorter span lengths if the same cross section is used — as excess strength is provided. (See large guideway)

PROJECT Small Guideway — ACC. NO. 8
SUBJECT Simply Supported Spans — SHEET NO. A07 OF
DATE 27 Dec 1976
COMP. L.E — CHECK — CONT. NO. 2791.200

100' Span - Cont'd

CAMBERS — using 2 point drape

CONSTANTS: $I = 192{,}859$ $E = 3.6\times10^3$ $e_{\mathbb{C}} = 19.0''$ $e_{end} = 7.61''$ $P^T = 1330.3^k$

$$\Delta\, P/S\, \mathbb{C} = \frac{L^2}{8EI}\left[M_2 + M_1 - \frac{M_1}{3}\left(\frac{2a}{L}\right)^2\right] \qquad a = \frac{L}{4} = 25'$$

$y_1 = e_{\mathbb{C}} - e_{end} = 19.0 - 7.61 = 11.39''$ $\qquad M_1 = P^T y_1 = 1330.3 \times 11.39 = 15{,}152$

$y_2 = e_{end} = 7.61$ $\qquad M_2 = P^T y_2 = 1330.3 \times 7.61 = 10{,}124$

$$\Delta\, P/S = \frac{100^2 \times 144}{8 \times 3.6\times10^3 \times 192{,}859}\left[10{,}124 + 15{,}152 - \frac{15{,}152}{3}\left(\frac{2\times25}{100}\right)^2\right] = -6.23'' \uparrow$$

$$\Delta\, DL\ Box = \frac{5wL^4}{384EI} = \frac{5 \times 1.17 \times 100^4 \times 1728}{384 \times 3.6\times10^3 \times 192{,}859} = 3.79'' \downarrow$$

Initial Camber = $6.23 - 3.79 = 2.44'' \uparrow$

Final Camber = $1.143 \times 2.44 = 2.79'' \uparrow$

$\Delta\, DL$ Parapet $= \frac{0.375}{1.17} \times 3.79 = 1.21'' \downarrow$

$\mathbb{C}$ CAMBER (before L.L.) $= 2.79 - 1.21 = \underline{1.58'' \uparrow}$

(was 1.91" for large guideway!)

PROJECT Small Guideway — ACC. NO. 9
SUBJECT Simply Supported Spans — SHEET NO. 412 OF
Parapet — DATE 29 Dec 19 76
COMP. L.E. — CHECK — CONT. NO. 2791.200

Parapet Side Wall

Parapet to be 3000 psi c.i.p. Concrete

For criteria see sh. B — General Criteria

Horizontal Force = Wt of Vehicle = 10,000 lb

Distribute the force over an area equal to width of vehicle and parapet height minus 6"

$$\text{Area} = 7' \times (2'0" - 0'6") = 10.5\ ft^2$$

$$\text{Uniform load} = \frac{P}{A} = \frac{10{,}000}{10.5} = 952\ \#/SF$$

Apply the uniform load over the whole 2'0" height of parapet

$$M = 1/2 \times 0.952 \times 2^2 = 1.90\ ^{1k}/ft$$

$$d\ req'd = \sqrt{\frac{1.90}{0.178}} = 3.27" < 7" - 1\tfrac{1}{2}"\ cov. = 5\tfrac{1}{2}"$$

$$A_s\ req'd = \frac{1.90}{1.78 \times 5.5} = 0.19\ in^2$$

Conservatively use #5@12" Inside face

Outside face use #4@12"

Horizontally use 3-#4 each face

PROJECT SMALL GUIDEWAY ACC. NO. 10
SUBJECT Simply Supported Spans SHEET NO. 413 OF
DATE 30 Dec 1976
COMP. LE CHECK CONT. NO. 2791.200

SHEAR REINFORCEMENT

$$A_v = \frac{(V_u - V_c)s}{2 f_{sy}\, jd}$$

$$V_c = 0.06 f_c' b' jd = 0.06 \times 5 \times (2 \times 5) \times 7/8 \times 32.5 = 85.3^k$$

$$\text{or } V_c = \frac{180\, b' jd}{1000} = \frac{180\,(2\times5)\,7/8 \times 32.5}{1000} = 51.2^k \leftarrow \text{governs}$$

$V_{u\,max}$ @ support, $L = 100'$ $= 1.3\left[(58.5+18.8) + 1.67(37.5)\right] = 181.9^k$

Critical shear for design is at 1/4 point of span

V_{DL+SDL} @ 1/4 pt $= 1/2\,(58.5+18.8) = 38.7^k$

V_{LL} static @ 1/4 pt = approx. $90\% \times 37.5 = 33.8^k$

Design Shear $= 1.3\left[38.7 + 1.67(33.8)\right] = 123.7^k$

$V_u - V_c = 123.7 - 51.2 = 72.5^k$

Assume #4 double leg stirrups in each of two webs

$A_v = 2 \times 2 \times 0.20 = 0.80\ in^2$

$$\text{Spacing of \#4 stirrups} = \frac{2 f_{sy}\, jd\, A_v}{V_u - V_c} = \frac{2 \times 60 \times 7/8 \times 32.5 \times 0.80}{72.5} = 37.7''$$

Use 18" max. spacing thruout for all spans

$$\text{Min. } A_v \text{ req'd} = 100\, b's / f_{sy} = \frac{100\,(2\times5)(18)}{60{,}000} = 0.3\ in^2 < 0.80 \quad \underline{\text{o.k.}}$$

<u>use double #4 stirrups @ 18" o.c. for all webs for all spans</u>

PROJECT SMALL GUIDEWAY ACC. NO. 11
SUBJECT Simply Supported Spans SHEET NO. 414 OF
DATE 30 Dec 19 76
COMP. L.E. CHECK CONT. NO. 2791.200

CONVENTIONAL REINF. IN BOX SECTIONS

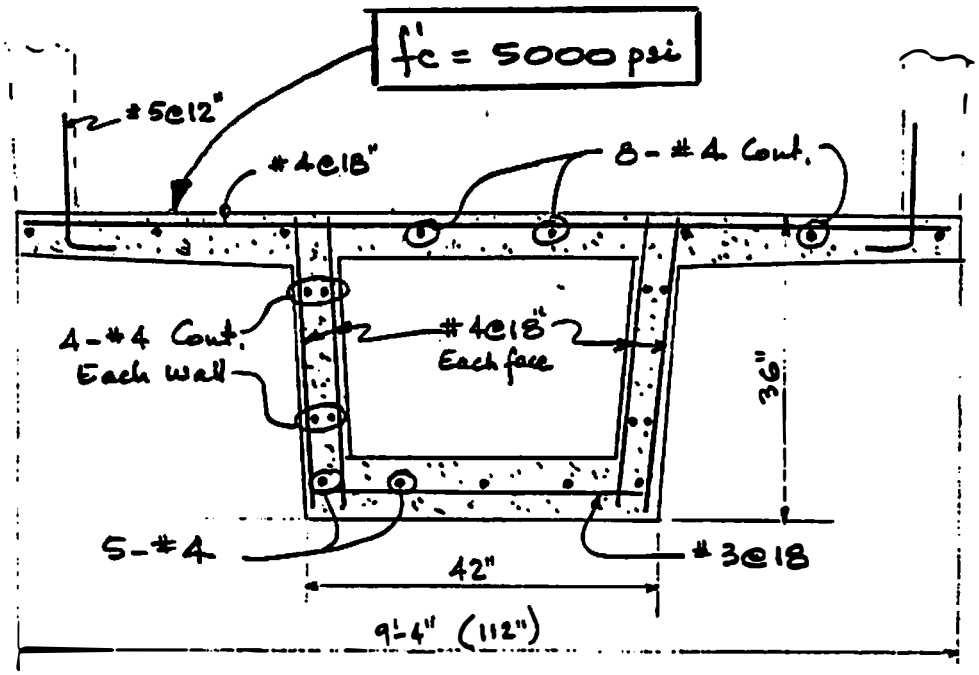

The above reinf. is Typical for all spans

CAST-IN-PLACE PARAPET REINFORCING

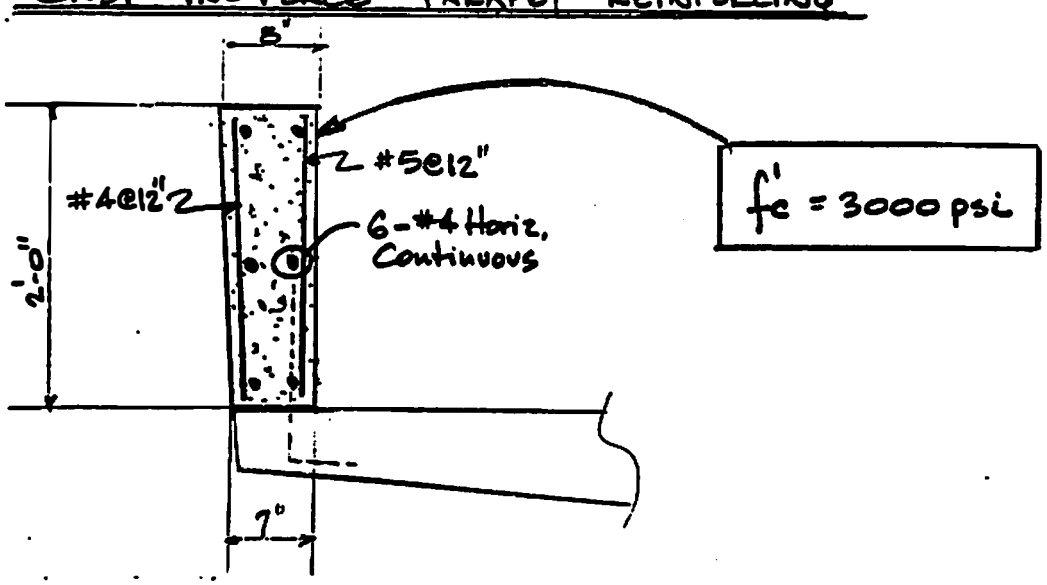

PROJECT Small Guideway — ACC. NO. 12
SUBJECT Simply Supported Spans — SHEET NO. 415 OF
DATE 30 Dec 1976
COMP. L.E — CHECK — CONT. NO. 2791.200

ELASTOMERIC BEARINGS @ PIERS

Reactions:

Span	Total React.	Load per Bearing
100	114.8^k	58^k
80	93.3^k	47^k
60	70.1^k	35^k

Allow. press on concrete = 800 psi

Span	Req'd Area = $\frac{P}{0.800}$	Req'd Size	Area Furnished
100	72.5 in^2	6" x 14" x 1½	84 in^2
80	58.75	6 x 10 x 1¼	60
60	43.75	6 x 8 x 1"	48

Based on max. movement per Conveco Catalogue

ELASTOMERIC BEARING SUMMARY (Small Guideway - Simple Spans)

Span Length	No. of Bearings per Span	Size of Bearing Width x Length x Thickness	Hardness
100'	4	6" x 14" x 1½"	60 Durometer
80'	4	6" x 10" x 1¼"	"
60'	4	6" x 8" x 1"	"

Pier Design (Small Guideway - Simply Supported Spans)

Wind on Superstructure (Gr. III @ 30% of Full Wind)

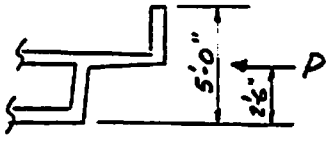

$P_{TR} = 0.30 \times 50\#/SF \times 5' =$ 75#/LF of span

$P_{long} = 0.30 \times 12\#/SF \times 5' =$ 18#/LF of span (24% of P_{TR})

Mom. @ Bott. of Col.

$L = 100'$ $M_{TR} = 0.075 \times 100 (18 + 2.5) = 154^{'k}$
$M_{long} = 0.24\ M_{TR} = 37^{'k}$

$L = 80'$ $M_{TR} = 0.075 \times 80 (18 + 2.5) = 123^{'k}$
$M_{long} = 30^{'k}$

$L = 60'$ $M_{TR} = 0.075 \times 60 (18 + 2.5) = 92^{'k}$
$M_{long} = 22^{'k}$

Wind on Live Load (Apply @ 6' above deck — arm = 24')

Mom @ Bott of Col.

$L = 100'$ $M_{TR} = 0.100 \times 100 \times 24 = 240^{'k}$
$M_{long} = 0.040 \times 100 \times 24 = 96^{'k}$

$L = 80'$ $M_{TR} = 0.100 \times 80 \times 24 = 192^{'k}$
$M_{long} = 0.040 \times 80 \times 24 = 77^{'k}$

$L = 60'$ $M_{TR} = 0.100 \times 60 \times 24 = 144^{'k}$
$M_{long} = 0.040 \times 60 \times 24 = 58^{'k}$

Overturning Wind Force (6 psf)

$L = 100'$ $M_o = 0.006 \times 9 \times \frac{9}{4} \times 100 = 12^{'k}$

$L = 80'$ $M_o =$ 80% $10^{'k}$

$L = 60'$ $M_o =$ 60% $8^{'k}$

PROJECT SMALL GUIDEWAY — ACC. NO. 14
SUBJECT Simply Supported Spans — SHEET NO. 419 OF
Substructure — DATE 30 Dec 19 76
COMP. L.E — CHECK — CONT. NO. 2791.200

PIER DESIGN - Cont'd

Summary of Group III Wind Moments @ Bot. of Col.

$L = 100'$ $\quad \Sigma M = \sqrt{(154+240+12)^2 + (37+96)^2} = 427^{'k} = 5124^{''k}$

$L = 80'$ $\quad \Sigma M = \sqrt{(123+192+10)^2 + (30+77)^2} = 342^{'k} = 4104^{''k}$

$L = 60'$ $\quad \Sigma M = \sqrt{(92+144+8)^2 + (22+58)^2} = 257^{'k} = 3084^{''k}$

Column Vertical Loads

$L = 100'$	Superstr. DL+SDL	$(1.17+0.38)\times 100$	=	155
	Superstr. L.L.	2×35	=	70
	Pier Col & Cap		=	32
				257^k
$L = 80'$	DL+SDL	$(1.17+0.38)\times 80$	=	124
	LL	2×25	=	50
	Col & Cap		=	28
				202^k
$L = 60'$	DL+SDL	$(1.17+0.38)\times 60$	=	93
	LL	2×20	=	40
	Col. & Cap		=	24
				157^k

COLUMN DESIGN ($f'_c = 3000$, $f_y = 60{,}000$, $g = 0.8$)

Span	P kips	M in-kips	Diamet. in	$f'_c A_g$	$\frac{P}{f'_c A_g}$	$\frac{M}{f'_c t A_g}$	P_g chart	A_s Req'd	No of Bars
100	257	5124	36	3054	0.084	0.047	2.2%	22.4	15 - #11
80	202	4104	33	2565	0.079	0.048	2.2%	18.8	13 - #11
60	157	3084	30	2121	0.074	0.048	2.3%	16.3	11 - #11

Use #4 spiral @ 3" pitch for all columns

11-72B

PROJECT Small Guideway — ACC. NO. 15
SUBJECT Simply Supported Spans — SHEET NO. 420 OF
Substructure — DATE 3 Jan. 1977
COMP. LE — CHECK — CONT. NO. 2791.200

Pier Footing Design

100' Span

Try 16×8×2 Ftg. Weight = $16\times8[2\times0.150 + 2\times0.120] = 69^k$ (0.54)

$A = 16\times8 = 128$ $S_T = \frac{1}{6}\times8\times16^2 = 341$ $S_L = \frac{1}{6}\times16\times8^2 = 171$

$P = 257+69 = 326^k$ $M_T = 406^{'k}$ $M_L = 133^{'k}$

$f = \frac{326}{128} \pm \frac{406}{341} \pm \frac{133}{171} = 2.55 \pm 1.19 \pm 0.78 = 4.52$ ksf < 5 ok (0.58)

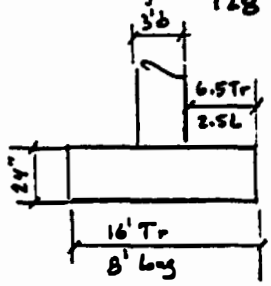

Net press = 4.52 − 0.54 = 3.98 ksf ↑

$M_T = \frac{1}{2}\times3.98\times6.5^2 = 84.1^{'k}/ft$

$d_{req'd} = \sqrt{\frac{84.1}{0.178}} = 21.7$ say ok 21" provided

$A_{s\,req'd} = \frac{84.1}{1.78\times21} = 2.25\ in^2/ft \times 8' = 18\ in^2$ Total

Use 15 - #10 Bot. Transv.

$M_L = \frac{1}{2}\times3.98\times2.5^2 = 12.4^{'k}/ft$ $A_{s\,req'd} = \frac{12.4}{1.78\times21} = 0.33$ use #5@12 Bot.

Top — use #5@12" Both ways

80' Span

Try 14×7×2 Ftg Weight = $14\times7[2\times0.150 + 2\times0.120] = 53^k$ (0.54)

$A = 14\times7 = 98$ $S_T = \frac{1}{6}\times7\times14^2 = 229$ $S_L = \frac{1}{6}\times14\times7^2 = 114$

$P = 202+53 = 255^k$ $M_T = 325^{'k}$ $M_L = 107^{'k}$

$f = \frac{255}{98} \pm \frac{325}{229} \pm \frac{114}{107} = 2.60 \pm 1.42 \pm 1.07 = 5.09 \simeq 5$ ksf ok (0.11)

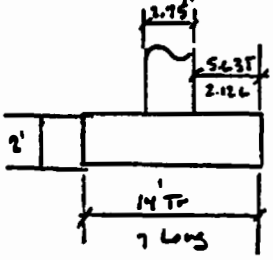

Net press = 5.09 − 0.54 = 4.55 ksf ↑

$M_T = \frac{1}{2}\times4.55\times5.63^2 = 72.1^{'}/ft$

$A_{s\,req'd} = \frac{72.1}{1.78\times21}\times7' = 13.5\ in^2$ Total Use 11 - #10 Bot. Transv

All other reinf #5@12"

11-72B

PROJECT Small Guideway — ACC. NO. 16
SUBJECT Simply Supported Spans — SHEET NO. 421 OF
Substructure — DATE 3 Jan. 1977
COMP. LE — CHECK — CONT. NO. 2791.200

Pier Footing Design

60' Span

Try 12 x 7 x 2 Ftg Weight = $12 \times 7 \left[2 \times 0.150 + 2 \times 0.120\right] = 45^k$ (0.54)

$A = 12 \times 7 = 84$ $S_T = \frac{1}{6} \times 7 \times 12^2 = 168$ $S_L = \frac{1}{6} \times 12 \times 7^2 = 98$

$P = 157 + 45 = 202^k$ $M_T = 244'^k$ $M_L = 80'^k$

$f = \frac{202}{84} \pm \frac{244}{168} \pm \frac{80}{98} = 2.40 \pm 1.45 \pm 0.82 = 4.67$ ksf < 8.0
0.13

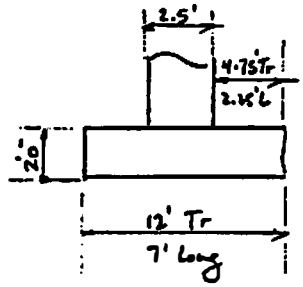

Net press = 4.67 - 0.54 = 4.13 ksf ↑

$M_T = \frac{1}{2} \times 4.13 \times 4.75^2 = 46.6'^k$

As reqd = $\frac{46.6}{1.78 \times 21} \times 7' = 8.73 in^2$ Total

Use 7 - #10 Bot Transv

All other reinf #5 @ 12"

Footing Quantities (For Estim)

Concrete

100'	16 x 8 x 2 x 1/27 =	9.5 c.y.
80'	14 x 7 x 2 x 1/27 =	7.3 c.y.
60'	12 x 7 x 2 x 1/27 =	6.2 cy

Reinforcing

	L = 100'		L = 80'		L = 60'	
Bot. Long	15 - #10 x 16' @ 4.303 =	1033	11 - #10 x 14' @ 4.303 =	663	7 - #10 x 12' @ 4.303 =	362
Bot Trans	16 - #5 x 8' @ 1.043 =	134	14 - #5 x 7' @ 1.043 =	102	12 - #5 x 7' @ 1.043 =	88
Top Long	8 - #5 x 16' " =	134	7 - #5 x 14' " =	102	7 - #5 x 12' " =	88
Top Trans	16 - #5 x 8' " =	134	14 - #5 x 7' " =	102	12 - #5 x 7' " =	88
		1435#		969#		626#

PROJECT Small Guideway — ACC. NO. 17
SUBJECT Simply Supported Spans — SHEET NO. 422 OF
Pier Design Summary — DATE 3 Jan 1977
COMP. LE — CHECK — CONT. NO. 2791.200

Pier Design Summary (Small Guideway - Simply Supported Spans)

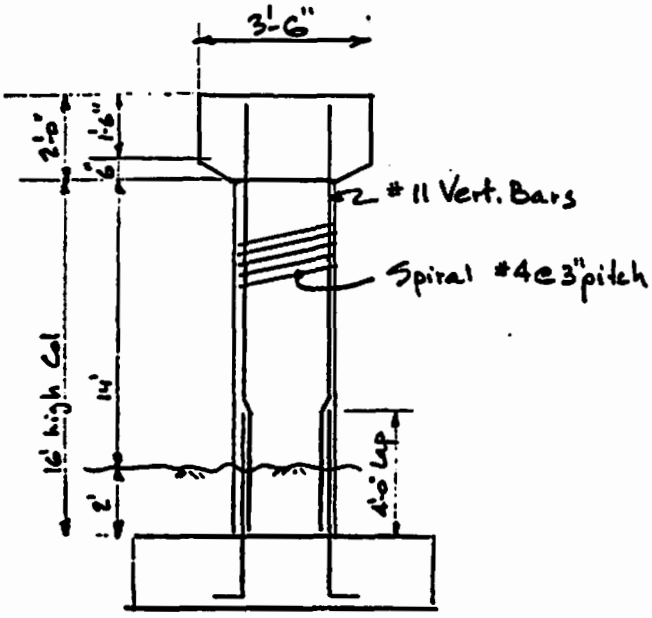

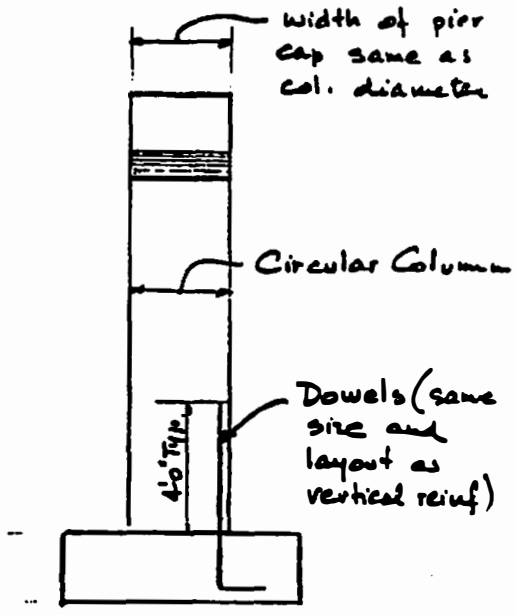

ALL PIER CONCRETE f'_c = 3000 psi

Span (Simply Supported)	Columns: Col. Diameter inches	Columns: Column Vertical Reinf and Dowels	Pier Cap: Width of pier cap	Pier Cap: Cu. yds Concrete in pier cap	Pier Cap: Pounds Reinforc'g in Pier Cap	Footing: Size of Footing Length, Width Thickness	Footing: Cu Yds Concrete in Footing	Footing: Pounds of Reinforc'g in Footing
100'	36"	15 - #11	3'-0"	0.78	120	16' x 8' x 2'	9.5	1435
80'	33"	13 - #11	2'-9"	0.71	115	14' x 7' x 2'	7.3	969
60'	30"	11 - #11	2'-6"	0.65	110	12' x 7' x 2'	6.2	626

APPENDIX B

SUMMARY DESIGN COST CALCULATIONS

DESIGN I SUMMARY

Large Guideway, Simply Supported AASHTO I-Beams

DIV.	ITEM DESCRIPTION	LABOR	MATERIAL	HAULING	ERECTION	TOTAL
1.1	60' SPAN COST PER L.F.					
	Earthwork	1 02	1 10			2 12
	Concrete Footing	5 91	8 63			14 54
	Conc. Pier	5 77	9 98			15 75
	Conc. Cap	3 32	2 71			6 03
	Beam Girders	25 55	39 74	6 12	7 19	78 60
	Diaphrams	5 55	4 65			10 20
	Upper Section	41 51	28 13	9 69	17 10	96 43
	Joint Sealer	0 28	1 26			1 54
	Elast. Bearings	0 15	3 03			3 18
	Anchorage	3 53	1 29			4 82
	SUB-TOTAL	92 59	100 52	15 81	24 29	233 21
1.2	80' SPAN COST PER L.F.					
	Earthwork	0 93	1 02			1 95
	Conc. Footing	5 15	7 65			12 80
	Conc. Pier	5 14	8 91			14 05
	Conc. Cap	2 63	2 17			4 80
	Beam Girders	34 51	57 20	10 95	9 09	111 75
	Diaphrams	6 07	5 09			11 16
	Upper Section	41 51	28 13	9 69	17 10	96 43
	Joint Sealer	0 21	1 01			1 22
	Elast. Bearings	0 14	2 84			2 98
	Anchorage	3 53	1 29			4 82
	SUB-TOTAL	99 82	115 31	20 64	26 19	261 96
1.3	100' SPAN COST PER L.F.					
	Earthwork	0 83	091			1 74
	Conc. Footing	5 08	7 71			12 79
	Conc. Pier	4 80	8 83			13 63
	Conc. Cap	2 22	1 86			4 08
	Beam Girders	43 59	74 17	15 68	11 98	145 42
	Diaphrams	6 85	5 73			12 58
	Upper Section	41 51	28 13	9 69	17 10	96 43
	Joint Sealer	0 17	1 13			1 30
	Elast. Bearings	0 14	2 73			2 87
	Anchorage	3 53	1 29			4 82
		108 72	132 49	25 37	29 08	295 66

DESIGN 2 SUMMARY

Large Guideway, Simply Supported Vertical Box Beams

DIV.	ITEM DESCRIPTION	LABOR	MATERIAL	HAULING	ERECTION	TOTAL
2.1	60' SPAN COST PER L.F.					
	Earthwork	1 09	1 17			2 26
	Conc. Footing	5 27	7.40			12 67
	Conc, Pier	6 96	11 77			18 73
	Conc. Cap	2 67	2 25			4 92
	P. C. Box Section	76 72	36 02			112 74
	Hauling			12 64		12 64
	Erection				20 18	20 18
	Joint Sealer	0 28	1 26			1 54
	Elast. Bearings	0 04	0 80			0 84
	7/8" Railings	19 47	11 45			30 92
	SUB-TOTAL	112 50	72 12	12 64	20 18	217 44
2.2	80' SPAN COST PER L.F.					
	Earthwork	0 93	1 02			1 95
	Conc. Footing	4 65	6 69			11 34
	Conc. Pier	6 26	10 58			16 84
	Conc. Cap	2 09	1 81			3 90
	P. C. Box Section	79 55	44 52			124 07
	Hauling			13 78		13 78
	Erection				21 68	21 68
	Joint Sealer	0 28	1.26			1 54
	Elast. Bearings	0 05	1 05			1 10
	7/8" Railings	19 47	11 45			30 92
	SUB-TOTAL	113 28	78 38	13 78	21 68	227 12
2.3	100' SPAN COST PER L.F.					
	Earthwork	0 87	0 96			1 83
	Conc. Footing	4 42	6.48			10 90
	Conc. Pier	5 86	10.43			16 29
	Conc. Cap	1 74	1 53			3 27
	P. C. Box Section	83 33	55.86			139 19
	Hauling			15 04		15 04
	Erection				24 18	24 18
	Joint Sealer	0 17	1 14			1 31
	Elast. Bearings	0 07	1.30			1 37
	7/8" Railings	19 47	11 45			30 92
	SUB-TOTAL	115 93	89 15	15 04	24 18	244 30

DESIGN 3A SUMMARY

Large Guideway, Simply Supported Sloping Box Beams

DIV	ITEM DESCRIPTION	LABOR	MATERIAL	HAULING	ERECTION	TOTAL
3A.1	60' SPAN - COST PER L.F.					
	Earthwork	1 09	1 17			2 26
	Concrete Footing	5 27	7 40			12 67
	Concrete Pier	6 96	11 77			18 73
	Concrete Cap	2 01	1 72			3 73
	P. C. Box Section	31 25	54 69			85 94
	Hauling			12 98		12 98
	Erection				21 66	21 66
	Joint Sealer	0 28	1 27			1 55
	Elast. Bearings	0 04	0 80			0 84
	7 7/8" Railings	19 47	11 45			30 92
	SUB-TOTAL	66 37	90 27	12 98	21 66	191 28
3A.2	80' SPAN - COST PER L.F.					
	Earthwork	0 93	1 02			1 95
	Concrete Footing	4 65	6 69			11 34
	Concrete Pier	6 26	10 58			16 84
	Concrete Cap	1 58	1 36			2 94
	P. C. Box Section	34 05	63 26			97 31
	Hauling			14 22		14 22
	Erection				21 66	21 66
	Joint Sealer	0 21	1 01			1 22
	Elast. Bearings	0 05	1 05			1 10
	7 7/8" Railings	19 47	11 45			30 92
	SUB-TOTAL	67 20	96 42	14 22	21 66	199 50
3A.3	100' SPAN - COST PER L.F.					
	Earthwork	0 87	0 96			1 83
	Concrete Footing	4 42	6 48			10 90
	Concrete Pier	5 86	10 43			16 29
	Concrete Cap	1 32	1 14			2 46
	P. C. Box Section	37 83	74 87			112 70
	Hauling			15 44		15 44
	Erection				21 66	21 66
	Joint Sealer	0 17	1 14			1 31
	Elast. Bearings	0 07	1 30			1 37
	7 7/8" Railings	19 47	11 45			30 92
	SUB-TOTAL	70 01	107 77	15 44	21 66	214 88

DESIGN 4A SUMMARY

Large Guideway, 6-Span Continuous Sloping Box Beams

DIV	ITEM DESCRIPTION	LABOR	MATERIAL	HAULING	ERECTION	TOTAL
4A.1	60' SPAN - COST PER L.F.					
	Earthwork	1 21	1 26			2 47
	Conc. Footing	4 98	6 75			11 73
	Conc. Pier	5 83	10 05			15 88
	Conc. Cap	1 95	1 60			3 55
	P. C. Box Section	31 44	53 35			84 79
	Hauling			12 98		12 98
	Erection				21 66	21 66
	Joint Sealer	0 50	3 25			3 75
	Elast. Bearing	0 57	0 95			1 52
	7/8" Railings	19 47	11 45			30 92
	SUB-TOTAL	65 95	88 66	12 98	21 66	189 25
4A.2	80' SPAN - COST PER L.F.					
	Earthwork	1 03	1 08			2 11
	Conc. Footing	4 50	6 30			10 80
	Conc. Pier	5 17	9 02			14 19
	Conc. Cap	1 51	1 26			2 77
	P. C, Box Section	33 78	60 76			94 54
	Hauling			14 22		14 22
	Erection				21 66	21 66
	Joint Sealer	0 47	4 38			4 85
	Elast. Bearing	0 46	1 29			1 75
	7/8" Railings	19 47	11 45			30 92
	SUB-TOTAL	66 39	95 54	14 22	21 66	197 81
4A.3	100' SPAN - COST PER L.F.					
	Earthwork	0 92	0 97			1 89
	Conc. Footing	4 37	6 32			10 69
	Conc. Pier	4 89	8 52			13 41
	Conc. Cap	1 24	1 02			2 26
	P. C. Box Section	37 29	71 53			108 82
	Hauling			15 44		15 44
	Erection				21 66	21 66
	Joint Sealer	0 63	5 50			6 13
	Elast. Bearings	0 40	1 66			2 06
	7/8" Railings	19 47	11 45			30 92
	SUB-TOTAL	69 21	106 97	15 44	21 66	213 28

DESIGN 5 SUMMARY

Large Guideway, 3-Span Continuous Sloping Box Beams

DIV.	ITEM DESCRIPTION	LABOR	MATERIAL	HAULING	ERECTION	TOTAL
5.1	60' SPAN - COST PER L.F.					
	Earthwork	1 05	1 14			2 19
	Concrete Footing	4 69	6 28			10 97
	Concrete Pier	5 28	8 87			14 10
	Concrete Cap	2 25	1 75			4 00
	P. C. Box Section	31 34	53 28			84 62
	Hauling			12 98		12 98
	Erection				21 66	21 66
	Joint Sealer	0 41	1 86			2 26
	Elast. Bearing	0 51	1 22			1 73
	7"/8" Railings	19 47	11 45			30 92
	SUB-TOTAL	64 94	85 85	12 98	21 66	185 43
5.2	90' SPAN - COST PER L.F.					
	Earthwork	0 90	0 98			1 88
	Concrete Footing	4 24	5 89			10 13
	Concrete Pier	4 66	8 41			13 07
	Concrete Cap	1 76	1 39			3 15
	P. C. Box Section	33 84	61 08			94 92
	Hauling			14 22		14 22
	Erection				21 66	21 66
	Joint Sealer	0 30	1 49			1 79
	Elastic Bearing	0 43	1 84			2 27
	7"/8" Railings	19 47	11 45			30 92
	SUB-TOTAL	65 60	92 53	14 22	21 66	194 01
5.3	100' SPAN - COST PER L.F.					
	Earthwork	0 79	0 84			1 63
	Concrete Footing	4 04	5 76			9 80
	Concrete Pier	3 98	7 42			11 40
	Concrete Cap	1 45	1 17			2 62
	P. C. Box Section	37 35	71 86			109 21
	Hauling			15 44		15 44
	Erection				21 66	21 66
	Joint Sealer	0 24	1 67			1 91
	Elast. Bearings	0 38	2 29			2 67
	7"/8" Railings	19 47	11 45			30 92
	SUB-TOTAL	67 70	102 46	15 44	21 66	207 26

DESIGN 6 SUMMARY

Small Guideway, Simply Supported Sloping Box Beams

DIV.	ITEM DESCRIPTION	LABOR	MATERIAL	HAULING	ERECTION	TOTAL
6.1	60' SPAN - COST PER L. F.					
	Earthwork	0 76	0 82			1 58
	Concrete Footing	4 12	5 47			9 59
	Concrete Pier	5 26	8 97			14 23
	Concrete Cap	1 47	1 24			2 71
	P. C. Box Section	22 92	41 38			64 30
	Hauling			9 64		9 64
	Erection				17 11	17 11
	Joint Sealer	0 23	1 04			1 27
	Elast. Bearings	0 03	0 64			0 67
	7"/8" Conc. Railings	14 77	6 86			21 63
	SUB-TOTAL	49 56	66 42	9 64	17 11	142 73
6.2	80' SPAN - COST PER L.F.					
	Earthwork	0 67	0 79			1 46
	Concrete Footing	3 83	5 31			9 14
	Concrete Pier	3 61	6 41			10 02
	Concrete Cap	1 15	0 98			2 13
	P. C. Box Section	25 13	48 00			73 13
	Hauling			10 56		10 56
	Erection				17 11	17 11
	Joint Sealer	0 17	0 83			1 00
	Elast. Bearings	0 04	0 75			0 79
	7"/8" Conc. Railings	14 77	6 86			21 63
	SUB-TOTAL	49 37	69 93	10 56	17 11	146 97
6.3	100' SPAN - COST PER L.F.					
	Earthwork	0 65	0 77			1 42
	Concrete Footing	4 01	5 81			9 82
	Concrete Pier	4 17	7 22			11 39
	Concrete Cap	0 95	0 83			1 78
	P. C. Box Section	27 65	55 56			83 21
	Hauling			11 46		11 46
	Erection				17 11	17 11
	Joint Sealer	0 14	0 93			1 07
	Elast. Bearings	0 05	1 01			1 06
	7"/8" Conc. Railings	14 77	6 86			21 63
	SUB-TOTAL	52 39	78 99	11 46	17 11	159 95

DESIGN 7 SUMMARY

Small Guideway, 6-Span Continuous Sloping Box Beams

DIV.	ITEM DESCRIPTION	LABOR	MATERIAL	HAULING	ERECTION	TOTAL
7.1	60' SPAN - COST PER L.F.					
	Earthwork	0 98	1 04			2 02
	Concrete Footing	4 43	5 93			10 36
	Conc. Pier	5 53	9 67			15 20
	Conc. Cap	1 30	1 06			2 36
	P. C. Box Section	23 11	40 39			63 50
	Hauling			9 64		9 64
	Erection				17 11	17 11
	Joint Sealer	0 40	2 60			3 00
	Elast. Bearing	0 53	1 66			2 19
	7"/8" Railing	14 77	6 36			21 63
	SUB-TOTAL	51 05	69 21	9 64	17 11	147 01
7.2	80' SPAN - COST PER L.F.					
	Earthwork	0 84	0 90			1 74
	Concrete Footing	3 93	5 42			9 35
	Concrete Pier	4 56	8 17			12 73
	Concrete Cap	1 00	0 84			1 84
	P. C. Box Section	25 03	46 10			71 13
	Hauling			10 56		10 56
	Erection				17 11	17 11
	Joint Sealer	0 38	3 50			3 88
	Elast. Bearing	0 41	1 51			1 92
	7"/8" Railing	14 77	6 86			21 63
	SUB-TOTAL	50 92	73 30	10 56	17 11	151 89
7.3	100' SPAN - COST PER L.F.					
	Earthwork	0 75	0 81			1 56
	Concrete Footing	3 70	5 23			8 93
	Concrete Pier	4 03	7 29			11 32
	Concrete Cap	0 82	0 70			1 52
	P. C. Box Section	27 57	53 68			81 25
	Hauling			11 46		11 46
	Erection				17 11	17 11
	Joint Sealer	0 50	4 40			4 90
	Elast. Bearing	0 36	1 86			2 22
	7"/8" Railing	14 77	6 86			21 63
	SUB-TOTAL	52 50	80 83	11 46	17 11	161 90

APPENDIX C

VEHICLE-GUIDEWAY MODEL DESCRIPTION

C.1 Guideway Representation

The general guideway configuration is shown in Figure C.1. A guideway span of length ℓ_s, is supported at its ends by rigid piers. The guideway spans under study have a large enough length to width ratio to be considered beams. If the guideway is a multispan (semi-continuous) type, reinforcing strands of steel are run between the adjoining ends of the beams to provide continuity, as shown in Figure C.2. Given the same cross-section, multispan guideway have less deflection than a single span guideway for a given load because the inter-span connection allows the transfer of moments from one span to another.

The guideway presents two different types of disturbances to the vehicle. The first type of input is due to the static profile of the guideway and is represented by construction induced irregularities as described in Section 2. The second type of guideway input is due to vehicle induced deflections of the guideway. Vehicle vertical forces on the guideway are due to the vehicle weight, whereas lateral forces are caused by the bias inherent in the steering controller. Because of the small magnitudes of the lateral forces, the guidewall is assumed not to deflect as the vehicle passes. Vertical guideway deflections are significant and depend on guideway span stiffness and end conditions and also on the vehicle velocity and spacing.

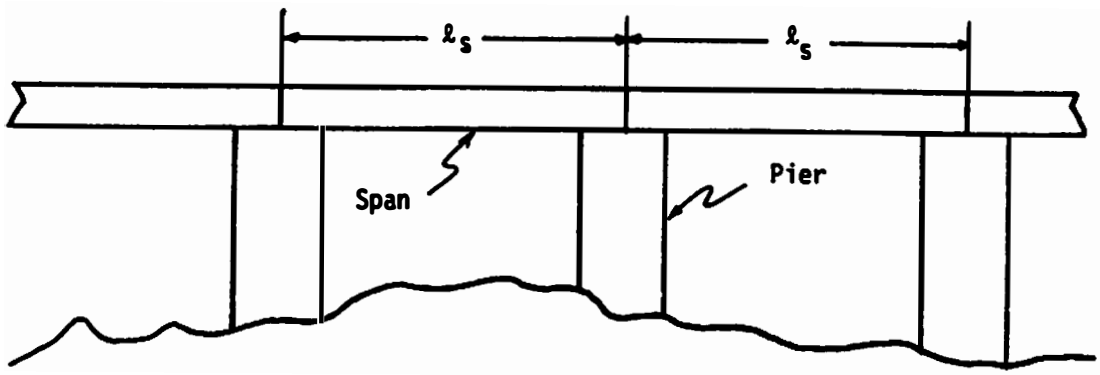

FIGURE C.1 : GENERAL ELEVATED GUIDEWAY CONFIGURATION

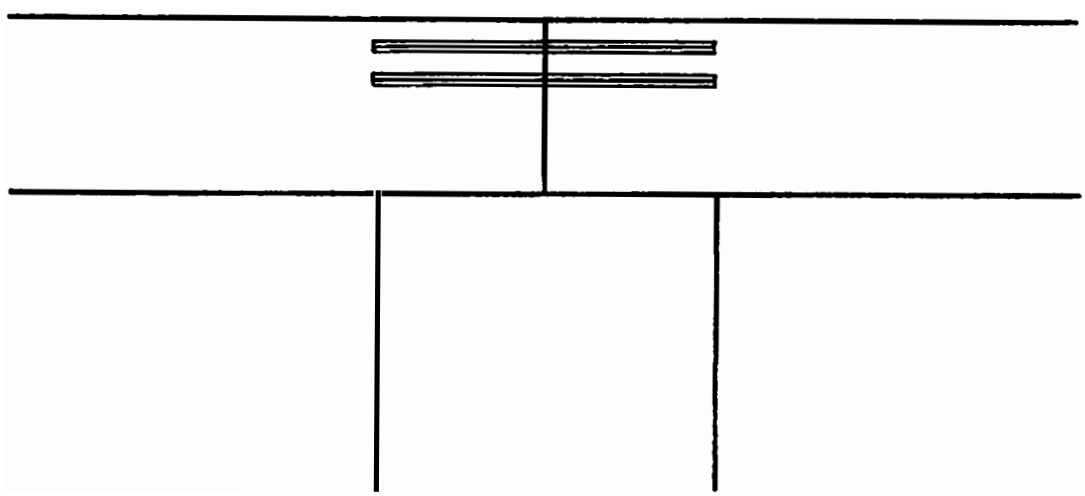

FIGURE C.2: MULTISPAN REINFORCING STRANDS

Therefore guideway inputs to the vehicle in the vertical plane are derived from two sources, guideway surface irregularities and guideway dynamic deflections. The total vertical input to the vehicle is therefore:

$$y_t = y_s + y_d \tag{C.1}$$

where:

y_t = total vertical guideway shape

y_s = vertical static guideway shape

y_d = vertical deflection guideway shape

The lateral input to the vehicle is only due to the static lateral profile Z_s.

Modeling of Dynamic Deflection

Modal analysis techniques are adopted to compute the dynamic motion of the guideway spans. The guideway span is modeled using the Bernoulli-Euler beam theory. The beam deflection which is a function of time and position along the beam, is expressed as a summation of the natural modes of vibration. Therefore,

$$y(x,t) = \sum_{m=1}^{\infty} A_m(t)\ \phi_m(x) \tag{C.2}$$

where the $\phi_m(s)$'s are mode shapes determined from the beam end conditions and the unforced Bernoulli-Euler beam equation and the $A_m(t)$'s are time varying functions determined from loading conditions and the forced beam equation. To obtain exact beam deflection equation (C.2) must be summed over an infinite number of modes. For vehicle speeds

under consideration it has been shown [7] that for a k span per beam guideway in which the number of modes m are integer multiples of k, the contribution for each higher set of modes to the deflection is proportional to $1/(m/k)^4$. Therefore, for a single span guideway system the contribution to the deflection of the second mode is 6.25 per cent. The modal description of the guideway deflections is applicable to single span and multispan guideways by using the appropriste end conditions when determining the modal shapes $\phi_m(x)$.

For a single span guideway the modal shape functions are:

$$\phi_m(x) = \sin \frac{m\pi x}{\ell_s} \tag{C.3}$$

where:

ℓ_s = span length

m = mode number

Each modal amplitude is determined from the ordinary differential equation:

$$\frac{d^2A_m}{dt^2} + 2\xi_m\omega_m \frac{dA_m}{dt} + \omega_m^2 A_m = \frac{2}{\rho A_b \ell_b} \int_0^{\ell_b} f(x,t)\, \phi_m(x)dx \tag{C.4}$$

where:

ℓ_b = beam length ($n\ell_s$)

ξ_m = beam damping ratio for m^{th} mode

ω_m = beam m^{th} mode natural frequency

A_b = beam cross sectional area

ρ = beam mass density

$f(x,t)$ = vehicle force distribution

The natural frequency for a single span beam is expressed as:

$$\omega_m = \frac{m^2 \pi^2}{\ell_b^2} \sqrt{\frac{E\ I_b}{\rho\ A_b}} \tag{C.5}$$

where:

E = beam elastic modulus

I_b = beam cross section moment of inertia

For a multispan beam the modal shape functions are more complicated because of the presence of interior pier supports. The beam no longer takes the shape of a simple sine wave, but is described as:

$$\phi_m(s) = a_m \sin\lambda_m x + b_m \cos\lambda_m x + c_m \sinh\lambda_m x + d_m \cosh\lambda_m x \tag{C.6}$$

where the parameter λ_m is defined as:

$$\lambda_m^4 = \frac{\rho\ A_b}{E\ I_b}\ \omega_m^2 \tag{C.7}$$

and where, a_m, b_m, c_m, d_m are coefficients determined by boundary conditions. The boundary conditions for the internal supports of the beam require that moment and slope are continuous across the pier, whereas the boundary conditions at the external supports require that zero moment develop.

Table C.1 shows the first NS values of $\overline{\lambda_m}$ for the multispan beams determined in [7]. $\overline{\lambda_m}$ is defined as:

$$\overline{\lambda_m} = \lambda_m \ell_s \tag{C.8}$$

where λ_m is calculated from equation (3.7).

TABLE C.1

FIRST NS EIGENVALUES $\bar{\lambda}_m = \lambda_m \ell_s$ FOR SEMICONTINUOUS BEAMS

NUMBER OF SPANS

1	2	3	4	5	6
π	π	π	π	π	π
	3.927	3.556	3.393	3.309	3.261
		4.298	3.927	3.700	3.556
			4.463	4.153	3.927
				4.550	4.298
					4.601

TABLE C.2

NONDIMENSIONAL MODAL COEFFICIENTS OF ϕ_m FOR THREE SPAN SEMICONTINUOUS BEAMS

Span Number	Mode Number	a_{ms}	b_{ms}	c_{ms}	d_{ms}
1	1	1.42	0.0	0.0	0.0
	2	1.67	0.0	.038	0.0
	3	1.12	0.0	.028	0.0
	1	-1.42	0.0	0.0	0.0
2	2	-1.42	-.673	-.713	.673
	3	1.56	-1.02	-.99	1.02
	1	1.41	0.0	.01	0.0
3	2	-1.53	.675	.675	-.674
	3	.442	-1.02	-1.02	1.02

In order to satisfy the boundary conditions, the values of a_m, b_m, c_m, and d_m in equation (C.6), are different in each span, therefore it is more convenient to express $\phi_m(x)$ as:

$$\phi_m(x) = \sum_{s=1}^{NS} \phi_{ms}(x_s) \qquad (C.9)$$

where:

s = span number 1,2,3....NS

ϕ_{ms} = individual shape function for mode m of span s, defined as zero outside of span s.

x_s = horizontal coordinate for span s extending over the interval $0 < x_s < \ell_s$

Each $\phi_{ms}(x_s)$ may be expressed as a function of each span's modal coefficients:

$$\phi_{ms}(x_s) = a_{ms} \sin\lambda_m x_s + b_{ms} \cos\lambda_m x_s + c_{ms} \sinh\lambda_m x_s + d_{ms} \cosh\lambda_m x_s$$

where a_{ms}, b_{ms} and d_{ms} are the individual span coefficients.

Table C.2 shows the normalized modal coefficients for a three span beam. To obtain a normalized function, the value of modal coefficients are scaled so that:

$$\sum_{s=1}^{NS} \frac{1}{\ell_s} \int_0^{\ell} \overline{\phi_{ms}(x_s)}^{\,2} \, dx_s = 1 \qquad (C.10)$$

where:

$\overline{\phi_{ms}(x_s)}$ = normalized span shape function

The resulting first NS mode shapes are given in Figure C.3 for both the three and six span beam.

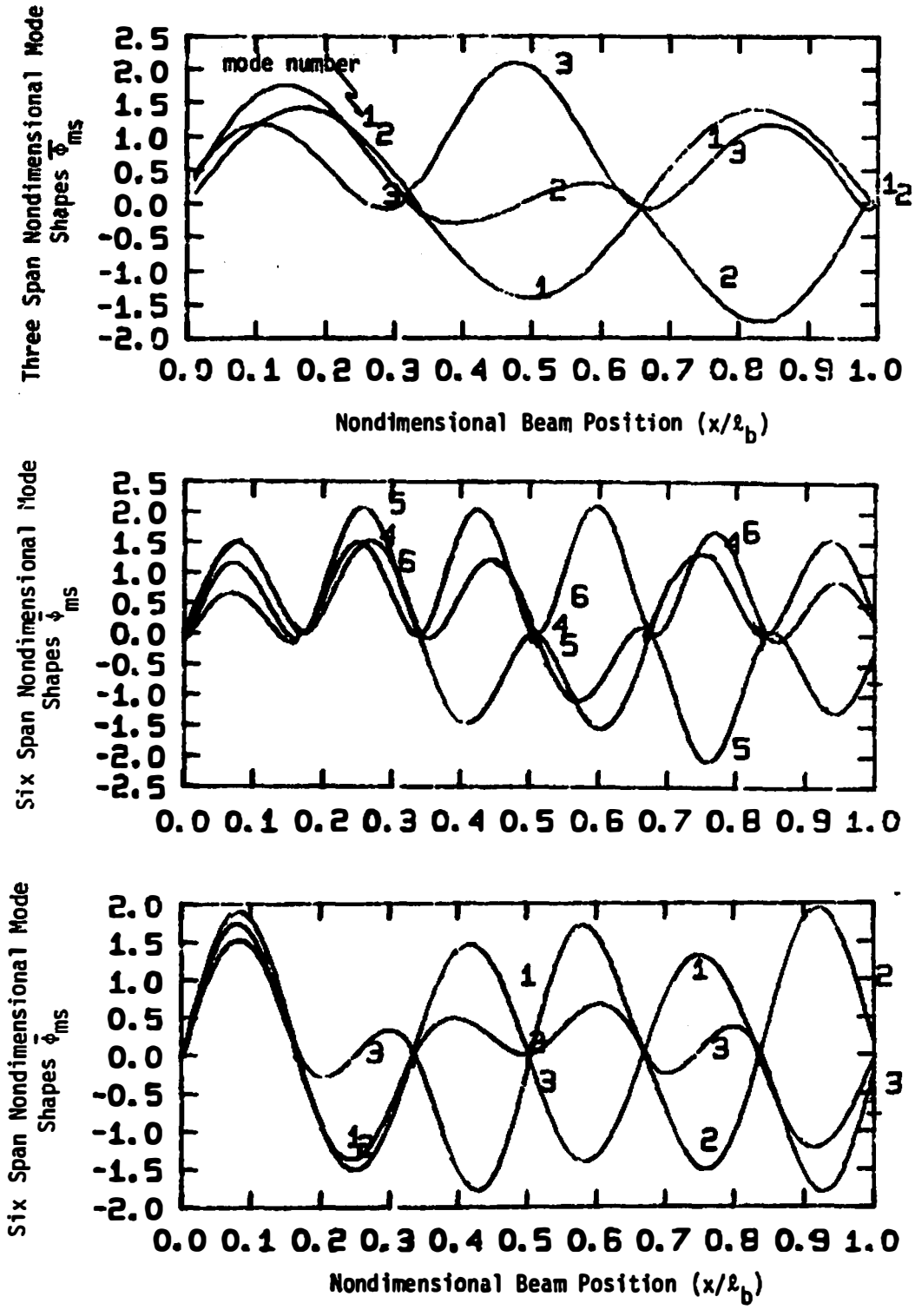

FIGURE C.3 : MODE SHAPES FOR MULTISPAN GUIDEWAYS

When the guideway is forced by a string of vehicles, the span natural frequency can be excited, depending on vehicle speed and spacing. Under these conditions, the guideway deflections increase considerably because the damping of beams is by nature very low (ξ_b = .025).

Static Profile Representation

The profile of the guideway before it has been disturbed by vehicle passage is determined by guideway construction practices. The degree to which the guideway spans are aligned is determined by the amount of effort devoted to beam manufacture and erection. Alignment errors that are present in the guideway surface disturb the vehicle and decrease ride quality. Four types of irregularities are shown in Fiugre 3.3. The magnitude of each irregularity is determined by a design specification, which gives the maximum allowable value of the misalignment. Because of this type of specification, precise values of the irregularity magnitudes are not known for every span. Therefore irregularity amplitude probability density functions (PDF) are assumed to describe the distribution of the irregularity amplitude. The irregularity amplitude PDF is described as either a Gaussian or uniform distribution.

The power spectral density (PSD) describing each static irregularity is formulated analytically [7]. The vertical and lateral total irregularity description include different combinations of the four irregularity types. Guideway construction procedures determine the presence and magnitude of the particular irregularity input. Each individual ir-

regularity source is described along with a brief development of the associated analytical PSD.

Surface Roughness

Surface roughness is due to imperfections in the concrete mold and wear of the surface. A method of defining the surface roughness in terms of a construction tolerance presents the major problem in the development of the surface roughness PSD. In this study, the magnitude of the surface roughness is described in terms of the mid chord deviation of the guideway under a straight edge. A schematic of how the mid chord deviation, δ_m, is measured is shown in Figure C.4. The output due to a sinusoidal input for this measurement device has been calculated to be [6]:

$$\frac{y(x)}{\delta_m(x)} = \sin^2 \left(\frac{L_c}{4} \Omega\right) \qquad \text{(C.11)}$$

where:

Ω = wavenumber, rad/ft

L_c = chord length

$y(x)$ = guideway profile

$\delta_m(x)$ = mid chord deviation

The assumptions that are implicit in this development are:

1) Stationary guideway profile ($y(x)$)
2) Gaussian distribution input amplitude ($y(x)$)
3) Stationary response ($\delta_m(x)$)
4) Gaussian distribution of output amplitude ($\delta_m(x)$)

As these assumptions state, the distribution of the mid chord deviation δ_m, is Gaussian.

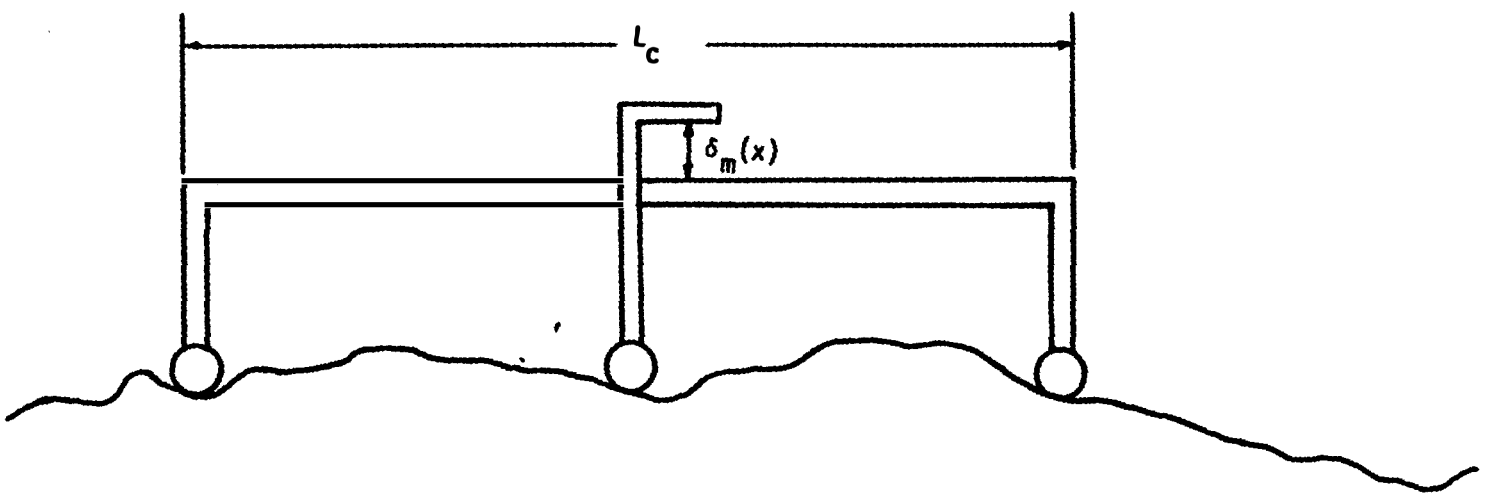

FIGURE C.4 : SURFACE ROUGHNESS MEASUREMENT DEVICE

Surface roughness measurements have been made on existing concrete roadway surfaces and show the resulting PSD to have the form [23]

$$S_{sr}(\Omega) = \frac{A}{\Omega_c^2 + \Omega^2} \tag{C.12}$$

where:

$S_{sr}(\Omega)$ = single sided surface roughness PSD

Ω = wavenumber

Ω_c = cut-off wavenumber

A = guideway roughness coefficient

The cut-off wavelength is assumed equal to the span length in all cases, because surface roughnesses are not described for a longer wavelength than one span length.

Equation (C.12) describes the PSD input, to the measurement device in Figure C.4. The response PSD of the measurement device is:

$$S_{\delta m}(\Omega) = 4 \sin^4\left(\frac{L_c}{4}\Omega\right) S_{sr}(\Omega) \tag{C.13}$$

Since the mid chord deviation is assumed to have a zero mean, the integral of (C.14) over Ω results in the mean square of the mid chord deviation $\sigma^2_{\delta m}$.

$$\sigma^2_{\delta m} = \frac{A\pi}{\Omega_c}\left[\frac{3}{4} + \frac{1}{4} e^{-L_c\Omega_c} - e^{-\left(\frac{L_c}{2}\Omega_c\right)}\right] \tag{C.14}$$

Solving for the surface roughness coefficient A,

$$A = \frac{\sigma^2_{\delta m}\,\Omega_c}{\pi\left[\frac{3}{4} + \frac{1}{4} e^{-L_c\Omega_c} - e^{-\left(\frac{L_c}{2}\Omega_c\right)}\right]} \tag{C.15}$$

Equation (C.15) is the required relationship between the construction tolerance $\sigma_{\delta m}$ and the magnitude of the analytical surface roughness PSD, A.

As a vertification of the above analysis, roughness profiles with a particular value of A were numerically created. These profiles, for various random number generation seeds, (3) are plotted in Figure C.5. They show that the magnitude of the largest mid chord variation is approximately 3 $\sigma_{\delta m}$ when $\sigma_{\delta m}$ is calculated by equation (C.14) and thus verifies the analysis.

Camber Irregularity

The amplitude PDF of the camber irregularity is the only one of the four types to have a mean value. An unloaded prestressed beam is deflected upward due to the prestressing moment. This upward deflection is defined as the mean camber. Variation of the camber magnitude about the mean value is due to variations in the prestressing force and location among spans. Since the nature of the span's prestressing is dependent on strength requirements which are different for each particular vehicle-guideway configuration, the mean camber magnitude varies with the vehicle-guideway configuration also. The shape of the cambered beam is given in Figure C.6 along with a Fourier sine series curve fit.

The PSD for a sine wave shaped camber variation is developed in [7]. A similar procedure is followed to derive the analytical PSD description for a sine series camber variation resulting in:

$$S_c(\Omega) = \frac{\sigma_c^2}{2\pi} \left[A_1 \sin\left(\frac{\Omega \ell_i - \pi}{2}\right) + A_2 \sin\left(\frac{\Omega \ell_i + \pi}{2}\right)\right]^2 \quad (C.16)$$

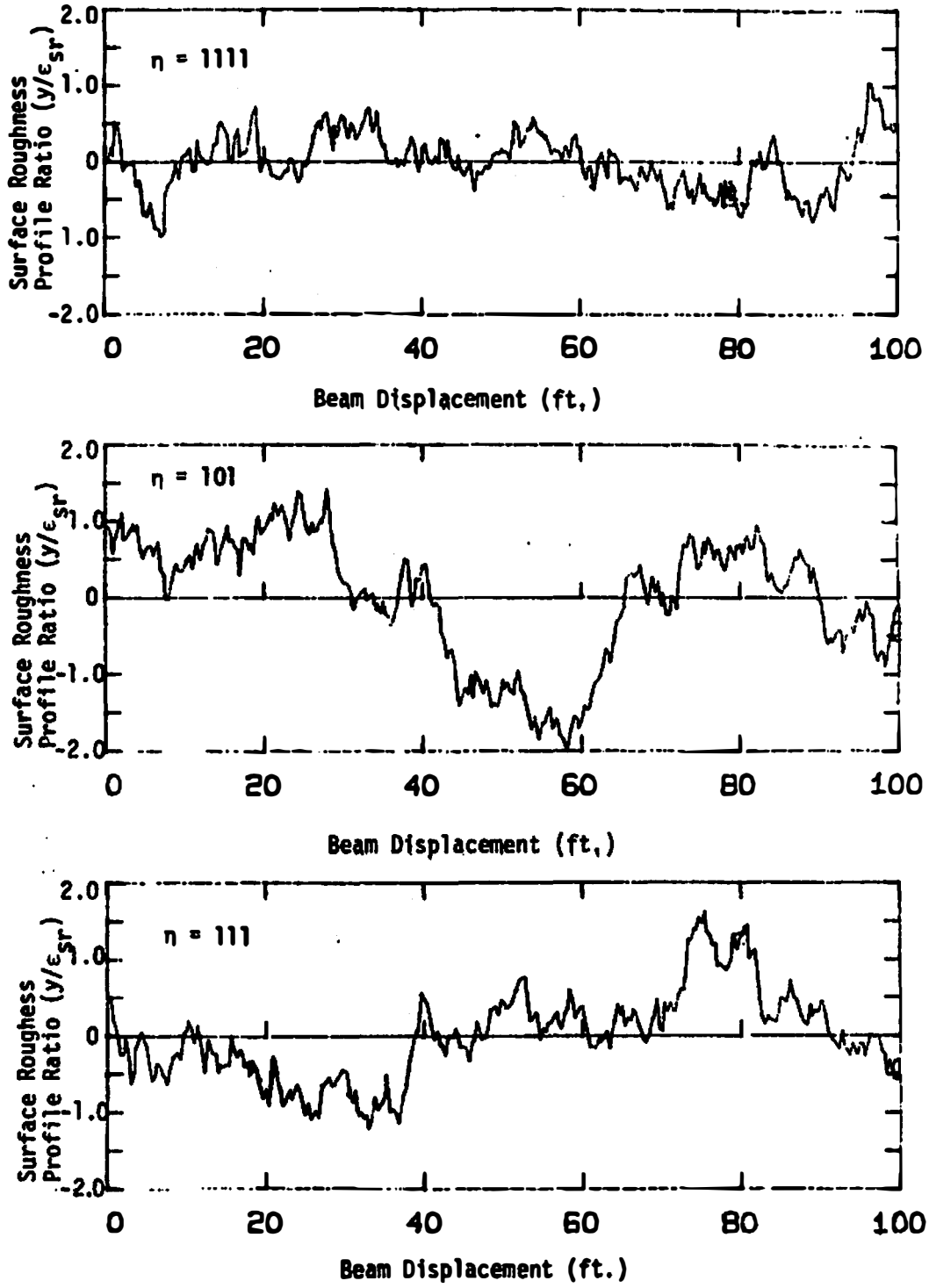

FIGURE C.5: GUIDEWAY SURFACE ROUGHNESS PROFILES

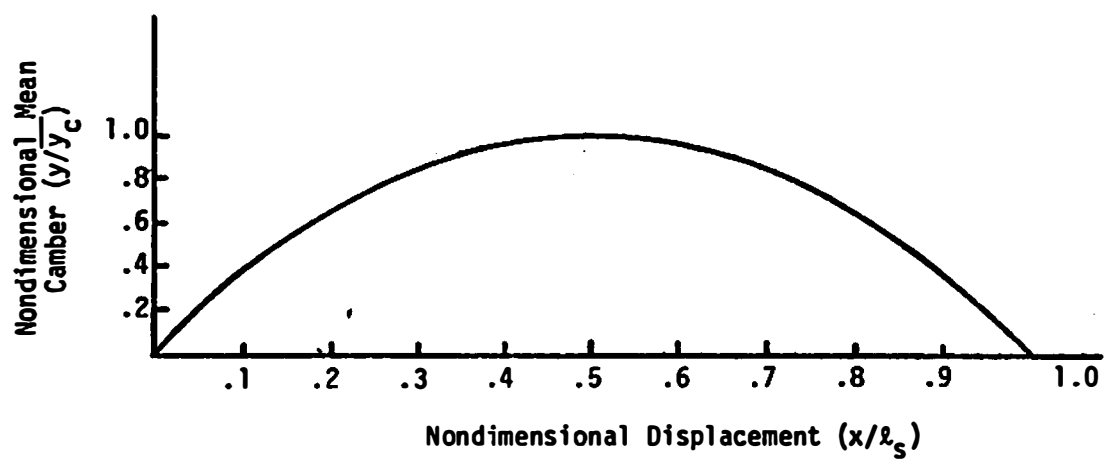

$$y(x/\ell_s) = 1.03 \sin(\pi x/\ell_s) + .04 \sin(3\pi x/\ell_s) + .01 \sin(5\pi x/\ell_s)$$

FIGURE C.6: MEAN CAMBER PROFILE

where:

$$A_1 = \left[\frac{2\,b_1}{(\Omega\ell_i - \pi)} - \frac{2\,b_2}{(\Omega\ell_i - 3\pi)} + \frac{2\,b_3}{(\Omega\ell_i - 5\pi)}\right]$$

$$A_2 = \left[\frac{2\,b_1}{(\Omega\ell_i + \pi)} + \frac{2\,b_2}{(\Omega\ell_i + 3\pi)} + \frac{2\,b_3}{(\Omega\ell_i + 5\pi)}\right]$$

b_1 = first coefficient of Fourier sine camber shape

b_2 = third coefficient of Fourier sine camber shape

b_3 = fifth coefficient of Fourier sine camber shape

ℓ_i = camber irregularity characteristic wavelength

Span Joint Misalignment

The joint misalignment irregularity represents a discontinuous alignment of adjacent spans in the guideway. This irregularity is created by lack of beam height uniformity and inaccurate installation practices. The magnitude of the irregularity is a random variable which is described by a uniform or Gaussian PDF. The uniform distribution is used to describe the span joint offset magnitude because it is assumed that the misalignment is limited to less than a specified maximum value, which is equal to the construction tolerance, ε_o. The single sided PSD has been derived analytically in [7] as:

$$S_o(\Omega) = \frac{\sigma_o^2\,\ell_i}{\pi}\,\frac{\sin^2(.5\Omega\ell_i)}{(.5\Omega\ell_i)^2} \qquad \text{(C.17)}$$

where:

S_o = joint offset PSD

σ_o = joint offset amplitude variance

ℓ_i = irregularity characteristic wavelength

Span Angular Alignment

Two distinct types of angular irregularities are considered. One irregularity results from survey errors when the position at one pier is determined by survey from the position at the previous pier. Deviations from the desired position are relative to a datum determined during the survey at the previous pier.

Deviations in position measured relative to a fixed datum describe the other type of angular irregularity. Instead of redefining a new datum at each measurement, a fixed reference is used to measure the survey errors. The two models for angular irregularities described above result in different power spectral densities derived in [7] as:

For pier reference datum:

$$S_{rw}(\Omega) = \frac{\sigma_{rw}^2}{\pi\,\Omega^2\,\ell_i}\;\frac{\sin^2(.5\Omega\ell_i)}{(.5\Omega\ell_i)^2} \qquad \text{(C.18)}$$

where:

S_{rw} = angular misalignment PSD

σ_{rw} = amplitude variance

ℓ_i = irregularity characteristic wavelength

For fixed datum:

$$S_a(\Omega) = \frac{\sigma_a^3\;\ell_s}{\pi}\;\frac{\sin^4(\Omega\ell_i/2)}{(\Omega\ell_i/2)^4} \qquad \text{(C.19)}$$

where:

S_a = angular fixed datum irregularity PSD

σ_a = angular fixed datum amplitude variance

ℓ_i = irregularity characteristic wavelength

C.2 Vehicle Representation

This section describes the lateral and vertical vehicle models used to find the response of the vehicle as it traverses different guideway designs. Throughout the study, vehicles are assumed to travel over equal length spans at a constant forward velocity. The major criteria for determining system performance is the magnitude of the accelerations transmitted to the passenger compartment due to guideway disturbances.

Vertical Model

The rigid body vertical vehicle model is shown in Figure 3.4. The passenger compartment has a sprung mass, m_v, and pitch moment of inertia, I_v. The sprung mass has two degrees of freedom, pitch and heave. The front and rear suspension system, separated by a length ℓ_a, are assumed to be identical. Each suspension consists of an unsprung mass $\frac{m_u}{2}$, a secondary stiffness k_b, a secondary damper b_b, and a primary stiffnes k_{sr}. The displacement of the guideway under the vehicles tires (y_{or} and y_{of}) are the inputs to the vehicle. The accelerations at the suspension attachment points ($\ddot{y}_{2f}$ and $\ddot{y}_{2r}$) are the passenger compartment accelerations of interest.

In the vertical vehicle model the forces the vehicle exerts on the guideway are assumed to be equal to the weight support by each tire and vehicle vertical acceleration forces are neglected. This constant force vehicle model has been evaluated in [7] and shown to be a good representation of a vehicle when the vehicle body accelerations are low as is required by ride quality. Thus the vehicle model is excited by the guideway inputs, but only forces the guideway through constant forces equal to the weight.

The acceleration transfer functions for this vertical model expressed in terms of nondimensional frequency $\hat{\omega}_i$ they are:

$$T_s(j\hat{\omega}_i) = \frac{C_{s7}(j\hat{\omega}_i)^7+C_{s6}(j\hat{\omega}_i)^6+C_{s5}(j\hat{\omega}_i)^5+C_{s4}(j\hat{\omega}_i)^4+C_{s3}(j\hat{\omega}_i)^3+C_{s2}(j\hat{\omega}_i)^2}{DNM(j\hat{\omega}_i)} \tag{C.20}$$

$$T_c(j\hat{\omega}_i) = \frac{C_{c7}(j\hat{\omega}_i)^7+C_{c6}(j\hat{\omega}_i)^6 + C_{c5}(j\hat{\omega}_i)^5 + C_{c4}(j\hat{\omega}_i)^4}{DNM(j\hat{\omega}_i)} \tag{C.21}$$

$$DNM(j\hat{\omega}_i) = d_8(j\hat{\omega}_i)^8 + d_7(j\hat{\omega}_i)^7 + d_6(j\hat{\omega}_i)^6 + d_5(j\hat{\omega}_i)^5 + d_4(j\hat{\omega}_i)^4$$

$$+d_3(j\hat{\omega}_i)^3 + d_2(j\hat{\omega}_i)^2 + d_1(j\hat{\omega}_i) + d_o \tag{C.22}$$

where:

$T_s(j\hat{\omega}_i)$ = Nondimensional front (rear) acceleration transfer function due to input at front (rear)

$T_c(j\hat{\omega}_i)$ = Nondimensional front (rear) acceleration transfer function due to input at rear (front)

$DNM(j\hat{\omega}_i)$ = Characteristic equation of vertical vehicle

$\hat{\omega}_i = \dfrac{\omega_i}{\omega_v}$ = Nondimensional frequency

The coefficients in equations (C.20) to (C.22) are given in Table C.3 in terms of the pitch inertia ratio $\bar{I}_v$, the damping ratio ξ_v, the unsprung mass ratio M_u and the suspension stiffness ratio K. Note that the normalized attachment point accelerations ($\ddot{y}_{2f}$, $\ddot{y}_{2r}$) due to guideway inputs are expressed by:

$$\hat{\ddot{Y}}_{2f}(\hat{s}) = T_s(\hat{s})\,\hat{Y}_{of}(\hat{s}) + T_c(\hat{s})\,\hat{Y}_{or}(\hat{s}) \qquad \text{(C.23)}$$

$$\hat{\ddot{Y}}_{2r}(\hat{s}) = T_c(\hat{s})\,\hat{Y}_{of}(\hat{s}) + T_s(\hat{s})\,\hat{Y}_{or}(\hat{s}) \qquad \text{(C.24)}$$

where:

$\hat{s} = \dfrac{j\omega_i}{\omega_v}$ = Nondimensional Laplace operator

$\hat{Y}_{of(r)}(s)$ = Laplace transform of nondimensional input

$\hat{\ddot{Y}}_{2f(r)}(s)$ = Laplace transform of nondimensional passenger compartment acceleration

ω_v = Vehicle sprung natural frequency

Figure C.7 illustrates the magnitude of the two transfer functions T_s and T_c. The peaks in the transfer functions are from the natural frequency excitation of the sprung and unsprung masses. The location of the peaks are functions of ω_v and the unsprung natural frequency, ω_u, which is defined as:

TABLE C.3

VERTICAL VEHICLE TRANSFER FUNCTION COEFFICIENT

$$c_{s7} = K\xi_v M_u [1 + \frac{\bar{I}_v}{3}]$$

$$c_{s6} = K\ M_u [\frac{1}{2} + \frac{\bar{I}_v}{6}] + 4\xi_v^2\ K[M_u + \frac{1}{2} + \frac{\bar{I}_v}{6}]$$

$$c_{s5} = K\xi_v [4M_u + (2 + K)(1 + \frac{\bar{I}_v}{3})]$$

$$c_{s4} = K[M_u + (1 + K)\ (\frac{1}{2} + \frac{\bar{I}_v}{6})] + 4\xi_v^2\ K^2$$

$$c_{s3} = 4K^2\ \xi_v$$

$$c_{s2} = K^2$$

$$c_{c7} = -K\xi_v M_u [1 - \frac{\bar{I}_v}{3}]$$

$$c_{c6} = -K(M_u + 4\xi_v^2)(\frac{1}{2} - \frac{\bar{I}_v}{3})$$

$$c_{c5} = -K\xi_v (2 + K)(1 - \frac{\bar{I}_v}{3})$$

$$c_{c4} = -K(1 + K)(\frac{1}{2} - \frac{\bar{I}_v}{6})$$

TABLE C.3 (cont.)

$$d_8 = M_u^2 \left[\left(\frac{1}{2} + \frac{\bar{I}_v}{6}\right)^2 - \left(\frac{1}{2} - \frac{\bar{I}_v}{6}\right)^2\right]$$

$$d_7 = 4\xi_v M_u \left[\left(\frac{1}{2} + \frac{\bar{I}_v}{6}\right)\left(M_u + \frac{1}{2} + \frac{\bar{I}_v}{6}\right) - \left(\frac{1}{2} - \frac{\bar{I}_v}{6}\right)^2\right]$$

$$d_6 = \xi_v^2 \left[2M_u + 1 + \frac{\bar{I}_v}{3}\right] - \left[4\xi_v^2 + 2M_u(1 + K)\right]\left(\frac{1}{2} - \frac{\bar{I}_v}{6}\right)^2$$
$$+ M_u\left[1 + \frac{\bar{I}_v}{3}\right]\left[(1 + K)\left(\frac{1}{2} + \frac{\bar{I}_v}{6}\right) + M_u\right]$$

$$d_5 = 2\xi_v K M_u\left[1 + \frac{\bar{I}_v}{3}\right] - \xi_v\left(1 - \frac{\bar{I}_v}{3}\right)^2(1 + K) + 2\xi\left[2M_u + 1 + \frac{\bar{I}_v}{3}\right]$$
$$+ \xi_v\left[2M_u + 1 + \frac{\bar{I}_v}{3}\right]\left[(1 + K)\left(1 + \frac{\bar{I}_v}{3}\right) + 2M_u\right]$$

$$d_4 = KM_u\left[1 + \frac{\bar{I}_v}{3}\right] + 4K\xi_v^2\left[2M_u + 1 + \frac{\bar{I}_v}{3}\right] - (1 + K)^2\left(\frac{1}{2} - \frac{\bar{I}_v}{6}\right)^2$$
$$+ \left[(1 + K)\left(\frac{1}{2} + \frac{\bar{I}_v}{6}\right) + M_u\right]^2$$

$$d_3 = 2\xi_v K\left[(2 + K)\left(1 + \frac{\bar{I}_v}{3}\right) + 4M_u\right]$$

$$d_2 = 4\xi_v^2 K^2 + K\left[(1 + K)\left(1 + \frac{\bar{I}_v}{3}\right) + 2M_u\right]$$

$$d_1 = 4\xi_v K^2$$

$$d_0 = K^2$$

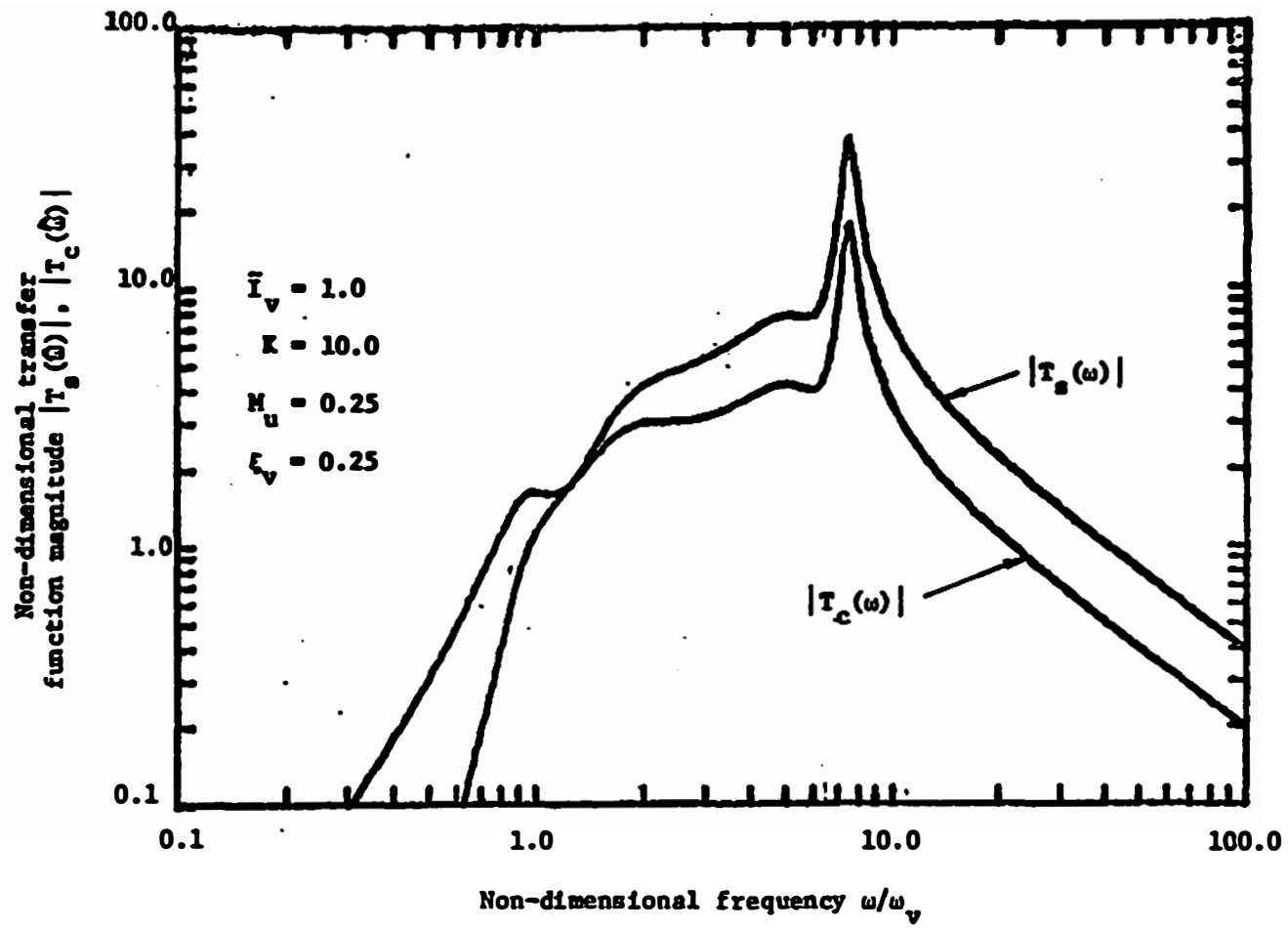

FIGURE C.7: NON-DIMENSIONAL VEHICLE ACCELERATION TRANSFER FUNCTION MAGNITUDE AS A FUNCTION OF NON-DIMENSIONAL FREQUENCY

$$\omega_u = \sqrt{\frac{2k_{sr}}{m_u}} = \sqrt{\frac{\bar{K}}{\bar{M}_u}}\ \omega_n \qquad (C.25)$$

Lateral Model

The lateral model used is illustrated in Figure 3.7. The vehicle is represented by a rigid body with mass $m_T (m_T = m_u + m_v)$ and yaw inertia I_y. This model assumes that only the front axle is steerable and that the vehicle is symmetric about its longitudinal axis. The lateral displacement of the center of gravity, z, measured from a reference position and the yaw angle of the vehicle centerline, ψ, represent degrees of freedom. The vehicle has one sensor which is located at the front axle. This sensor measures the error in the vehicle position in relation to the guideway. The controller adjusts the steering angle, δ, to keep the sensor error as small as possible. In the control law, L^*, is physically the distance from the c.g. to the sensor location. L^* translates a sensor error to an error in yaw angle at the c.g., and it should be chosen as large as possible to minimize yaw errors. However, it is impractical to place the sensing device in front of the vehicle's bumper. Therefore, L^* in all cases studied is set equal to the c.g. to front bumper distance. The guidewall surface irregularities are denoted by Z_s, which is the only input to the lateral vehicle model. The outputs of interest are the lateral errors, measured from the vehicle position to the guidewall profile transposed to the guideway centerline, and accelerations at the front axle, center of gravity and rear axle.

The equations of motion for the lateral model are derived in [20] for a two degree of freedom model as:

$$\dot{\beta} = \frac{k_5}{V}\beta + \left(\frac{k_6}{V^2} - 1\right)r + \frac{k_4}{V} + \frac{k_4}{V}\delta \qquad (C.26)$$

$$\dot{r} = k_2\beta + \frac{k_3}{V}r + k_1\delta \qquad (C.27)$$

where:

β = vehicle sideslip angle

r = yaw rate

δ = steering angle

Figure C.8 is a schematic diagram of the model while Table C.4 defines the lateral vehicle nomenclature.

The lateral forces on the vehicle include the inertial forces at the c.g. and the forces at the tire road contact. For small angles:

$$F_y = C_f\,\alpha_f + C_r\,\alpha_r \qquad (C.28)$$

where:

$\alpha_{f,r}$ = front, rear slip angle

From Figure C.8 and geometry the front and rear slip angles can be expressed as:

$$\alpha_f = \beta - \alpha + \frac{ar}{V} \qquad (C.29)$$

$$\alpha_r = \beta - \frac{br}{V} \qquad (C.30)$$

and the sideslip velocity of the vehicle, $\dot{z}$, is

$$\dot{z} = V(\dot{\beta}+r) \qquad (C.31)$$

TABLE C.4

LATERAL VEHICLE MODEL NOMENCLATURE

$$K_1 = \frac{aC_f}{I_y}$$

$$K_2 = \left(\frac{aC_f - bC_r}{I_y}\right)$$

$$K_3 = \left(\frac{a^2C_f + b^2C_r}{I_y}\right)$$

$$K_4 = \frac{C_f}{m_T}$$

$$K_5 = \frac{C_f + C_r}{m_T}$$

$$K_6 = \left(\frac{aC_f - bC_r}{m_T}\right)$$

C_f = Front axle combined tire stiffness

C_r = Rear axle combined tire stiffness

I_y = Yaw moment of inertia

a = c.g. to front axle distance

b = c.g. to rear axle distance

δ = Steering angle

β = Vehicle sideslip angle

ψ = Yaw angle

r = Yaw rate ($\dot{\psi}$)

TABLE C.4 (cont.)

α_f = Front tire slip angle

α_r = Rear tire slip angle

Z = Lateral displacement

C_1 = Controller gain on lateral displacement

C_2 = Controller gain on yaw angle

C_3 = Controller gain on lateral velocity

C_4 = Controller gain on yaw rate

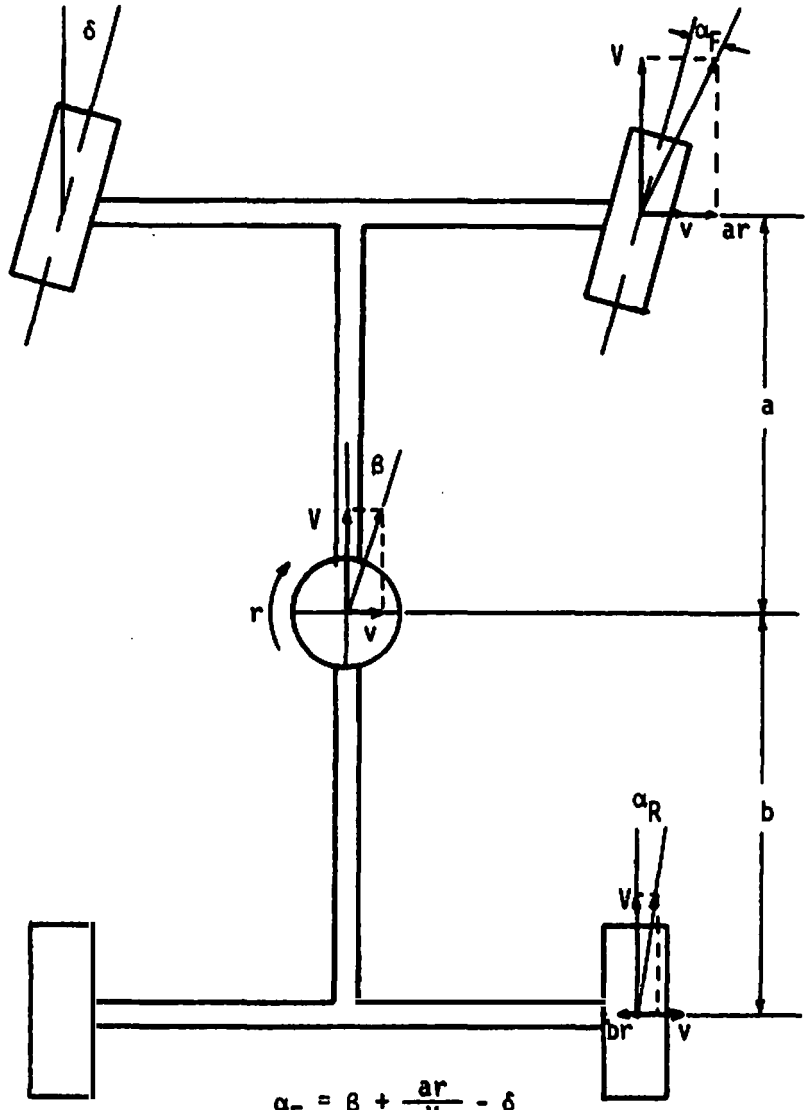

$$\alpha_F = \beta + \frac{ar}{V} - \delta$$

$$\alpha_R = \beta - \frac{br}{V}$$

FIGURE C.8: LATERAL VEHICLE SCHEMATIC

Substituting equations (C.29) - (C.31) into equation (C.28) and (C.27) leads to

$$\ddot{z} = \frac{k_5}{V}\dot{z} + \frac{k_6}{V}\dot{\psi} - k_5\psi + k_4\delta \tag{C.32}$$

$$\ddot{\psi} = \frac{k_2}{V}\dot{z} + \frac{k_3}{V}\dot{\psi} - k_5\psi + k_1\delta \tag{C.33}$$

Changing these equations into state variable matrix form:

$$\frac{d}{dt}\begin{bmatrix}\dot{z}\\ z\\ \dot{\psi}\\ \psi\end{bmatrix} = \begin{bmatrix}\frac{k_5}{V} & 0 & \frac{k_6}{V} & -k_5\\ 0 & 1 & 0 & 0\\ \frac{k_2}{V} & 0 & \frac{k_3}{V} & -k_2\\ 0 & 0 & 1 & 0\end{bmatrix}\bullet\begin{bmatrix}\dot{z}\\ z\\ \dot{\psi}\\ \psi\end{bmatrix} + \begin{bmatrix}k_4\\ 0\\ k_1\\ 0\end{bmatrix}\delta \tag{C.34}$$

The control law in its most general form can be expressed as:

$$\delta = C_1 z - C_1 z_o + C_2\psi + C_3\dot{z} + C_4\dot{\psi} \tag{C.35}$$

Incorporating this control law into equation (C.35) yields:

$$\frac{d}{dt}\begin{bmatrix}\dot{z}\\ z\\ \dot{\psi}\\ \psi\end{bmatrix} = \begin{bmatrix}(\frac{k_5}{V} + k_4C_3) & k_4C_1 & (k_4C_4 + \frac{k_6}{V}) & (-k_5+C_2k_4)\\ 0 & 1 & 0 & 0\\ (k_1C_3 + \frac{k_2}{V}) & k_1C_1 & (k_4C_4 + \frac{k_3}{V}) & (-k_2-k_1C_2)\\ 0 & 0 & 1 & 0\end{bmatrix}\bullet\begin{bmatrix}\dot{z}\\ z\\ \dot{\psi}\\ \psi\end{bmatrix} + \begin{bmatrix}-k_4C_1\\ 0\\ -k_1C_1\\ 0\end{bmatrix}z_o \tag{C.36}$$

The transfer functions relating lateral and yaw accelerations at a point on the vehicle to the guideway input can be found analytically from the matrix form of equation (C.36) by:

$$G(s) = C^T(sI - \bar{A})^{-1}\bar{B} \qquad (C.37)$$

where: $\bar{A}$, $\bar{B}$ = state and control matrices given in (C.36)

$G(s)$ = transfer function

$\bar{I}$ = identity matrix

s = Laplace operator

$\bar{C}$ = measurement matrix

The accelerations at the vehicle front and rear may be expressed in terms of the lateral and yaw accelerations as:

$$\ddot{Z}_{fa} = \ddot{Z} + a\,\ddot{\psi} \qquad (C.38)$$

$$\ddot{Z}_{ra} = \ddot{Z} + b\,\ddot{\psi} \qquad (C.39)$$

where:

a = c.g. to front axle distance

b = c.g. to rear axle distance

The front and rear tracking errors are defined as:

$$\Delta Z_{fa} = Z + a\,\psi - Z_o \qquad (C.40)$$

$$\Delta Z_{ra} = Z + -b\,\psi - Z_o \qquad (C.41)$$

where:

$Z_{fa(ra)}$ = front (rear) axle tracking error

Z_o = guideway profile input

In this study, the following controller gains are used:

$$C_1 = K_c$$
$$C_2 = K_c L^*$$
$$C_3 = C_4 = 0$$

A plot of roots of the denominator of the yaw and lateral acceleration transfer functions as the overall control gain K_c is varied is given in Figures C.9 and C.10 for both small and large vehicles, with $L^* = 7.5$ ft for the small vehicle and $L^* = 11.0$ ft for the large vehicle. From these root locus plots the value of K_c is chosen that gives the system the desired response. It can be seen, for example, that when $K_c = .1$ rad/foot the roots corresponding to the yaw response have good damping, but the Z roots are unstable (in the right half plane). Therefore a compromise must be made in order to place both poles in an acceptable position. For both large and small vehicles the value of K_c is chosen to be .3 rad/foot, because the damping for both roots is acceptable throughout the range of vehicle velocities studied.

Further modification on these choices of K_c may be necessary depending on the vehicle response. As K_c is increased, it has been shown [20] that the tracking errors of the vehicle are decreased, and the accelerations increased. Therefore, if the accelerations of either vehicle are unacceptable, the values of K_c can be decreased until the system goes unstable or the value of the tracking error becomes excessive. If the tracking errors are excessive, K_c can be increased until the accelerations exceed the ride comfort boundary.

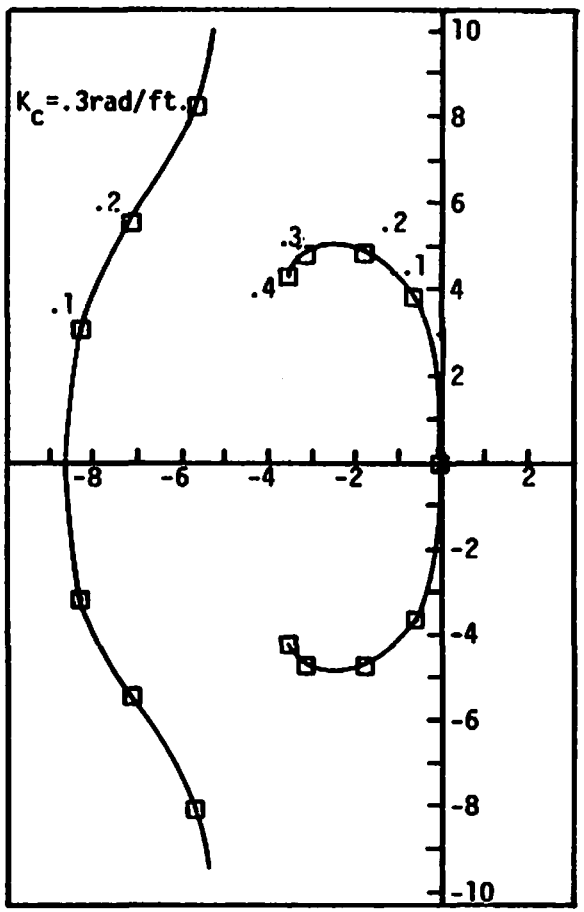

V = 30 MPH

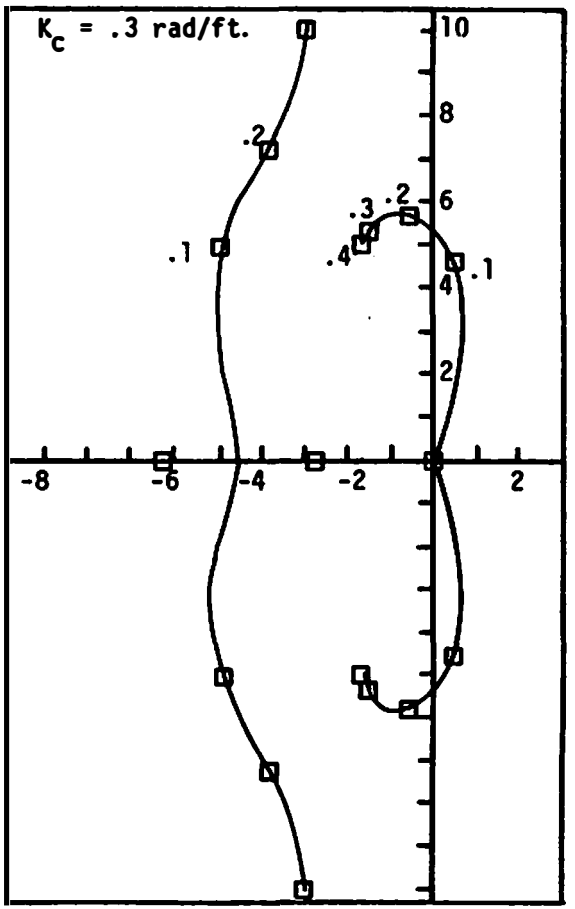

V = 60 MPH

FIGURE C.9: SMALL VEHICLE ROOT LOCUS

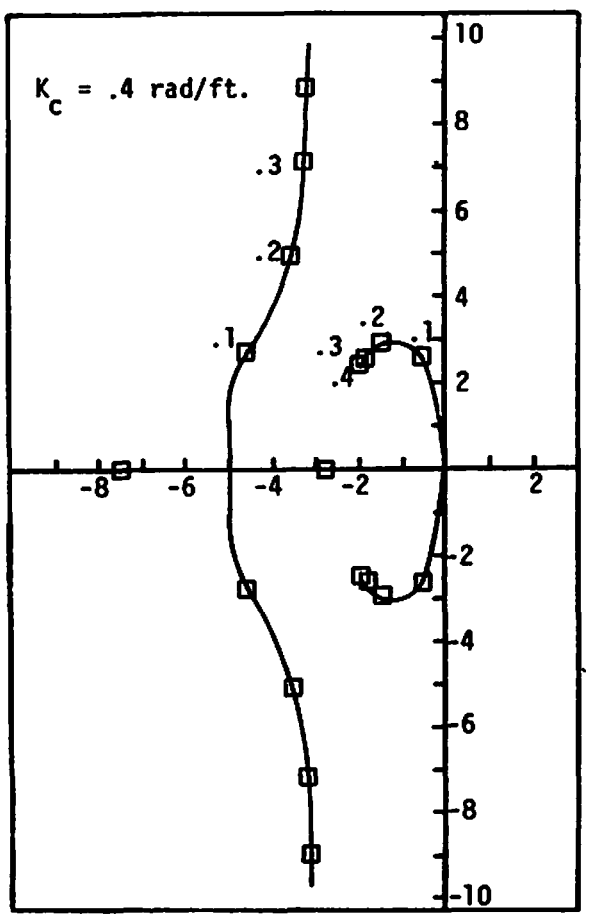

V = 30 MPH

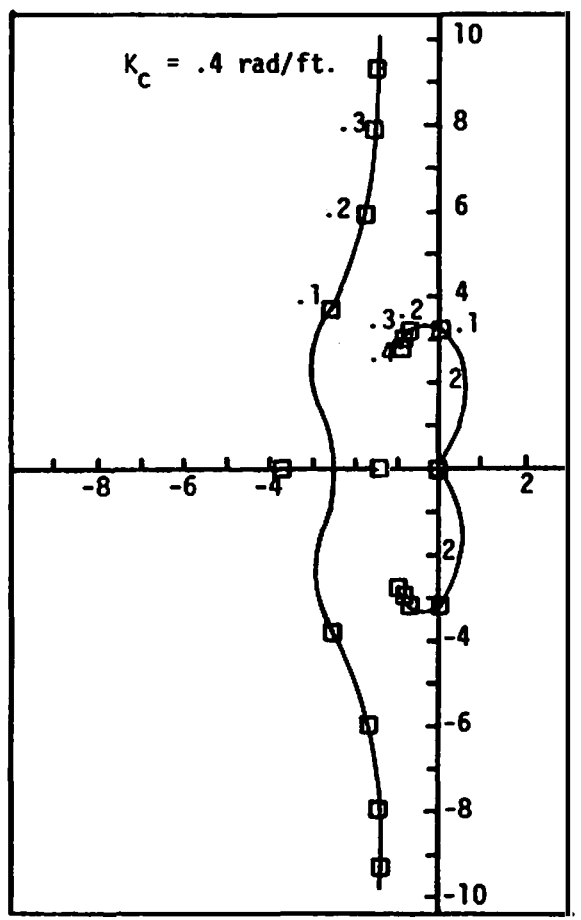

V = 60 MPH

FIGURE C.10: LARGE VEHICLE ROOT LOCUS

C.3 Computation of Vehicle Acceleration

The analysis techniques used to compute ride quality are discussed below. Because inputs to the vehicle are described both statistically (irregularities) and deterministically (guideway deflection and mean camber), two different algorithms are used to determine the total vehicle response. The basic framework of these algorithms is presented here. More specific algorithm details are provided in the computer programs listed in [7].

Irregularity Response

The response of a linear system forced by a stationary random input that is described as a PSD, can be found by:

$$S_{out}(\omega) = |H(\omega)|^2 \, S_{in}(\omega) \tag{C.42}$$

where:

$S_{out}(\omega)$ = Response PSD

$S_{in}(\omega)$ = Input PSD

$H(\omega)$ = Frequency response function of system

ω = Temporal frequency

The irregularity input to the vehicle is given as a PSD in terms of spatial frequency Ω. For a vehicle traveling at a constant velocity, the spatial frequency is related to the temporal frequency, ω, by

$$\omega = \Omega V \tag{C.43}$$

For the vertical model, inputs force the vehicle at the front and rear wheels. The input at the rear wheels is identical to that at the front wheels except that it has been delayed by a lag time $\frac{\ell_a}{V}$. Or,

$$y_r(t + \frac{\ell_a}{V}) = y_f(t) \tag{C.44}$$

Finding the frequency response relationship of equation (C.44) leads to

$$\frac{y_r}{y_f} = e^{-j(\omega \frac{\ell_a}{V})} = e^{-j(\phi)} \tag{C.45}$$

where:

ϕ = Phase angle

Therefore if the input at the front wheel is the total irregularity input, $S_{y_f}(\omega)$, the input at the rear wheel, from equation (C.44) is

$$S_{y_r}(\omega) = |e^{-j\phi}|^2 \, S_{y_f}(\omega) \tag{C.46}$$

For the vertical response, the transfer functions, of equations (C.23) and (C.24) and equation (C.34) combine to give the response PSD for the front wheel nondimensional accelerations.

$$S_{\ddot{y}_{2f}}(\omega) = |T_s(\frac{j\omega}{\omega_v}) + T_c(\frac{j\omega}{\omega_v})^{-j\phi}|^2 \, S_{tot}(\frac{\omega}{V}) \tag{C.47}$$

where:

$S_{\ddot{y}_{2f}}(\omega)$ = Front nondimensional acceleration PSD

$S_{tot}(\frac{\omega}{V})$ = Total irregularity input PSD

A similar expression can be found to describe the vehicle rear response.

The lateral response only has one input location and thus a phasing of inputs is not necessary. The responses at front and rear axles are respectively:

$$\frac{\ddot{Z}_{fa}}{Z_o}(\omega) = \frac{\ddot{Z}}{Z_o}(\omega) + a\,\frac{\ddot{\psi}}{Z_o}(\omega) \qquad (C.48)$$

$$\frac{\ddot{Z}_{ra}}{Z_o}(\omega) = \frac{\ddot{Z}}{Z_o}(\omega) + b\,\frac{\ddot{\psi}}{Z_o}(\omega) \qquad (C.49)$$

The response of the front axle to the PSD is found by using Equation (C.48) in Equation (C.42):

$$S_{fa}(\omega) = \left|\frac{\ddot{Z}}{Z_o}(\omega) + a\,\frac{\ddot{\psi}}{Z_o}(\omega)\right|^2 S_{tot}\left(\frac{\omega}{V}\right) \qquad (C.50)$$

To evaluate the lateral and vertical response in 1/3 octave bands, so the accelerations can be compared to the ISO spec., the value of the output PSD's are calculated at a number of frequencies in each third octave band. The PSD values are integrated over the 1/3 octave band which gives the mean square acceleration response and taking the square root defines the 1/3 octave band r.m.s. acceleration to be compared to the ISO spec.

<u>Deflection and Mean Camber Algorithm for the Vertical Response</u>

By using the modal analysis outlined in C.1, the deflections of an initially flat beam forced by a vehicle traveling over it can be found. These deflections are summed with the initial camber shape of the beam caused by prestressing. The resulting guideway shape repre-

sents the path of the vehicle front wheel as it passes over the span. Because of the vehicle's constant velocity, the time history of wheel movement is identical to the wheel path when a change in the horizontal axis is made from displacement to time. To find the temporal frequency representation of the wheel travel a Fast Fourier Transform is performed. The frequency description of the front wheel travel can be phased, as in the irregularity algorithm, to produce the rear wheel input.

If a deterministic input is known as a function of frequency the response can be found by:

$$Y(\omega) = H(\omega)\ X(\omega) \tag{C.51}$$

where:

$Y(\omega)$ = Frequency response of system

$X(\omega)$ = Frequency input

$H(\omega)$ = Frequency response function of system

and the nondimensional acceleration frequency response of the front axle is

$$\hat{\ddot{Y}}_{2f}(\omega) = [T_s(\frac{j\omega}{\omega_v}) + T_c(\frac{j\omega}{\omega_v})\ e^{-j\phi}]\ X_f(\omega) \tag{C.52}$$

where:

$X_f(\omega)$ = Fourier transform of front wheel input

To calculate the third octave band response of the guideway deflection response, the frequencies of the accelerations must be distinguished. Since the analysis is performed using an FFT, the response acceleration have magnitudes in discrete frequencies. The

square of the accelerations whose frequencies are within a third octave band must be added, multiplied by 1/2, and square rooted to find the 1/3 octave r.m.s values.

The total vertical vehicle response is due to both the irregularity and deflection induced accelerations. Mean square accelerations calculated from the separate irregularity and deflection analysis are added in each 1/3 octave band. The square root of this sum is taken and the total r.m.s. 1/3 octave band acceleration is the result.

A vertical analysis program summarized in Figure C.11 has been developed to compute vehicle accelerations from the vehicle irregularity and guideway deflections. The vertical irregularity analysis calculates the vertical guideway roughness from the inputted irregularity amplitude standard deviations and the analytical PSD's. This total irregularity input PSD is used to calculate the irregularity output PSD for the front and rear suspension attachment points. By integrating the output PSD in third octave bands the ISO response to guideway irregularity disturbances is calculated. The beam deflection, under the front wheel of the vehicle is calculated by a time simulation of the modal guideway equations in C.1 and assuming initially flat beam. The resulting deflected beam shape is added to the mean camber shape to determine the total time history beam deflection under the front wheel of the vehicle. The frequency domain description of the front wheel input is calculated by the use of a Fast Fourier Transform (FFT) and from this the rear wheel input is calcu-

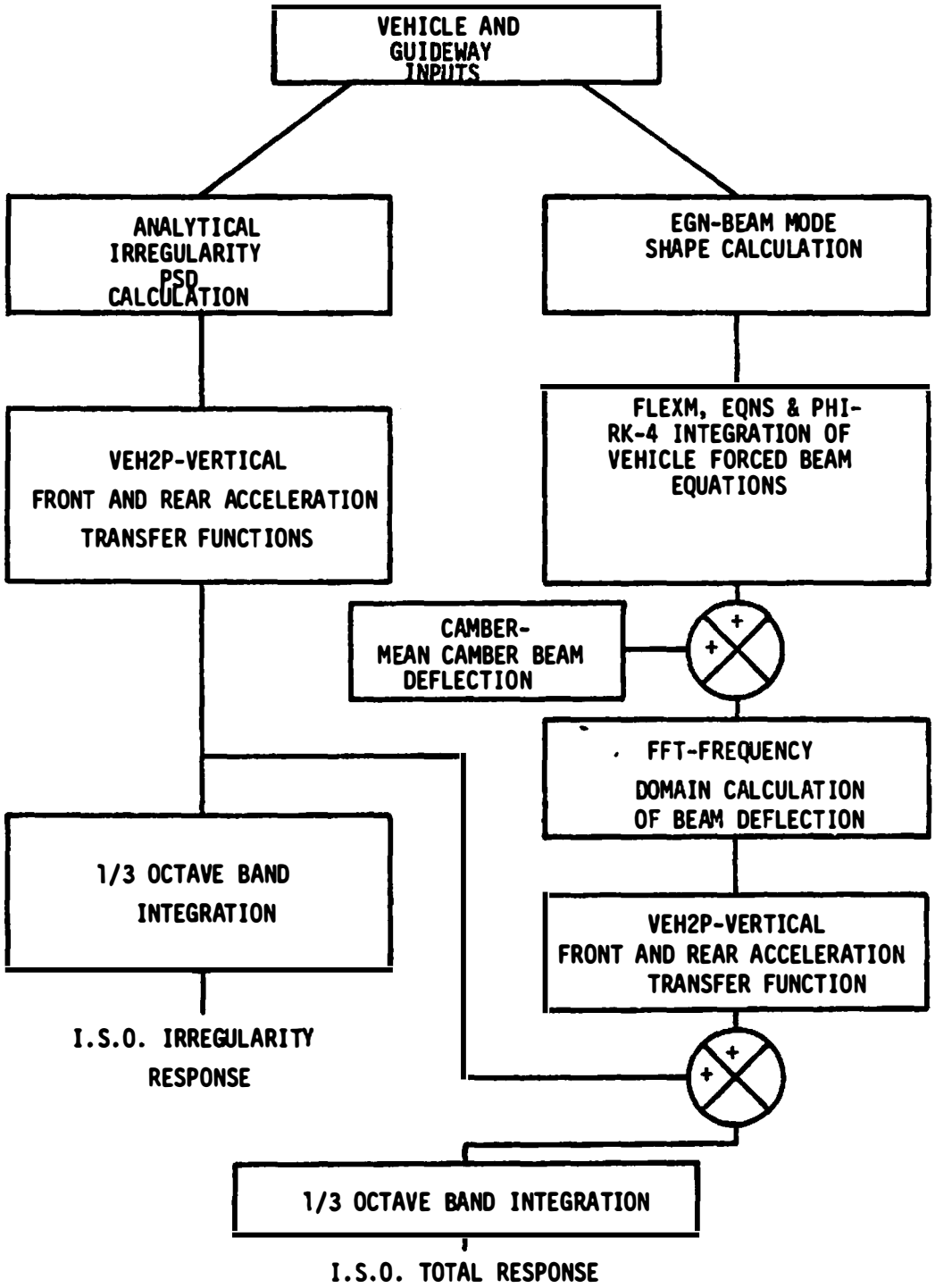

FIGURE C.11: VERTICAL VEHICLE ANALYSIS PROGRAM

lated. Vehicle response is calculated in the frequency domain and the resulting mean square response is added to irregularity response in third octave bands. The total I.S.O. response is calculated by taking the square root of the third octave band mean squares.

The lateral analysis program is similar to the vertical program and has as inputs vehicle and construction tolerance parameters. The lateral vehicle transfer functions are calculated at each frequency analyzed along with the total input irregularity PSD. Both acceleration and tracking error response PSD's are integrated over the total range of frequencies analyzed to determine total rms response.

The basic computer programs used to calculate the vertical and lateral response have been developed by modifying slightly the programs listed in [7].

APPENDIX D
REPORT OF INVENTIONS

The material in this report has been reviewed and does not contain patentable or copyrightable material. The innovations reported in this document are of an analytical and computational nature. The analytical innovations concern the development of techniques and methodology for elevated guideway design.

100 Copies